

NERVE AGENT INDUCED STATUS EPILEPTICUS: FROM SEIZURE ONSET TO
LONG LASTING PATHOLOGY

By

Eric Michael Prager

Dissertation submitted to the Faculty of the
Neuroscience Graduate Program
Uniformed Services University of the Health Sciences
In partial fulfillment of the requirements for the degree of
Doctor of Philosophy, 2014



DISSERTATION APPROVAL FOR THE DOCTORAL DISSERTATION IN THE
NEUROSCIENCE GRADUATE PROGRAM

Title of Dissertation: "Nerve Agent-induced Status Epilepticus: From Seizure Onset to Long- Lasting Pathology"

Name of Candidate: Eric Prager
Doctor of Philosophy Degree
January 24, 2014

DISSERTATION AND ABSTRACT APPROVED:

Dr. Gregory Mueller
DEPARTMENT OF ANATOMY, PHYSIOLOGY, AND GENETICS
Committee Chairperson

DATE:

01/31/2014

Dr. Maria Braga
DEPARTMENT OF ANATOMY, PHYSIOLOGY, AND GENETICS
Dissertation Advisor

1/23/14

Dr. Joseph McCabe
DEPARTMENT OF ANATOMY, PHYSIOLOGY, AND GENETICS
Committee Member

1/23/14

Dr. Thomas Flagg
DEPARTMENT OF ANATOMY, PHYSIOLOGY, AND GENETICS
Committee Member

1/23/14

Dr. Ann Marini
DEPARTMENT OF NEUROLOGY
Committee Member

1/23/14

Dr. James P. Aplan
USAMRIID, APG, MD

24 Jan 2014

ACKNOWLEDGMENTS

The work produced for my dissertation is the product of the efforts of many individuals. It is with my deepest gratitude that I thank all the individuals who made this work possible and helped build my capacity as a scientist and professional.

I am deeply indebted to Dr. Maria Braga for her unwavering support and mentorship throughout my years at USUHS. Without fail, I could always count on her to provide excellent guidance and provide a caring mentality. This thesis would not have been possible without her extreme level of enthusiasm, support, and patience. Her guidance and passion for teaching has helped me grow exponentially as a scientist and as a professional. Thank you for guiding and shaping this project, for all your help and support, especially as we sat for hours late into the evening talking about electrophysiology theory, and thank you for being my mentor.

I would also like to thank Dr. Vassiliki Aroniadou-Anderjaska. During my time in the program, Dr. Aroniadou-Anderjaska has taught me so much, to which I am forever indebted. With her mentorship, I have learned how to carefully design experiments, perform extracellular field recordings, and, most importantly, write scientific manuscripts. I thank her for her endless support and willingness to give me multiple opportunities to revise my own manuscripts, for taking the time to respond to countless emails, speak to me late into the night, help me understand each and every mistake I made, and enthusiastically encourage me to continue striving for perfection.

Drs. Volodymyr Pidoplichko, and Taiza Figueiredo have been instrumental in teaching me the skills I need to be an effective neuroscientist; I could not have completed this work without your guidance and wisdom. I would like to thank my colleagues in Dr.

Braga's lab, Dr. Franco Rossetti, Camila Almeida-Suhett, Steven Miller, Robert Long, and Katia Rossetti. You are all incredible individuals and helped ease the stress of running experiments. Thank you for cheering me up on stressful days (and weeks), when nothing was going right. I want to especially thank Camila Almeida-Suhett for spending countless hours with me at the bench.

I owe a great debt of gratitude to Dr. Luke Johnson, who urged me to apply to USUHS and gave me the opportunity to work in his laboratory, where I learned about basic science techniques, writing, and experimental design. Thank you for helping provide me the opportunity to also travel to Israel to work with Dr. Rafi Lamprecht. I would like to also thank Dr. Hadley Bergstrom for his mentorship and collaboration throughout my years at USUHS. His enthusiasm for science is a true inspiration. I deeply appreciate the roles played by Dr. Neil Grunberg, who helped lay the foundation for my professional career and gave me years of support and advice, and Dr. Sharon Juliano and the rest of the Neuroscience Program for their support throughout my studies.

I want to thank members of my dissertation committee – Dr. Gregory Muller (Chair), Dr. Thomas Flagg, Dr. Ann Marini, Dr. Joseph McCabe, and especially Dr. James Apland – for their invaluable input, criticism, suggestions, and comments, which greatly improved the quality of my work. My work could not have been completed with the help of Dr. Cara Olsen, who provided valuable input with my statistics and helped make all of my projects successful.

I cannot thank enough my parents, Jeffrey and Judy Prager, and my siblings, David, Susan, Jenny, and Daniel and their children Georgiana and Jonathan. You have all been a constant positive force in my life and have helped shape me into the person I am

today. Thank you for your patience and support throughout my 25+ years in school. We have been through so many twists and turns together, a lot of which I am sure we will never fully understand, but throughout each roadblock, you have helped me find my way. I would like to thank Drs. Marc and Nancy Hazan, David Hazan, and Drs. Emily Hazan and Jason Goldman, and their children, Eve and Wyatt. Thank you for always being there for me and supporting me throughout my education.

I was inspired to pursue this work by my grandparents, George and Margo Prager, and Margaret Levitt. Throughout my life, they have supported everything I did with enthusiasm. Even when they gave up trying to understand my work, they always approved and provided unrelenting encouragement. I am certain that they are extremely proud of this accomplishment, which I dedicate to them.

I would like to thank my friends, Nicholas and Elenna Sayers, Katya Tregub-Emrick and Steve Emrick, Drs. Craig Budinich, Jennifer Coyner, and John Buonora, and Carl Goforth. You have been a continued source of support to me.

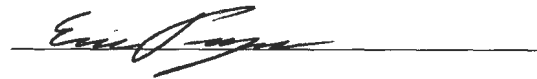
To my beautiful wife and best friend, Sarah Prager. Her outlook on life, unwavering support, patience, and belief in me, even through the tough periods, have helped strengthen my resolve and made me a better human being. She has been by my side each and every day and has been and continues to be a constant source of strength. This would not have been possible without your support, understanding, and love. Thank you for being by my side. Finally, to my constant source of happiness, Turtle: although you did not understand my long days, hours of studying, and lack of time to play with you and take you for runs, you brought a smile to my face each day. Thank you.

DEDICATION

To my grandparents, George and Margo Prager and Margaret Levitt,
for their love, inspiration, and unwavering support.

COPYRIGHT STATEMENT

The author hereby certifies that the use of any copyrighted material in the dissertation manuscript entitled: “Nerve Agent Induced Status Epilepticus: From Seizure Onset to Long Lasting Pathology” is appropriately acknowledged and, beyond brief excerpts, is with the permission of the copyright owner.

A handwritten signature in black ink, appearing to read "Eric Prager", is written over a horizontal line.

Eric Prager
Program in Neuroscience
Uniformed Services University
January 31, 2014

ABSTRACT

Title of Dissertation: Nerve Agent Induced Status Epilepticus: From Seizure Onset to
Long Lasting Pathology

By

Eric M. Prager, Doctor of Philosophy, 2014

Thesis directed by: Dr. Maria F.M. Braga, D.D.S., Ph.D.,
Professor, Department of Anatomy, Physiology, and Genetics,
Department of Psychiatry, Program in Neuroscience

The recent use of chemical nerve agents in Syria left countless civilians to deal with possible health consequences, including the development of anxiety disorders. Anxiety disorders were among the most debilitating neuropsychiatric symptoms reported by victims of the Japan sarin attack, more than a decade after exposure. Nerve agents are powerful neurotoxins that irreversibly inhibit acetylcholinesterase (AChE) activity. This leads to the generation of seizures, status epilepticus (SE), resulting in brain damage and long-term behavioral deficits. Uncovering the neuro-pathophysiological mechanisms underlying the development of seizures and the subsequent anxiety disorders observed after nerve agent exposure is necessary for developing successful treatments. Towards this goal, we examined AChE activity in three brain regions critically involved in nerve agent induced SE after subcutaneous injection of the nerve agent soman. Following the administration of soman, we observed that AChE activity was significantly reduced in the

hippocampus, piriform cortex, and basolateral amygdala (BLA) of rats that developed SE. In addition, animals that developed seizures went on to have significant neuronal loss and neurodegeneration after SE. In marked contrast, AChE activity was not inhibited in the BLA of animals that did not develop SE, even though AChE activity was reduced in the hippocampus and piriform cortex of these same animals. In addition, these animals did not display any neuropathology 7 days after SE. These results indicate that AChE inhibition in the BLA is necessary for the generation of seizures in response to nerve agent exposure and that only in animals that develop seizures will neuropathology and behavioral deficits ensue.

The BLA is known to play a major role in anxiety-like behavior and associated disorders. To identify the mechanisms underlying the development of anxiety disorders after a nerve agent exposure we examined neuropathological and pathophysiological alterations to the BLA during a 30-day period after soman exposure. Significant neuronal loss and neurodegeneration was observed in the BLA at 24 hours post soman exposure. By day 7, the number of GABAergic interneurons in the BLA were reduced by ~46% and by 14-days, an increase in anxiety-like behavior was evident. The loss of GABAergic interneurons led to deficits in inhibitory synaptic transmission as determined by whole-cell patch clamp recordings. Moreover, activation of α_7 -nicotinic acetylcholine receptors, a cholinergic receptor that participates in the regulation of BLA excitability and is involved in anxiety, was less effective in increasing spontaneous inhibitory postsynaptic currents (sIPSCs) in soman-exposed rats. Despite the loss of both interneurons and principal cells, the frequency of sEPSCs was increased in the soman-exposed rats. Thus, impaired function of the GABAergic system and impaired modulation by α_7 -nicotinic

acetylcholine receptors, along with an increase in excitatory neurotransmission, may explain the development of anxiety disorders after nerve agent exposure.

TABLE OF CONTENTS

LIST OF TABLES.....	xiv
LIST OF FIGURES.....	xv
CHAPTER 1: Introduction.....	23
Physical and Chemical Properties of Nerve Agents.....	24
Cholinergic Synaptic Transmission.....	25
Nerve Agent Mechanism of Action.....	26
Symptoms of Nerve Agent Exposure.....	29
Nerve Agent Induced Seizures.....	29
Acute and Long Term Neuropathology after Nerve Agent Exposure.....	32
The Amygdala and Long-Lasting Behavioral Deficits Associated with Amygdalar Hyperactivation After Soman Induced Status Epilepticus.....	34
The Amygdala's Anatomy and Physiology.....	34
Amygdala-Dependent Behavioral Deficits After Nerve Agent Exposure.....	36
Conclusions.....	37
Specific Aims.....	38
Specific Aim 1: To determine whether AChE must be sufficiently inhibited in the BLA for the generation of soman-induced seizures and examine the recovery of AChE in temporal lobe brain regions after soman exposure.....	39
Specific Aim 2: To identify the progression of neuropathological and pathophysiological alterations in the BLA after soman exposure and its association with anxiety-like behavior.....	39
Specific Aim 3: To identify alterations in GABA _A receptor mediated inhibitory synaptic transmission in the rat BLA after exposure to soman.....	40
Chapter 2: Acetylcholinesterase Inhibition in the Basolateral Amygdala Plays a Key role in the Induction of Status Epilepticus After Soman Exposure.....	42
Abstract.....	43
Introduction.....	45
Materials and Methods.....	46
Animals.....	46
Soman exposure.....	47
Electrode implantation for electroencephalographic (EEG) recordings.....	48
Acetylcholinesterase activity assay.....	48
Neuropathology assessments.....	49
Fixation and tissue processing.....	49
Stereological quantification.....	50
Fluoro-Jade C (FJC) staining.....	51
Statistical analysis.....	52
Results.....	52

Discussion	59
Acknowledgments.....	61
Chapter 3: The Recovery of Acetylcholinesterase Activity and the Progression of Neuropathological and Pathophysiological Alterations in the Rat Basolateral Amygdala After Soman-Induced Status Epilepticus: Relation to Anxiety-Like Behavior	
Abstract	64
Introduction.....	66
Materials and Methods.....	68
Animal Model	68
Soman administration and drug treatment	68
Acetylcholinesterase activity assay.....	69
Neuropathology experiments	70
Fixation and tissue processing	70
Fluoro-Jade C (FJC) staining.....	71
GAD-67 Immunohistochemistry	71
Stereological quantification	72
Behavioral Experiments.....	73
Open field test.....	73
Acoustic startle response test.....	73
Electrophysiological experiments.....	74
Statistical analysis.....	75
Results.....	76
Time course of recovery of AChE inhibition	76
Time course of neurodegeneration and neuronal loss in the BLA.....	79
Anxiety-like behavior after soman exposure	83
Time course of pathophysiological alterations in the BLA	85
Discussion	90
Inhibition and recovery of AChE.....	90
Acute and delayed neuropathology.....	92
Increased anxiety-like behavior and pathophysiological alterations	94
Acknowledgments.....	96
Chapter 4: Pathophysiological Mechanisms Underlying Increased Anxiety After Soman Exposure: Reduced GABAergic Inhibition in the Basolateral Amygdala.....	
Abstract	99
Significance Statement.....	100
Introduction.....	101
Results.....	102
Diminished GABAergic Inhibition after Soman-Induced SE	103
Impaired α_7 -nAChR Mediated Enhancement of Inhibitory Synaptic Transmission after Soman-Induced SE.....	106
Increased Spontaneous Excitatory Activity after Soman-Induced SE.....	110
Discussion.....	113
Materials and Methods.....	117
Animals	117

Experimental Procedures	118
Soman Administration and Drug Treatment.....	118
Electrophysiological Experiments	118
Statistical Analysis.....	120
Acknowledgements.....	121
CHAPTER 5: Discussion.....	122
AChE Inhibition and Recovery After Nerve Agent Exposure.....	123
Acute and Delayed Neuropathology After Nerve Agent Induced Status Epilepticus	128
Increased Anxiety-like Behavior and Pathophysiological Alterations After Exposure to a Nerve Agent	131
Conclusions and Future Directions.....	133
Appendix 1: α_7 -Containing Nicotinic Acetylcholine Receptors on Interneurons of the Basolateral Amygdala and Their Role in the Regulation of the Network Excitability ..	139
Abstract.....	140
Introduction.....	142
Materials and Methods.....	144
Animals.....	144
Electrophysiological Experiments.	144
Results.....	147
Functional α_7 -nAChRs are present on BLA interneurons	147
Glutamatergic excitation of interneurons following α_7 -nAChR activation.....	150
Activation of α_7 -nAChRs enhances spontaneous GABA _A receptor-mediated inhibitory postsynaptic currents (sIPSCs).....	153
The net effect of α_7 -nAChR activation in the BLA	156
α_7 -nAChRs are active in the basal state contributing to background inhibition.....	160
Discussion	163
Acknowledgments.....	168
REFERENCES	169

LIST OF TABLES

Table 1 Chemical Properties of Nerve Agents.....	25
Table 2: Reduction of AChE activity (in nmol/min/ng) and time course of recovery after soman-induced status epilepticus (SE).....	78

LIST OF FIGURES

- Figure 1 Structural formula of organophosphorus agents. (A) General formula of an organophosphate where R^{1-2} are hydrogen, alkyl (including cyclic), aryl, alkoxy, alkylthio, and amino groups, and R^3 is a dissociable group. (B) Structural formula of soman (pinacolyl methylphosphonate). Modified from (26).25
- Figure 2 Cholinergic synaptic transmission under basal conditions and in the presence of a nerve agent. (A) In the presynaptic terminal choline-acetyltransferase (ChAT) catalyzes the synthesis of acetylcholine (ACh) from choline and acetyl-coenzyme A (a). ACh is packaged in synaptic vesicles via a vesicular ACh transporter (vAChT) (b). ACh is released into the synaptic cleft (c) where it will bind to muscarinic acetylcholine receptors (mAChRs), leading to the activation of second messengers (d) that either increase intracellular calcium concentrations or inhibit activation of potassium channels (e). In addition, activation of post-synaptic α_7 -nAChRs increase calcium influx and activates second messengers that influence anti-apoptotic mechanisms (3) (f), whereas activation of presynaptic α_7 -nAChRs regulates ACh release via a feedback response. ACh is hydrolyzed in the synaptic cleft by AChE. Liberated choline is taken back up by a high affinity choline-uptake mechanism (267) where it will be resynthesized into ACh (g). (B) A nerve agent, such as soman, binds to and irreversibly inhibits AChE activity (black circles). While initially the synthesis and packaging of ACh is similar to basal conditions (a, b) AChE inhibition will cause ACh to accumulate at cholinergic synapses (c). Accumulation of ACh will increase activation of mAChRs, subsequently, increasing postsynaptic depolarization (d, e). α_7 -nAChRs, which are present on GABAergic interneurons in the BLA and act to increase inhibitory synaptic transmission will desensitize. The combined effects initiate SE activity, but subsequently give way to glutamatergic hyperactivity, which sustains and reinforces seizures, causing neuropathology and subsequent neurodegeneration via pro-apoptotic effects (f).28
- Figure 3 Comparison of EEG activity in two rats exposed to the same dose of soman (154 $\mu\text{g}/\text{kg}$). In rat (A), seizure activity appeared within 11 min after soman injection. The arrow points to the time point that the animal behavior was consistent with stage 3 seizures. In rat (B), there was no evidence of seizure activity in any of the 4 electrodes at the same time point as in (A), or 30 min after administration of soman. (C), Diagrammatic presentation of electrode placement. The numbers 1, 2, 3, 4 refer to the electrodes/sites from where electrical activity was sampled (1, left frontal; 2, right frontal; 3, left parietal; 4, right parietal; the reference electrode is in the cerebellum).....54
- Figure 4 Reduction of brain AChE activity after exposure to soman. The “raw data” of AChE activity are shown in (A), while the data are expressed as percent of the control mean in (B). Soman-exposed rats that developed SE (SE group, $n = 7$) were sacrificed at the onset of Stage 3 seizures. These rats had significantly reduced AChE activity in all three regions examined, compared to controls ($n =$

7). Soman-exposed rats that did not develop SE (no-SE group, n = 7) were sacrificed at 30 min after soman exposure. These rats had significantly reduced AChE activity in the piriform cortex and hippocampus, but not in the BLA ($p = 0.535$). $***p < 0.001$ compared to the control group. $\#p < 0.05$ for the difference between the SE group and the no-SE group.....	56
Figure 5 Neuronal loss in rats that developed SE versus rats that did not develop SE after soman exposure. (A) Panoramic photomicrographs of Nissl-stained sections of half hemispheres, outlining the BLA and the CA1 hippocampal subfield where stereological analysis was performed (red highlight). (B) Representative photomicrographs of Nissl-stained sections showing BLA and CA1 cells from a control rat, a SE rat, and a no-SE rat. Total magnification is 63x and scale bar is 50 μm . (C) Group data of stereological estimation of the total number of Nissl-stained neurons in the BLA (left) and CA1 (right), expressed as percent of the control (n = 6). Significant neuronal loss was present in SE rats (n = 5), while there was no neuronal loss in the no-SE rats (n = 5); $***p < 0.001$.	57
Figure 6 Neuronal degeneration in rats that developed SE versus rats that did not develop SE after soman exposure. (A) and (B) Panoramic photomicrographs of Nissl-stained sections showing the brain regions from where the FJC photomicrographs shown in C were taken. (C) Representative photomicrographs of FJC-stained sections from the brain regions where neuronal degeneration was evaluated, for the SE and the no-SE groups. Total magnification is 100x and scale bar is 50 μm . (D) Neurodegeneration scores for the amygdala (Amy), piriform cortex (Pir), entorhinal cortex (Ent), CA1 and CA3 hippocampal subfields, hilus, and neocortex (neo-Ctx), in the SE group and the no-SE group (n = 5 for each group).....	58
Figure 7 Time course of the recovery of AChE activity after soman-induced status epilepticus (SE). AChE activity was reduced by more than 90% in all four brain regions at the onset of SE (n = 7), as well as at 24 hours later (n = 11). At 7 days post-exposure (n = 11), AChE activity had recovered in the BLA, while at 14 days (n = 10) and 30 days (n = 12) post-exposure, it was not significantly different from the control levels in all 4 brain regions. $**p < 0.01$; $***p < 0.001$ compared to the controls (Welch F ANOVA with Games-Howell post hoc).....	79
Figure 8 Time course of neuronal degeneration in the BLA after soman-induced SE. A, B. The BLA region where neuronal degeneration was assessed. In A, the drawings are from Paxinos and Watson (2005), while in B the BLA is outlined on FJ-C stained sections. C. Representative photomicrographs of FJC-stained sections, at 24-hours, 7-, 14-, and 30-days after soman exposure. Rows correspond to the coordinates shown in B. Total magnification is 20x. Scale bar, 250 μm . D. Quantitative assessment of the extent of neurodegeneration at 24-hours (n = 4), 7- (n = 6), 14- (n = 4), and 30 days (n = 5) after soman exposure. Values are mean \pm SEM number of cells counted in the BLA from both hemispheres. $**p < 0.01$, $***p < 0.001$ (One-Way ANOVA with Tukey post hoc).	80

- Figure 9 Time course of neuronal loss in the BLA after soman-induced SE. A. Panoramic photomicrograph of a Nissl-stained section from half hemisphere, outlining the BLA where stereological analysis was performed (red highlight). B. Representative photomicrographs of Nissl-stained sections showing BLA cells from a control rat and from soman-exposed rats, analyzed at 24-hours, 7-, 14- and 30-days after exposure. Total magnification is 63x and scale bar is 50 μ m. C. Group data of stereological estimation of the total number of Nissl-stained neurons in the BLA, expressed as percent of the control group (n = 11). Significant neuronal loss was present in rats at 24 hours (n = 5), 7 days (n = 6), 14 days (n = 5), and 30-days (n = 6) after soman exposure. There were no differences in the extent of neuronal loss among the 24-hour, 7-, 14-, and 30-day groups; *** p < 0.001 (One-Way ANOVA with Dunnett's T post hoc).....81
- Figure 10 Delayed loss of GABAergic interneurons in the BLA after soman-induced SE. A. Panoramic photomicrograph of an immunohistochemically-stained section for GAD-67 (BLA is outlined in white). B. Representative photomicrographs of GABAergic interneurons in the BLA from a control rat and from soman-exposed rats, analyzed at 24-hours, 7-, 14- and 30-days after exposure. Total magnification is 630x; scale bar, 50 μ m. C. Group data showing the mean and standard error of the stereologically estimated total number of GAD-67-positive cells in the BLA. D. Group data showing the mean and standard error of the ratio of GABAergic interneurons to the total number of neurons. * p < 0.05, ** p < 0.01, *** p < 0.001 (Welch F ANOVA with Games-Howell post hoc and one-way ANOVA with Dunnett's T post hoc).....83
- Figure 11 Exposure to soman causes long-lasting increases in anxiety-like behavior, as measured by the open field and acoustic startle response (ASR) tests. A. Soman-exposed rats spent significantly less time in the center of the open field, at 14 and 30 days after exposure, compared to control rats. B. Exposure to soman significantly increased the amplitude of the ASR to both the 110 and 120 dB startle stimuli, at 14 and 30 days after exposure, compared to controls. There were no significant differences between the 14- and 30-day groups. * p < 0.05, ** p < 0.01; n = 17 (One-Way ANOVA with Dunnett's T post hoc).....85
- Figure 12 Alterations in the BLA field potentials after soman-induced SE. A to E show representative field potentials evoked in the BLA by paired-pulse stimulation of the external capsule, from control rats (n = 9) and soman-exposed rats, at 24-hours (n = 9), 7 days (n = 9), 14 days (n = 10), and 30 days (n = 11) after exposure; each trace is an average of 10 to 15 sweeps. In the soman-exposed rats, higher stimulus intensities were necessary to evoke field potentials compared to controls, the duration of the field potentials was prolonged (notice the decay of the waveforms), and the paired-pulse ratio was significantly increased (F). ** p < 0.01 (One-Way ANOVA with Dunnett's T post hoc).....87
- Figure 13 Effects of soman exposure on Long-Term Potentiation in the BLA. The plots show the time course of the changes in the amplitude of the field potentials after high-frequency stimulation (HFS). The amplitude of the 3 responses recorded in each min (stimulation at 0.05 Hz) was averaged, and

each data point on the plots is the mean and standard error of these averages, from 7 to 10 slices (see sample sizes in the text). Traces over the plots are examples from a control rat and from soman-exposed rats studied at the indicated time-point after exposure; the superimposed field potentials are a baseline response and a response at 50 to 60 min after HFS (each trace is the average of 10 to 15 sweeps). Potentiation of the responses, measured at 50 to 60 min after HFS, was significantly lower – compared to the control group – at 24 hours, 7 days and 14 days post-exposure, but not at 30 days post-exposure.

.....89

Figure 14 Exposure to soman reduces the frequency and amplitude of GABA_A receptor mediated spontaneous IPSCs. Recordings are from BLA principal cells at a holding potential of +30 mV and internal chloride concentration of 10 mM. (A) Representative traces of sIPSCs recorded from BLA pyramidal cells in slices obtained from control animals and from animals at 24 hours and 14 days after soman exposure. (B) Significant decreases in the frequency of sIPSCs was observed at 24 hours ($n = 18$; 6.63 ± 0.88 Hz; $P < 0.001$) and 14 days ($n = 24$; 7.78 ± 0.58 Hz; $P = 0.001$) after soman exposure compared to controls ($n = 20$; 11.35 ± 0.61 Hz). (C) Cumulative probability amplitude distributions of sIPSCs. The mean amplitude of sIPSCs was significantly reduced at 24 hours (47.39 ± 2.91 pA; $P = 0.005$) and 14 days (49.06 ± 3.52 pA; $P = 0.005$) after exposure compared to controls (75.51 ± 9.20 pA). *** $P < 0.001$ (One-way ANOVA with Tukey post hoc). 104

Figure 15 Exposure to soman reduces the frequency but not the amplitude of GABA_A receptor mediated miniature IPSCs. Recordings are from BLA principal cells at a holding potential of +30 mV and internal chloride concentration of 10 mM. (A) Representative traces of mIPSCs recorded from BLA pyramidal cells, in slices obtained from control animals and from animals at 24 hours and 14 days after soman exposure. (B) A significantly lower frequency of mIPSCs was observed at 24 hours ($n = 17$; 3.19 ± 0.24 Hz; $P < 0.001$) and 14 days ($n = 24$; 4.75 ± 0.28 Hz; $P < 0.001$) after exposure, compared to controls ($n = 20$; 7.41 ± 0.47 Hz). (C) Cumulative probability amplitude distributions of mIPSCs. *** $P < 0.001$ (One-way ANOVA with Tukey post hoc). 106

Figure 16 Exposure to soman impairs the α_7 -nAChR-mediated enhancement of spontaneous inhibitory synaptic transmission. Recordings are from BLA principal cells at a holding potential of +30 mV and internal chloride concentration of 10 mM. (A) Bath application of choline chloride (5 mM) increased the frequency and amplitude of sIPSCs in control slices, as well as in slices obtained from animals at 24 hours and 14 days after soman exposure. (B) The increase in the charge transferred by sIPSCs upon application of choline chloride was significantly lower at 24 hours after soman exposure ($n = 16$, $P < 0.001$) and 14 days after exposure ($n = 22$, $P = 0.032$) compared to the controls ($n = 17$). (C) Cumulative probability amplitude distributions of sIPSCs in the presence of choline. The mean amplitude of sIPSCs was significantly reduced at 24 hours ($P = 0.037$), but not at 14 days ($P = 0.938$) after exposure, compared

to controls. * $P < 0.05$; *** $P < 0.001$ (One-way ANOVA with Dunnett T post hoc).

..... 108

Figure 17 The α_7 -nAChR-mediated enhancement of spontaneous excitatory synaptic transmission is not impaired after soman exposure. Recordings were obtained from principal neurons at a holding potential of -58 mV and internal chloride concentration of 1 mM. (A-C) Bath application of choline chloride (5 mM) induced a transient increase in the frequency and amplitude of both sIPSCs (outward currents) and sEPSCs (inward currents). (D) The charge transferred by sEPSCs during choline application was not significantly altered at 24 hours or 14 days after soman exposure compared to controls. (E) The charge transferred by sIPSCs was significantly reduced at 24 hours ($n = 16$; $P = 0.017$) and 14 days ($n = 14$; $P = 0.002$) after soman exposure compared to controls ($n = 12$). * $P < 0.05$; ** $P < 0.01$ (One-way ANOVA with Dunnett T post hoc).

..... 110

Figure 18 Spontaneous excitatory synaptic transmission is increased after soman exposure. Recordings were obtained from principal neurons at a holding potential of -58 mV and internal chloride concentration of 1 mM. (A) The frequency of sEPSCs was greater at 24 hours ($P < 0.001$; $n = 16$) and 14 days ($P = 0.04$; $n = 14$) after soman exposure, compared to controls ($n = 28$). (B) Amplitude-frequency histograms showing the effects of soman on sEPSCs, at 24 hours ($n = 16$) and 14 days ($n = 14$) after exposure, compared to controls ($n = 28$). * $P < 0.05$; ** $P < 0.01$; *** $P < 0.001$ (One-way ANOVA with Dunnett T post hoc).

..... 112

Figure 19 Summary of mechanisms involved with the onset of nerve agent induced seizures and pathophysiological alterations after status epilepticus. (A) Excitation within the BLA is tightly regulated by GABAergic inhibition (blue neurons, red circles). ACh (green circles) released from cholinergic fibers in the basal forebrain synapse, in part, on α_7 -nAChRs. While activation of α_7 -nAChRs enhances both excitation (1) and inhibition (2), α_7 -nAChR mediated enhancement of GABAergic inhibition predominates (see Appendix 1). Nerve agent exposure rapidly and irreversibly inhibits AChE, leading to an accumulation of ACh at the synapse and hyperstimulation of cholinergic receptors. SE onset occurs only after AChE is sufficiently inhibited in the BLA, leading to hyperstimulation of mAChR and nAChR, and subsequent neuronal depolarization; α_7 -nAChRs rapidly desensitize and reduce α_7 -nAChR mediated enhancement of inhibitory synaptic transmission. SE is sustained and reinforced when excessive glutamate (gold circles) is released, subsequently causing hyperstimulation of glutamatergic receptors (e.g., AMPA, NMDA, kainate receptors). (B) Within 24 hours of SE onset, approximately 35% of neurons die in the BLA and within 7 days of SE 46% of GABAergic interneurons die. α_7 -nAChR mediated enhancement of excitatory transmission remains unchanged (1), but α_7 -nAChR mediated inhibitory synaptic transmission is reduced, likely because of the loss of GABAergic interneurons and not because of alterations to receptor activation (2). Reduced GABAergic inhibition, and deficits to mechanisms that modulate GABAergic inhibition, subsequently dysregulate the tight control GABAergic inhibition has over excitation in the

BLA; reduced GABAergic inhibition, leads to significant increases in excitatory synaptic transmission and subsequently BLA hyperexcitability, which may manifest as anxiety disorders..... 135

Figure 20 α_7 -nAChRs are present on BLA interneurons. Recordings were obtained from electrophysiologically identified interneurons in the BLA, in the presence of α -conotoxin Au1B (1 μ M), DH β E (10 μ M), atropine sulfate (0.5 μ M), D-AP5 (50 μ M), CNQX (20 μ M), SCH50911 (10 μ M), LY 3414953 (3 μ M), and bicuculline (20 μ M). *A*: Examples of fast and slow currents evoked by pressure-application of 10 mM choline chloride (arrowhead; 100 ms; 30 psi; $V_h = -70$ mV; $[Cl^-]_{int} = 10$ mM). The insets show the absence of the current activated by hyperpolarization (I_h). *B*: In the current-clamp mode, pressure application of 5 mM tricholine citrate (arrowhead) induced brief spiking (*upper left panel*; the membrane potential was held at -60 mV by passing low-amplitude depolarizing current). The *lower left panel* shows the inward current evoked in the same cell by tricholine citrate (5 mM; arrowhead) in the voltage-clamp mode (holding potential (V_h), -70 mV). The *right panel* shows the fast, non-accommodating spiking of the same neuron, in response to depolarizing current injections, and the absence of a "sag" in response to hyperpolarizing current injections (*upper panel*), as well as the linear changes in leakage current (absence of I_h) during 1 s-long, 10 mV hyperpolarizing steps, starting from the holding potential of -70 mV (*lower panel*). *C*: The fast current activated by sequential (40 s interval) pressure-application of 10 mM choline chloride (arrowheads; same settings as in "A") was blocked by bath application of either 250 nM α -BgTx (*upper trace*), or 1 μ M α -BgTx (*lower trace*). Upper and lower traces are from two different neurons. Grey bars over the recordings mark the duration of bath-application of α -BgTx. *D*: Example of the low sensitivity of choline-evoked, slow currents to α -BgTx. Arrowheads show the time point of pressure application of 10 mM choline chloride. α -BgTx was bath applied, initially at the concentration of 500 nM, followed by 1 μ M (duration of application, 8 min at each concentration; flow rate, 8 ml/min). 150

Figure 21 Indirect excitation of interneurons by activation of α_7 -nAChRs. Recordings are from electrophysiologically identified interneurons, in the presence of α -conotoxin Au1B (1 μ M), DH β E (10 μ M), atropine sulfate (0.5 μ M), D-AP5 (50 μ M), SCH50911 (10 μ M), LY 3414953 (3 μ M), and bicuculline (20 μ M). *A*: Pressure application of tricholine citrate (5 mM; arrowhead) induced high frequency firing in the current-clamp mode (*upper left panel*) and a transient inward current along with high-frequency sEPSCs in the voltage-clamp mode (*lower left panel*; V_h , -70 mV). The electrophysiological characteristics of this neuron are shown on the right panel. Responses to depolarizing or hyperpolarizing current injections (*upper right panel*) and hyperpolarizing voltage steps (*lower right panel*) are consistent with the properties of interneurons. *B*: In current-clamp mode, bath application of choline chloride (2.5 mM) induced high-frequency spiking..... 152

Figure 22 Activation of α_7 -nAChRs enhances spontaneous GABA_A receptor-mediated IPSCs. Recordings are from BLA principal cells, in the presence of α -conotoxin

Au1B (1 μ M), DH β E (10 μ M), atropine sulfate (0.5 μ M), D-AP5 (50 μ M), CNQX (20 μ M), SCH50911 (10 μ M), and LY 3414953 (3 μ M), at V_h +30 mV and internal chloride 10 mM. *A*: Bath application of choline chloride (5 mM) induced a transient outward cationic current and increased the frequency and amplitude of sIPSCs. The sIPSCs were blocked by 20 μ M bicuculline, indicating that they were mediated by GABA_A receptors. *B*: Amplitude-frequency histogram of the effect of choline on sIPSCs ($n = 12$, $***P < 0.001$). *C*: Group data (mean \pm SE) of the change in the frequency of sIPSCs by bath application of choline chloride ($n = 12$, $***P < 0.001$). *D*: Pretreatment of the slices with α -BgTx reduced significantly the effects of choline. Traces show an example of the response of a principal neuron to bath application of choline chloride (5 mM), and the response of the same neuron when choline chloride was applied in the presence of α -BgTx (1 μ M). The group data are shown in the bar graphs below ($***P < 0.001$, $**P < 0.01$, $n = 9$)..... 155

Figure 23 Effects of α_7 -nAChR activation on simultaneously recorded sIPSCs and sEPSCs. Recordings were obtained from principal neurons in the presence of α -conotoxin Au1B (1 μ M), DH β E (10 μ M), atropine sulfate (0.5 μ M), D-AP5 (50 μ M), SCH50911 (10 μ M), and LY 3414953 (3 μ M), at a holding potential of -58 mV and internal chloride concentration of 1 mM. *A*: Bath application of choline chloride (5 mM) induced a transient increase in the frequency and amplitude of both sIPSCs (outward currents) and sEPSCs (inward currents), but the increase in sIPSCs was more pronounced. *B*: Another example of the effects of choline chloride (5 mM) on sIPSCs and sEPSCs. The increase in sEPSCs is more apparent in this cell compared to the cell in *A*. *C*: Group data (mean \pm SE) showing the effects of 5 mM choline chloride on sIPSCs (*left*) and sEPSCs (*right*). Application of choline significantly increased the mean charge transferred by sIPSCs and sEPSCs ($n = 9$, $**P < 0.01$), measured during the 5 sec period after the initiation of the effect. During this 5 sec period, the charge transferred by sIPSCs was significantly larger than the charge transferred by sEPSCs ($n = 9$, $**P < 0.01$). *D*: Lower concentrations of choline produced a similar effect; an example is shown where 500 μ M choline chloride was bath applied..... 158

Figure 24 Activation of α_7 -nAChRs reduces evoked field potentials in the BLA. *A*: An example of field potentials evoked in the BLA by stimulation of the external capsule, before, during, and after wash out of choline chloride (20 mM). Each trace is an average of 10 sweeps. *B*: Same field potentials as in *A*, in control medium and in the presence of choline, superimposed for a clearer view of the effect of choline. *C*: Group data from 8 slices showing the amplitude of the field responses as percentages of the control responses before, during, and after bath application of choline ($n = 8$; $***P < 0.001$). 160

Figure 25 Blockade of α_7 -nAChRs in the basal state decreases the frequency of sIPSCs. *A*: An example from a principal cell displaying high inhibitory synaptic activity in control medium, and the effect of α -BgTx (1 μ M) on sIPSCs ($V_h = +30$ mV); the reduction of the sIPSCs by α -BgTx was irreversible. The slice medium contains α -conotoxin Au1B (1 μ M), DH β E (10 μ M), atropine sulfate (0.5 μ M),

CNQX (20 μ M), D-AP5 (50 μ M), SCH50911 (10 μ M), and LY 3414953 (3 μ M). *B*: Group data showing the effect of α -BgTx on the frequency of sIPSCs (n = 4, ***P* < 0.01). *C*: An example from another principal cell where sIPSCs and sEPSCs were recorded simultaneously (V_h = -58 mV, internal chloride concentration is 1 mM). The reduction of the sIPSCs by α -BgTx (1 μ M) was more pronounced than the reduction of sEPSCs. The slice medium contains α -conotoxin Au1B (1 μ M), DH β E (10 μ M), atropine sulfate (0.5 μ M), D-AP5 (50 μ M), SCH50911 (10 μ M), and LY 3414953 (3 μ M). *D*: Group data showing the effect of α -BgTx on the frequency of sIPSCs (n = 4, **P* < 0.05) and sEPSCs (n = 4, *P* > 0.05). 162

CHAPTER 1: Introduction

The most recent use of chemical nerve agents occurred on 21 August 2013, killing 1,429 Syrians including 426 children. Thousands of the survivors have been left to deal with the health consequences of the exposure, including the development of anxiety disorders. This highlights the importance of developing effective countermeasures that protect against the long-lasting neuropsychiatric deficits that result from nerve agent exposure (72). Nerve agents act by irreversibly inhibiting acetylcholinesterase (AChE), which leads to an accumulation of acetylcholine (ACh) at the cholinergic synapse, inducing convulsive activity. If pharmacological intervention is not immediately administered to inhibit seizure activity, cholinergic receptor hyperstimulation gives way to glutamatergic receptor hyperactivity, which sustains and reinforces seizures (status epilepticus; SE) (177).

Exposure to a nerve agent causes severe neuronal loss and long lasting behavioral abnormalities, including the development of anxiety disorders. The basolateral amygdala (BLA) — a temporal lobe brain region centrally involved in seizure generation and anxiety disorders (20) — is severely damaged after a nerve agent exposure; damage leads to BLA hyperactivity, which is often associated with anxiety disorders. However, the mechanisms underlying the progression from nerve agent exposure to BLA hyperexcitability and the development of anxiety disorders have not yet been evaluated. Identifying the mechanisms underlying the alterations that lead to anxiety disorders is essential for well-tolerated and efficacious treatment interventions to be developed to prevent or minimize long-term neuropsychiatric deficits that are often observed after nerve agent exposure.

PHYSICAL AND CHEMICAL PROPERTIES OF NERVE AGENTS

Nerve agents are extremely toxic relatives of organophosphate insecticides (203). The G-series of nerve agents (tabun [GA], sarin [GB], soman [GD], and cyclosarin [GF]) were invented in Nazi Germany, but were never used in battle during World War II; tabun and sarin have been used in more recent conflicts, including the Iran-Iraq war (202), the Aum Shinrikyo terrorist attacks in Matsumoto and Tokyo (271; 278), and most recently in the 2013 Syrian conflict (72; 276). Nerve agents remain a major threat to both military and civilians because of the relative ease with which to produce, transport, and deploy agents (19). Moreover, because pharmacological intervention does not protect against the long-term effects of nerve agent exposure (72), their use on civilians can have lasting neurological and psychological effects. It is therefore essential that their mechanism of action and the pathophysiological deficits that arise after exposure are well understood so that effective countermeasures may be developed to prevent or reduce the deficits that occur after exposure to a nerve agent.

Nerve agents are organic esters of phosphoric acid derivatives similar to the organophosphorus pesticides (109). Nerve agents have a central phosphorus atom bonded to three heteroatoms, where R^{1-2} are hydrogen, alkyl (including cyclic), aryl, alkoxy, alkylthio and amino groups (26), and R^3 is a dissociable group (e.g., halogens, cyano, alkylthio group, or inorganic or organic acid) (26) (Figure 1). Their toxicity generally is determined depending on specific conditions including species, sex, age, genetic disposition, body weight, diet, hormonal factors, etc. (26). The physical characteristics of the G-agents are summarized in Table 1. Nerve agents show a volatility that increases with temperature; sarin is the most volatile of the G-agents (276). However, soman is

most persistent; that is, soman has the greatest ability to remain active in the environment after deployment (289).

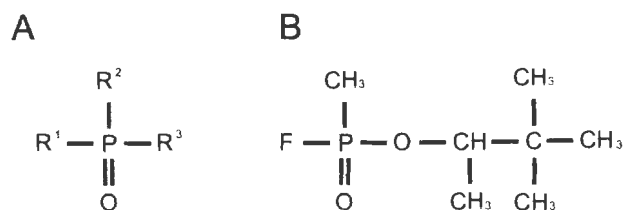


Figure 1 Structural formula of organophosphorus agents. (A) General formula of an organophosphate where R¹⁻² are hydrogen, alkyl (including cyclic), aryl, alkoxy, alkylthio, and amino groups, and R³ is a dissociable group. (B) Structural formula of soman (pinacolyl methylphosphonate). Modified from (26).

Table 1 Chemical Properties of Nerve Agents

	Sarin (GB)	Soman (GD)	Tabun (GA)	Cyclosarin (GF)
Boiling point (°C)	147	167-200	240	239
Melting point (°C)	-57	-42	-50	-30
Vapor Pressure (mmHg at 25°C)	2.9	0.4	0.057	0.068
Volatility (mg/m³ at 25°C)	22,000	3,900	490	581
Vapor LC₅₀ (ppm)	1.2-0.6	0.9-0.5	2.0-1.0	0.5
Liquid LD₅₀ Skin g/70 kg man	1.7	0.35	1	0.35
Persistency	2-24 hours at 5-25°C	Relatively Persistent	T1/2 = 24-36 hours	Unknown
Ageing half-time for human	~3-5 hours	~2-6 min	~13.3>14 hours	~7.5-40 hours

Note: Adapted from (259; 276; 289)

CHOLINERGIC SYNAPTIC TRANSMISSION

To understand nerve agents' mechanism of action and subsequent pathological and pathophysiological alterations that occur after nerve agent exposure, cholinergic synaptic transmission must first be explained. Choline-acetyltransferase (ChAT) catalyzes the synthesis of ACh from choline and acetyl-coenzyme A in cholinergic synapses in the peripheral (PNS) and central nervous system (CNS). ACh is packaged into synaptic vesicles via a vesicular ACh transporter (vAChT) and released upon

stimulation (267) (Figure 2). ACh acts at muscarinic (mAChRs) and nicotinic acetylcholine receptors (nAChRs). Activation of $M_{1,3,5}$ -mAChRs, in turn, activate secondary messenger processes that result in depolarization of the postsynaptic neuron, whereas activation of $M_{2,4}$ -mAChRs activate secondary messenger processes that hyperpolarize the postsynaptic neuron (42; 76). Release of ACh also activates nAChRs. Brain nAChRs are pentameric receptors composed of 5 subunits (α_2 - α_{10} , β_1 - β_4) (7); nAChRs containing the homomeric α_7 and heteromeric $\alpha_4\beta_2$ are the two major subtypes found in the brain. The α_7 homomeric pentamer binds to α -bungarotoxin (α -BgTx) with high affinity, is calcium permeable (95), and is rapidly desensitized (8; 283), whereas the heteromeric $\alpha_4\beta_2$ (configured in a $2\alpha_3\beta$ stoichiometry) subtype has a high affinity binding for nicotine and slowly desensitizes (7). In the BLA, the α_7 -nAChRs are expressed on both glutamatergic neurons and GABAergic interneurons, but predominantly enhance inhibitory synaptic transmission (141; 225).

NERVE AGENT MECHANISM OF ACTION

AChE, which is synthesized in the endoplasmic reticulum and transported along the motor axon via anterograde transport (137), rapidly hydrolyzes ACh, effectively reducing its concentration in the synapse. AChE is a glycoprotein that consists of six main forms (G1, G2, G4, A4, A8, A12) (137); G4 is primarily found in the brain, with a lesser extent being G1 (137). AChE molecules have two active sites, known as the anionic and esteratic sites. The anionic site positions ACh in the active site through an electrostatic interaction with the quaternary nitrogen in choline (289), whereas the hydroxyl group of the serine residue in the esteratic site covalently binds to the ester carbonyl group forming an unstable tetrahedral intermediate that rapidly decomposes,

liberating choline and leaving the enzyme covalently bound to acetate (289). The acyl enzyme then undergoes hydrolysis, releasing acetic acid and regenerating the free enzyme.

AChE is rapidly and irreversibly inhibited when nerve agents bind to the serine hydroxyl residue at the esteratic site of the AChE molecule, forming a phosphonate ester (28; 190; 263), subsequently blocking the hydrolysis of ACh. With the loss of one of the R groups (Figure 1A), a conformational change ensues, resulting in the formation of a stable and permanent bond that is resistant to spontaneous hydrolysis and reactivation by oximes (167; 289). When the bond is strengthened, the enzyme-nerve agent complex is said to have aged. The aging time varies greatly between the different nerve agents (Table 1); the aging half time, or time for half of involved cholinesterase to age (289), ranges from approximately 2 min for soman to up to 40 hours for cyclosarin (259; 276; 289). Because soman ages AChE most rapidly, symptoms of intoxication will appear rapidly, severely limiting the therapeutic window; for this reason soman is the nerve agent used in the experiments performed in this dissertation.

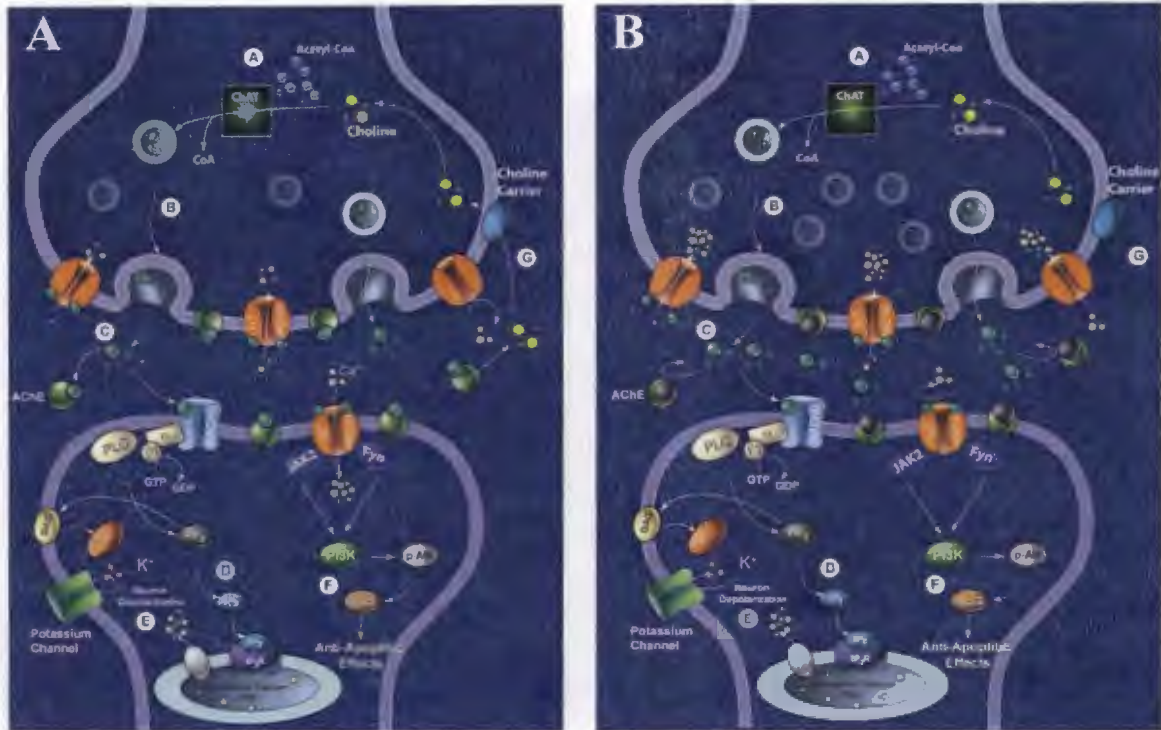


Figure 2 Cholinergic synaptic transmission under basal conditions and in the presence of a nerve agent. (A) In the presynaptic terminal choline-acetyltransferase (ChAT) catalyzes the synthesis of acetylcholine (ACh) from choline and acetyl-coenzyme A (a). ACh is packaged in synaptic vesicles via a vesicular ACh transporter (vAChT) (b). ACh is released into the synaptic cleft (c) where it will bind to muscarinic acetylcholine receptors (mAChRs), leading to the activation of second messengers (d) that either increase intracellular calcium concentrations or inhibit activation of potassium channels (e). In addition, activation of post-synaptic α_7 -nAChRs increase calcium influx and activates second messengers that influence anti-apoptotic mechanisms (3) (f), whereas activation of presynaptic α_7 -nAChRs regulates ACh release via a feedback response. ACh is hydrolyzed in the synaptic cleft by AChE. Liberated choline is taken back up by a high affinity choline-uptake mechanism (267) where it will be resynthesized into ACh (g). (B) A nerve agent, such as soman, binds to and irreversibly inhibits AChE activity (black circles). While initially the synthesis and packaging of ACh is similar to basal conditions (a, b) AChE inhibition will cause ACh to accumulate at cholinergic synapses (c). Accumulation of ACh will increase activation of mAChRs, subsequently, increasing postsynaptic depolarization (d, e). α_7 -nAChRs, which are present on GABAergic interneurons in the BLA and act to increase inhibitory synaptic transmission will desensitize. The combined effects initiate SE activity, but subsequently give way to glutamatergic hyperactivity, which sustains and reinforces seizures, causing neuropathology and subsequent neurodegeneration via pro-apoptotic effects (f).

SYMPTOMS OF NERVE AGENT EXPOSURE

Acute symptoms of nerve agent intoxication arise from hyperactivation of mAChRs and nAChRs in the CNS and PNS. ACh receptors are defined by their affinities for nicotine and muscarine, are present in different anatomic locations, and utilize different signal transduction mechanisms. Muscarinic receptors, for example, exert their effects through G-proteins and are found in the CNS, at postganglionic parasympathetic nerve endings, and in postganglionic sympathetic receptors (289), whereas nicotinic receptors are present in the CNS, both sympathetic and parasympathetic autonomic ganglia, and at the neuromuscular junction (289). Hyperactivation of peripheral mAChRs after nerve agent exposure causes salivation, lacrimation, urination and defecation, diaphoresis, gastric emesis, excessive secretion of nasal mucosa (rhinorrhea), miosis, failure of accommodation (ciliary muscle paralysis), and abdominal cramps (26; 289). As symptoms progress, bronchorrhea, bronchoconstriction, and bradycardia manifest. Peripheral nicotinic symptoms include pallor, tachycardia, hypertension, muscle weakness, fasciculations, convulsions, and paralysis (skeletal muscles including diaphragm and intercostal muscles) (26). In the CNS, muscarinic and nicotinic symptoms include anxiety, restlessness, headache, confusion, tremor, convulsions, and respiratory depression (26; 289). Death may result from a failure of heart and ventilation functions.

Nerve Agent Induced Seizures

Without immediate treatment to arrest the toxic effects of nerve agents, a common symptom is the development of seizures. Seizures were common, for example, in a small percentage of moderately to severely poisoned patients from the sarin attack in the Tokyo subway (207; 210) and were reported in victims of the Syrian nerve agent attack. While

seizures are not the primary cause of death in an individual after nerve agent exposure, prolonged seizure activity causes severe neuropathology (174), which may lead to long lasting behavioral deficits.

The initiation of seizures after nerve agent exposure is due to hyperstimulation of cholinergic receptors. While evidence indicates that nAChRs are not implicated in seizure generation and, in fact, have been found to be relatively ineffective in antagonizing seizures (62), hyperactivation of M₁-mAChRs activate second messenger processes that increase intracellular calcium concentrations, effectively depolarizing neurons (42) and generating seizures. Evidence in support of this view include: 1) administration of 240 mg/kg pilocarpine, a potent mAChR agonist, induces seizures resembling 1.6-2.0 x LD₅₀ soman exposure (274); 2) administration of VU0225035, a selective M₁-mAChR antagonist, reduces pilocarpine-induced seizures (251); 3) administration of the M₁-mAChR antagonist, methoctramine, abolished carbachol-induced seizures (62).

If treatment is not immediately administered to mitigate seizure activity, cholinergic hyperactivation gives way to glutamatergic hyperstimulation, which sustains and reinforces seizures (177). This transition occurs when activation of M₁-mAChRs increase neuronal depolarization and subsequently enhance the frequency and amplitude of spontaneous excitatory postsynaptic currents (sEPSCs) (144). Support that a transition from cholinergic receptor hyperstimulation to glutamatergic receptor hyperactivation has been documented biochemically and pharmacologically. For example, after nerve agent exposure, ACh returns to baseline concentrations within 50 min in septohippocampal areas and within 90 min in the amygdala (145), whereas extracellular glutamate concentrations have been found to rise within minutes of exposure and remain elevated at

least 90 minutes after SE onset in multiple brain regions (146; 147; 177).

Pharmacological evidence confirms that the cholinergic system is responsible for initiating but not sustaining seizures; administration of an anti-cholinergic drug (e.g., scopolamine, atropine, benactyzine, or trihexyphenidyl) within 5 min of SE onset terminates seizure activity, whereas delaying treatment up to 20 min after exposure increases the concentration of drug needed to terminate seizures. Delaying treatment up to 40 min renders cholinergic antagonists ineffective in terminating seizures (176).

Alternatively, the GABA_A receptor agonist, diazepam, and the NMDA receptor antagonist, MK-801, exerted powerful anticonvulsant effects against soman-induced seizures, even when given up to 20 min after exposure (176), indicating that the initial phases of nerve agent-induced seizures are modulated by mAChR activation, whereas glutamatergic receptors are recruited and sustain seizures after a period of time (176). However, benzodiazepines such as diazepam lose anticonvulsant effectiveness if there is a delay between seizure onset and treatment (179).

Controlling and eliminating seizures is essential to protect against neuropathology and subsequent behavioral and neurological disorders. Military personnel are deployed with autoinjectors, which contain an oxime (e.g., pralidoxime or HI-6) and atropine (mAChR antagonist). Immediate administration of the autoinjectors will prevent the deleterious effects of ACh binding to mAChRs, but atropine must be re-administered every 5-10 min when an adult is severely poisoned (203; 259). In the event of a civilian attack, however, such as in Japan and more recently Syria, it may take at least 30 min for emergency personnel to access individuals exposed to a nerve agent (196; 296). As time elapses after the initial exposure, neuropathology will develop; there is a strong positive

correlation between seizure duration and neuropathology after soman nerve agent exposure (174). It is therefore essential that treatments be rapidly administered after exposure to a nerve agent to prevent the ensuing neuropathology.

ACUTE AND LONG TERM NEUROPATHOLOGY AFTER NERVE AGENT EXPOSURE

Prior to the nerve agent attack in Syria, the last known use of nerve agents occurred in Japan; evidence of long term neuropsychiatric deficits have been amassed from victims of the Tokyo Subway and Matsumoto terrorist attacks. One to three years after those attacks, individuals reported, among other symptoms, a chronic decline in memory function (199; 205). Five years after the attacks individuals showed continued ocular and cognitive symptoms (134) and significant decreases in regional gray matter volume in the right insular, right temporal cortices, and left hippocampal region (295). In addition, a significant decrease in amygdalar gray matter volume was observed in victims of the Tokyo subway sarin attack, of whom many reported symptoms of posttraumatic stress disorder (PTSD) (243). Similarly, neurological follow-up surveys monitored between 5 and 7 years after the Tokyo attack showed that the main neurological symptoms were neuropsychiatric disorders, including PTSD (124; 209).

While accumulated data regarding the neuropathological alterations that occur after nerve agent exposure in humans is sparse, animal models are often used to evaluate the acute and long lasting neuropathological deficits that occur in the brain after exposure to a nerve agent such as soman. The amount of damage in the brain correlates with the duration of the seizure (174; 255). If seizures are terminated within 20 minutes of onset, only approximately 10% of animals developed neuropathology; however, approximately 98% of animals display severe neuropathology if seizures are not terminated (174).

Neuronal loss occurring within the first 24 hours of nerve agent induced seizures is primarily caused by a process known as necrosis (114; 177); necrosis typically occurs when excessive glutamate is released into the synaptic cleft, which in turn activates NMDA receptors and triggers calcium influx. The intracellular calcium then activates intracellular proteases, neuronal nitric oxide synthase, and generates free radicals, damaging the cell membrane, structural proteins, and enzymes essential for cell survival (96). Neuronal loss within the first 24 hours of nerve agent induced seizures has been documented in many brain regions including the fibers of fornix, cortico-fugal projections to the thalamus, spinal cord, optic tract, lateral geniculate bodies, pre-tectal area, superior colliculus, substantia nigra, and temporal lobe regions including hippocampal formation, amygdala, and piriform cortices (68; 222). However, the most severe damage in rats has been found in the amygdala, piriform cortex, and hippocampus (53; 68; 90).

In addition to the loss of neurons immediately after nerve agent exposure, cells continue to undergo neurodegeneration via mechanisms of secondary necrosis (69; 93) and apoptosis. Secondary necrosis, which has been found to contribute to ongoing neuronal loss up to 14 days after SE (93), involves the early release of cytochrome c into the cytoplasm, the subsequent activation of caspase-9 and caspase-3, but does not require an upregulation of immediate early genes (71; 204). Apoptosis, on the other hand, is triggered by the activation of glutamate receptors that increase calcium influx; the result is the activation of harmful metabolic cascades, including lipases, proteases, kinases, phosphatases, and endonucleases (261), which deprive the cell of enzymes or trophic factors essential for survival (53; 171; 261), causing fragmentation of nuclear DNA, cell

shrinkage, chromatin degradation, mitochondrial breakdown, and cell death (53; 261). Secondary neuronal loss (i.e., neurodegeneration) is prominent in brain regions including the piriform cortex, hippocampus, amygdala, thalamus and cortex after nerve agent exposure (53). Although neurodegeneration appears to be severe in multiple brain regions, the frequency of damage in the amygdala is more severe than most other brain regions (90; 174). Eventually, however, these degenerating neurons die due to delayed toxicity (57; 60). The result may be long lasting behavioral and neurological deficits (57; 91).

THE AMYGDALA AND LONG-LASTING BEHAVIORAL DEFICITS ASSOCIATED WITH AMYGDALAR HYPERACTIVATION AFTER SOMAN INDUCED STATUS EPILEPTICUS

Over a decade after the sarin attack in Japan, many victims reported ongoing symptoms associated with PTSD (124; 209). The loss of gray matter volume may lead to hyperactivity within a structure that plays a central role in anxiety disorders, the amygdala. The amygdala modulates emotional processing by assigning emotional significance to external stimuli to produce the appropriate behavioral responses (154; 245). Amygdala activation is also implicated in fear conditioning (34); trauma to the amygdala plays a key role in anxiety disorders (67; 82; 102; 152) and the generation of seizures (20; 230). To understand why the amygdala plays a key role in fear and anxiety, its anatomy and physiology must be briefly described.

The Amygdala's Anatomy and Physiology

The amygdala is comprised of approximately 13 nuclei divided into three groups: 1) the basolateral (complex) group, which consists of the lateral nucleus, basal nucleus, and accessory basal nucleus; 2) the cortical-like group, which consists of cortical nuclei

and the nuclei of the lateral olfactory tract; and 3) centromedial group, which consists of the medial and central nuclei (245). The basolateral nuclei (BLA), the complex that is the center of this dissertation, receives afferent stimuli (e.g., sensory information from all modalities) from cortical areas (166), including the anterior cingulate, insular, orbitofrontal cortices, and basal forebrain (183; 212), and subcortical brain areas, including the thalamus and hypothalamus (245), among other regions. Although the BLA has reciprocal projections with many cortical areas, the major efferent pathway is to the central nucleus of the amygdala (217). The BLA also projects to the medial temporal lobe memory system with afferents to hippocampus, nucleus accumbens, perirhinal cortex, but also to the prefrontal cortex and thalamus (245). The central amygdala sends robust projections to hypothalamic, pontine, and medullary regions, as well as the brainstem and basal forebrain structure (166; 215), modulating autonomic responses. Via the robust projections to neuromodulatory cell groups of the brainstem and basal forebrain as well as to regions associated with memory, the amygdala can not only directly influence major cell groups, but it can also influence excitability in brain regions to which it is not directly connected (215).

A defining feature of the amygdala is its ability to regulate its intrinsic excitability. The amygdala is comprised of pyramidal (glutamatergic) neurons and GABAergic interneurons. Pyramidal neurons constitute the majority of the neurons in the BLA (80-85%), whereas GABAergic interneurons form approximately 15-20% of the neuronal population (245; 268) and express parvalbumin or calbindin and/or calretinin in their cytosol (136). GABAergic interneuronal excitability is regulated by excitatory inputs from cortical and thalamic glutamatergic neurons that converge onto GABAergic

interneurons in the BLA (162; 163; 217) to regulate their activity. In addition, feed-forward and feedback inhibition from local circuit interneurons in the BLA are also present to regulate their excitability (149; 268; 293). Evidence also indicates that GABAergic interneuronal excitability is regulated by a number of different systems, including the dopaminergic (208), serotonergic (238), and cholinergic system (193). One mechanism recently found to powerfully modulate GABAergic inhibition, but also mitigate anxiety-like behavior, is activation of α_7 -containing nicotinic acetylcholine receptors (α -nAChRs) (88; 225; see also Appendix 1). Thus, although GABAergic interneurons only comprise a fraction of the total cell population, they have a powerful ability to regulate BLA excitability and the expression of anxiety (148; 163; 216; 293).

Amygdala-Dependent Behavioral Deficits After Nerve Agent Exposure

More than a decade after the 1994 terrorist attack in Matsumoto, 73% of exposed individuals reported psychological problems (296). Similarly, a decade after the Tokyo attack, victims reported ongoing neuropsychiatric disturbances, including irritability and restlessness, avoidance of places that triggered recollection of the trauma, tension, and insomnia (209; 296), all symptoms of PTSD. Sarin exposed individuals suffering from PTSD also had significantly smaller mean bilateral amygdala volumes than those that did not develop PTSD (243). However, individuals with PTSD (not exposed to nerve agents) also have greater amygdala activation (262). Although reduced amygdala volume in conjunction with increased amygdala activity may seem inconsistent, numerous studies of related disorders have shown increased activation in brain regions with reduced volume (45; 253). Similarly, animal models have also demonstrated that anxiety- or fear-

like behavior is associated with reduced amygdala volume (297) and increased activity (67).

After nerve agent exposure, animals display reduced amygdalar volume (50; 107) and increased anxiety- and fear-like behavior (61; 91; 150; 187; 231). Both lethal or sublethal doses of soman cause greater anxiety-like behavior 30 to 90 days after exposure (61; 165) compared to respective controls. Similarly, although auditory fear conditioning, which is primarily amygdala dependent, was impaired up to 10 days after soman exposure, animals display greater freezing behavior in response to a conditioned tone 30 days after exposure (58; 187) and elevated startle response even after convulsions were pharmacologically terminated (150). These results indicate that long-lasting increases in anxiety- and fear-like behaviors are present after exposure to a nerve agent.

CONCLUSIONS

Both animal and human studies have revealed that exposure to nerve agents cause severe neuropathology within the BLA and persistent increases in anxiety disorders or anxiety-like behaviors. This demonstrates a real health consequence in survivors of a nerve agent attack. The latest nerve agent attack in Syria left thousands of civilians susceptible to the development of neurological and neuropsychiatric illnesses. To help mitigate the symptoms associated with these disorders, it is essential to develop new and efficacious treatments. However for treatments to be successful, the mechanisms underlying the development of anxiety after nerve agent exposure must be uncovered. Therefore, the purpose of this dissertation is to identify the underlying pathological and pathophysiological alterations that lead to long-lasting increases in anxiety-like behavior.

SPECIFIC AIMS

The recent sarin attack in Syria killed 1,429 people, including 426 children, and left countless more to deal with the health consequences of the exposure. Prior to the Syrian chemical assault, the nerve agent attacks in Japan left many victims suffering from neuropsychiatric illnesses, particularly anxiety disorders. The biological mechanisms underlying the development of anxiety after nerve agent exposure are not known; uncovering these mechanisms is necessary for successful treatment. Nerve agents rapidly and irreversibly inhibit acetylcholinesterase (AChE), causing an accumulation of acetylcholine (ACh) at the cholinergic synapse; hyperstimulation of cholinergic receptors raises the excitation level to the point of seizure generation, initiating seizure activity. If treatment is not immediately administered, cholinergic receptor hyperstimulation gives way to excessive activation of the glutamatergic system, sustaining and intensifying seizure activity (status epilepticus, SE), causing profound brain damage and long-term behavioral impairments. For treatments to be successful, it is essential to define the brain regions associated with the generation of seizures as well as the underlying pathophysiological alterations that follow nerve agent exposure that lead to long-lasting neuropsychiatric deficits.

The **long-term goal** of the proposed research is to develop effective and well-tolerated pharmacological strategies for ameliorating seizure activity immediately after soman intoxication. The immediate goal of this research is to identify the cellular and molecular mechanisms underlying the development of epileptiform activity after soman exposure and the subsequent increases in anxiety-like behavior. The **central hypotheses** are: 1) that inhibition of AChE in the basolateral amygdala (BLA) is necessary for the generation of nerve agent induced seizures; and 2) the pathophysiological alterations

underlying increases in anxiety-like behavior result from impairments in GABAergic synaptic transmission and impaired synaptic plasticity. Our specific aims are:

Specific Aim 1: To determine whether AChE must be sufficiently inhibited in the BLA for the generation of soman-induced seizures and examine the recovery of AChE in temporal lobe brain regions after soman exposure.

No study has conclusively identified whether AChE inhibition in the BLA is required for the generation of seizures after nerve agent exposure. Understanding where seizures are generated and how AChE activity recovers after nerve agent intoxication is imperative for developing treatment options towards ameliorating toxic symptoms after nerve agent exposure. We hypothesize that AChE inhibition in the BLA leads to the generation of seizures after soman exposure, but also hypothesize that AChE will recover and return to baseline values. To accomplish this aim, we will use spectrophotometry to establish a time course for the recovery of AChE activity.

Specific Aim 2: To identify the progression of neuropathological and pathophysiological alterations in the BLA after soman exposure and its association with anxiety-like behavior.

To identify the underlying mechanisms responsible for increased neuropsychiatric deficits, it is essential to examine the pathological and pathophysiological alterations that occur in the BLA. We hypothesize that soman exposure will cause severe neuronal and interneuronal loss in the BLA. The neuropathology will lead to alterations in BLA excitability, mechanisms responsible for learning and memory (e.g., long term potentiation of synaptic transmission), and subsequently lead to increases in anxiety-like behavior. To accomplish this aim, we will use immunohistochemistry and stereology to determine the loss of GABAergic interneurons and principal neurons. In addition, we will use extracellular field potentials to identify alterations to network excitability and

mechanisms associated with learning and memory. Finally, we will correlate these alterations with increases in anxiety-like behavior, as determined by the open field and acoustic startle response tests.

Specific Aim 3: To identify alterations in GABA_A receptor mediated inhibitory synaptic transmission in the rat BLA after exposure to soman.

Indirect evidence suggests that GABAergic inhibition is impaired after nerve agent exposure. However, no study, to date, has directly examined whether GABAergic transmission and mechanisms that modulate GABAergic inhibition are altered after soman exposure. We hypothesize that soman exposure severely damages the GABAergic inhibitory system. In addition, we will examine whether soman exposure alters the function of α_7 -nAChRs, which has previously been found to powerfully modulate GABAergic inhibition in the BLA and mitigate anxiety-like behavior. To accomplish this aim we will use whole-cell patch clamp to examine the long-term alterations in GABAergic synaptic transmission and alterations to α_7 -nAChR mediated enhancement of inhibitory synaptic transmission.

Because victims of nerve agent attacks report ongoing neuropsychiatric deficits, including anxiety disorders, long after the initial attack, it is essential that safe and efficacious treatments are developed to mitigate these illnesses. To date, the mechanisms underlying the neuropsychiatric deficits are not known. However, our results will provide conclusive evidence that the BLA plays a central role in seizure generation after nerve agent intoxication. In addition, our results will demonstrate that pathological and pathophysiological alterations to the BLA will lead to reduced inhibition, increased excitation, and subsequently, long-lasting increases in anxiety-like behavior. Establishing

the mechanisms underlying the progression of alterations that occur after nerve agent exposure will provide for novel treatments to reduce or mitigate these alterations and improve therapeutic outcome for those exposed to a nerve agent.

Chapter 2: Acetylcholinesterase Inhibition in the Basolateral Amygdala Plays a Key role in the Induction of Status Epilepticus After Soman Exposure

Eric M. Prager^{1,3}, Vassiliki Aroniadou-Anderjaska^{1,2,3}, Camila P. Almeida-Suhett^{1,3},
Taiza H. Figueiredo¹, James P. Apland⁴, Maria F.M. Braga^{1,2,3*}

¹Department of Anatomy, Physiology, and Genetics

² Department of Psychiatry

³ Program in Neuroscience

Uniformed Services University of the Health Sciences

4301 Jones Bridge Road

Bethesda, MD 20814, USA

⁴Neurotoxicology Branch

United States Army Medical Research Institute of Chemical Defense

Aberdeen Proving Ground, MD 21010, USA

*Corresponding Author:

Maria F.M. Braga, D.D.S., Ph.D.

Department of Anatomy, Physiology, and Genetics

Uniformed Services University of the Health Sciences

4301 Jones Bridge Road

Bethesda, MD 20814

Phone: (301) 295-3524

Fax: (301) 295-3566

Email: maria.braga@usuhs.edu

ABSTRACT

Exposure to nerve agents induces intense seizures (status epilepticus, SE), which cause brain damage or death. Identification of the brain regions that are critical for seizure initiation after nerve agent exposure, along with knowledge of the physiology of these regions, can facilitate the development of pretreatments and treatments that will successfully prevent or limit the development of seizures and brain damage. It is well-established that seizure initiation is due to excessive cholinergic activity triggered by the nerve agent-induced irreversible inhibition of acetylcholinesterase (AChE). Therefore, the reason that when animals are exposed to lethal doses of a nerve agent, a small proportion of these animals do not develop seizures, may have to do with failure of the nerve agent to inhibit AChE in brain areas that play a key role in seizure initiation and propagation. In the present study, we compared AChE activity in the basolateral amygdala (BLA), hippocampus, and piriform cortex of rats that developed SE (SE rats) after administration of the nerve agent soman (154 $\mu\text{g}/\text{kg}$) to AChE activity in these brain regions of rats that received the same dose of soman but did not develop SE (no-SE rats). The levels of AChE activity were measured at the onset of SE in SE rats, 30 min after soman administration in no-SE rats, as well as in controls, which received saline in place of soman. In the control group, AChE activity was significantly higher in the BLA compared to the hippocampus and piriform cortex. Compared to controls, AChE activity was dramatically lower in the hippocampus and the piriform cortex of both the SE rats and the no-SE rats, but AChE activity in the BLA was reduced only in the SE rats. Consistent with the notion that soman-induced neuropathology is due to intense seizures, rather than due to a direct neurotoxic effect of soman, no-SE rats did not present any neuronal loss or degeneration, 7 days after exposure. The results suggest that inhibition of

AChE activity in the BLA is necessary for the generation of seizures after nerve agent exposure, and provide strong support to the view that the amygdala is a key brain region for the induction of seizures by nerve agents.

Keywords: Acetylcholinesterase, Soman, Status Epilepticus, Basolateral Amygdala, Piriform Cortex, Hippocampus

INTRODUCTION

Organophosphorus nerve agents are among the most toxic of the chemical warfare agents. Their primary mechanism of action is the irreversible inhibition of acetylcholinesterase (AChE), which produces an accumulation of acetylcholine and overstimulation of cholinergic receptors; an important consequence is the initiation of brain seizures, which rapidly progress to status epilepticus (SE), causing profound brain damage or death (177).

Identifying which brain regions are primarily responsible for seizure initiation and propagation after exposure to a nerve agent, along with knowledge of the biochemistry and physiology of these regions, may facilitate the development of effective pharmacological treatments that will prevent or limit seizures and the associated brain damage during exposure. Previous studies have suggested that the amygdala, a seizure-prone limbic structure (20), plays a central role in the generation of seizures by nerve agents (19). Thus, the amygdala displays the earliest increase in extracellular glutamate after exposure to soman (147), generates ictal-like discharges after in vitro application of soman (15), and suffers very severe nerve agent-induced damage (17; 255). Moreover, microinjection of nerve agents into different brain regions can elicit convulsions only when the nerve agent is injected into the basolateral nucleus of the amygdala (BLA; (175). Others, however, have argued that brain regions other than the amygdala, including the piriform cortex and the hippocampus, are likely seizure initiators after nerve agent exposure (195).

When lethal doses of a nerve agent are administered to experimental animals, a small percentage of these animals do not develop SE. This could be due to failure of

soman to sufficiently inhibit AChE in brain regions that play a key role in seizure initiation. Therefore, to gain some insight into the involvement of different brain regions in seizure generation after nerve agent exposure, in the present study we compared the extent of AChE inhibition at the onset of SE in the brains of rats exposed to the nerve agent soman, to the AChE inhibition in rats that received the same dose of soman but did not develop SE. We found that in both groups, AChE was significantly inhibited in the piriform cortex and the hippocampus, but only in the group that developed SE was AChE inhibited also in the BLA.

MATERIALS AND METHODS

Animals

Male, Sprague-Dawley rats (Taconic Farms, Derwood, MD), weighing 150 to 200 gr, were individually housed in an environmentally controlled room (20-23°C, ~44% humidity, 12-h light/12-h dark cycle [350-400 lux], lights on at 6:00 am), with food (Harlan Teklad Global Diet 2018, 18% protein rodent diet; Harlan Laboratories; Indianapolis, IN) and water available *ad libitum*. Cages were cleaned weekly (232). All animal experiments were conducted according to the Guide for the Care and Use of Laboratory Animals (Institute of Laboratory Animal Resources, National Research Council) and were approved by the U.S. Army Medical Research Institute of Chemical Defense and the Uniformed Services University of the Health Sciences Institutional Animal Care and Use Committees.

Soman exposure

Soman (pinacoyl methylphosphonofluoridate; obtained from Edgewood Chemical Biological Center, Aberdeen Proving Ground, MD, USA) was diluted in cold saline and administered via a single subcutaneous injection (154 $\mu\text{g}/\text{kg}$). Following exposure to soman, rats were monitored for signs of seizure onset. Rats that developed SE were sacrificed at the onset of Stage 3 seizures (see (89), according to the Racine scale (236; 237). Stage 3 seizures manifest behaviorally as unilateral/bilateral forelimb clonus without rearing, straub tail, and extended body posture, and coincide with the initiation of electrographically monitored SE, as determined in the present study (see below) and in previous studies (90; 150; 244). When 1.4 x LD₅₀ of soman is administered to rats, SE starts within 5 to 15 min. We sacrificed the rats at the onset of SE, rather than at a particular time point after soman injection, in order to avoid inter-subject variability in the “time from the onset of SE”, but also because we were interested in the level of AChE activity at the point of time that SE starts. Occasionally, SE takes longer than 15 min to develop (up to 23 minutes, in our observations). Therefore, in order to be certain that the rats included in the no-SE group were not “on their way” to develop SE, we sacrificed those rats at 30 min after soman administration. Some animals from both groups were sacrificed seven days after soman intoxication to assess neuronal loss and degeneration. Rats that developed SE and were needed for neuropathology studies were administered an intramuscular injection of atropine sulfate (2 mg/kg) at 20 min after soman injection to increase survival rate and minimize peripheral toxic effects.

Electrode implantation for electroencephalographic (EEG) recordings

A group of rats was anesthetized with 1.5-2% isoflurane, using a gas anesthesia system (Kent Scientific, Torrington, CT). Five stainless steel, cortical screw electrodes were stereotaxically implanted using the following coordinates (after Paxinos and Watson, 2005): two frontal electrodes, 2.0 mm posterior from bregma and 2.5 mm lateral from the midline; two parietal electrodes, 5.0 mm posterior from bregma and 2.5 mm lateral from the midline; a cerebellar reference electrode was implanted 1.0 mm posterior to lambda (Figure 1C). Each screw electrode (Plastics One Inc., Roanoke, VA, USA) was placed in a plastic pedestal (Plastics One Inc.) and fixed to the skull with dental acrylic cement. For EEG recordings, the rats were placed in the EEG chamber, and connected to the EEG system (Stellate, Montreal, Canada; 200 Hz sampling rate). Video-EEG recordings were performed in the freely moving rats. Recordings were visually analyzed offline with filter settings at 0.3 Hz for the low frequency filter, 60 Hz for the notch filter, and 70 Hz for the high frequency filter, using the Harmonie Viewer 6.1e from Stellate (Montreal). EEG recordings started 30 min prior to soman administration. The appearance of large amplitude, repetitive discharges (>1 Hz with at least double the amplitude of the background activity) was considered to signify the initiation of SE, and coincided with Stage 3 behavioral seizures.

Acetylcholinesterase activity assay

Total AChE activity was measured using a previously established spectrophotometric protocol (77; 213). Briefly, rats were anesthetized with 3-5% isoflurane and rapidly decapitated. The brain was removed and placed in ice-cold phosphate buffer (0.1 M, pH 8.0). Coronal brain slices (500 μ m-thick) containing the

BLA (Bregma -2.28 mm to -3.72 mm), piriform cortex (Bregma -1.72 mm to -3.00 mm), and hippocampus (Bregma -2.28 mm to -4.68 mm) were cut with a vibratome (series 1000; Technical Products International, St. Louis, MO). The three structures were isolated by hand, and placed in an Eppendorf tube containing 1:20 Triton + phosphate buffer, homogenized for 10 s, and centrifuged at 14,000g for 5 min. The supernatant was removed and placed into a separate container. On the day of sampling, a glutathione curve was constructed by adding glutathione (1 – 10 μ L) to DTNB [5,5'-dithio-bis(2-nitrobenzoic acid)] (up to 200 μ L; (213)). Tissue supernatants (10 μ L per well) were added to either 10 μ L eserine (an all-purpose cholinesterase inhibitor that inhibits both butyrylcholinesterase and acetylcholinesterase) or ethoprozine (a specific butyrylcholinesterase inhibitor), all in the presence of acetylthiocholine (5 μ L) and 175 μ L DTNB (all purchased from Sigma-Aldrich, St. Louis; MO). Samples were read by the Softmax Pro 5.2 kinetics every 20 s for 4 min. The total butyrylcholinesterase inhibition was subtracted from the absorbance sample to provide a difference score, which was multiplied by the slope and intercept to provide a total concentration of AChE activity. AChE specific activity was calculated by dividing the total activity by the calculated protein concentration assayed by the Bradford method (see (38) using a protein assay dye reagent (Bio-Rad, Hercules, CA).

Neuropathology assessments

Fixation and tissue processing

Seven days after soman exposure rats were deeply anesthetized with pentobarbital (75-100 mg/kg, i.p.) and transcardially perfused with PBS (100 mL) followed by 4% paraformaldehyde (200 mL). Brains were removed and post-fixed in 4%

paraformaldehyde overnight at 4°C then transferred to a solution of 30% sucrose in PBS for 72 h, and frozen with dry ice before storage at -80°C until sectioning. Sectioning was performed as previously described (90). A 1-in-5 series of sections from the rostral extent of the amygdala to the caudal extent of the entorhinal cortex was cut at 40 μm on a sliding microtome (Leica Microsystems SM2000R). One series of sections was mounted on slides (Superfrost Plus, Daigger, Vernon Hills, IL) for Nissl staining with cresyl violet, while the adjacent series of sections were mounted on slides for Fluro-Jade-C (FJC) staining.

Stereological quantification

Design-based stereology (Kristiansen and Nyengaard, 2012) was performed as previously described (90) to quantify neuronal loss on Nissl-stained sections from the BLA and the CA1 hippocampal area along the rostrocaudal extent of the hippocampus. The BLA and CA1 regions were identified on slide-mounted sections under a 2.5x objective, based on the atlas of Paxinos and Watson (220). Sampling was performed under a 63x oil-immersion objective. Nissl-stained neurons were distinguished from glial cells by their larger size and pale nuclei surrounded by darkly-stained cytoplasm containing Nissl bodies. The total number of Nissl-stained neurons was estimated using the optical fractionator probe, and, along with the coefficient of error (CE), was calculated using the Stereo Investigator 9.0 (MicroBrightField, Williston, VT). The CE was calculated by the software according to Gundersen ($m = 1$; (108)) and Schmitz-Hof (2nd estimation; (247)) equations.

A 1-in-5 series of sections (~7 sections per rat) was analyzed for Nissl-stained neurons in the BLA. The counting frame was 35 x 35 μm , the counting grid was 190 x

190 μm , and the dissector height was 12 μm . Nuclei were counted when the cell body came into focus within the dissector, which was placed 2 μm below the section surface. An average of 242 neurons per rat were counted, and the average CE was 0.05 for both the Gundersen and Schmitz-Hof equations. A 1-in-10 series of sections (~8 sections per rat) was analyzed for Nissl-stained neurons in the CA1 region of the hippocampus. The counting frame was 20 x 20 μm , the counting grid was 250 x 250 μm , and the dissector was 10 μm . An average of 232.6 neurons per rat were counted, and the average CE was 0.05 for Gundersen ($m = 1$) and 0.06 for Schmitz-hof (2nd Estimation) equation. For both the BLA and CA1 regions, section thickness was measured at every counting site (averaging 18 μm and 19 μm for the BLA and CA1, respectively).

Fluoro-Jade C (FJC) staining

FJC (Histo-Chem, Jefferson, AR) was used to identify irreversibly degenerating neurons (248) in the amygdala, piriform cortex, entorhinal cortex, hippocampal subfields CA1, CA3, and hilus, as well as neocortex (between coordinates -1.72 and -6.60 from bregma, extending from the retrosplenial cortex to the entorhinal cortex in the medial to lateral direction, based on the atlas of Paxinos and Watson, 2005). Qualitative assessments were made from 6 brain sections per animal, 600 μm apart, and the average derived from 3 to 6 sections per brain structure was used. Mounted sections were treated as previously described (90) and stained in a 0.0001% solution of FJC dissolved in 0.1% acetic acid. Tracings from the Nissl-stained sections were superimposed on the FJC-stained sections using the Stereo Investigator 9.0 (MicroBrightField, Williston, VT). A previously established rating system was used to score the extent of neuronal degeneration in each structure and substructures: 0 = no damage; 1 = minimal damage (1-

10%); 2 = mild damage (11-25%); 3 = moderate damage (26-45%); and 4 = severe damage (>45%; (16; 90). We have shown previously that this qualitative scoring method produces results very similar to those derived from quantitative analysis (234).

Statistical analysis

Data analysis for the AChE activity assay was performed using either a repeated measures ANOVA and paired t-tests or a Welch F ANOVA with a Games-Howell post hoc. Welch F ANOVA was used due to the lack of homogeneity of variance; the source of variance was primarily from the no-SE group. Statistical differences in neuronal loss between the groups were determined using independent t-tests. All data are presented as mean \pm standard error. Statistical analyses were made using the software package PAWS SPSS 20 (IBM, Armonk, NY, USA). Differences were considered significant when $p < 0.05$. Sample size “n” refers to the number of animals.

RESULTS

Forty-six rats were implanted with electrodes for EEG recordings. After a two-week recovery, the rats were administered soman. Eleven of these rats did not display seizures, while the remaining 35 rats developed SE. Figure 1 shows an example of EEG activity at the onset of SE, in comparison to the EEG activity in a rat that did not develop seizures after soman injection. The electrode-implanted rats were not used for analysis of AChE activity or neuropathology evaluation, to avoid any confounding variable related to the surgery affecting the parameters studied.

Soman was also administered to 72 rats that were not implanted with EEG electrodes. Sixty of these rats displayed stage 3 seizures (which coincide with the initiation of SE; see Figure 3 and (90; 150; 244)) within 5 to 15 min after soman

exposure, while 12 rats did not progress above stage 1 (behavioral arrest) or stage 2 (oral/ facial movements, chewing, head nodding). For the present study, we used all 12 rats that did not develop SE (no-SE group), and we randomly selected another 12 rats from the group that developed SE (SE group); the remaining rats were used in different studies (16 of the 60 rats that developed SE died). Seven rats from the SE group were sacrificed at the onset of Stage 3 seizures (8.7 ± 1.2 min after soman injection) for measurements of AChE activity; the remaining 5 rats from this group were used for neuropathology studies, 7 days later. From the no-SE group, 7 rats were sacrificed at 30 min after soman exposure, and 5 rats were used to study neuropathology. Rats injected with saline in place of soman were used for control measurements.

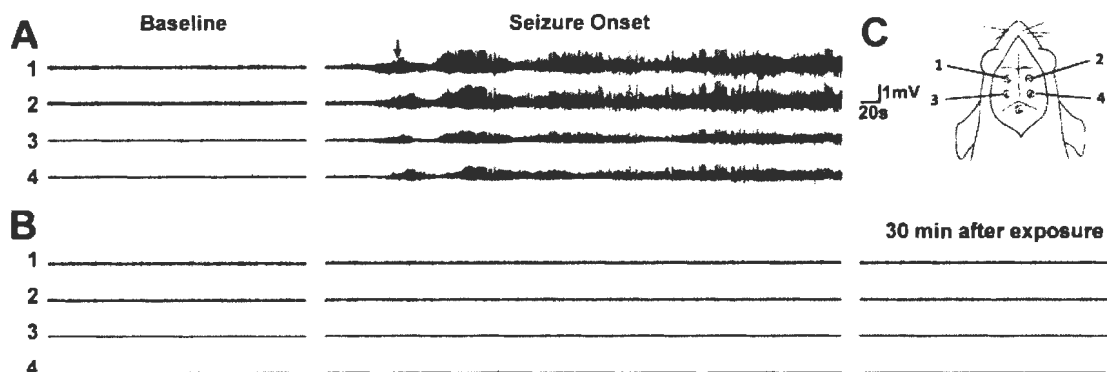


Figure 3 Comparison of EEG activity in two rats exposed to the same dose of soman (154 $\mu\text{g}/\text{kg}$). In rat (A), seizure activity appeared within 11 min after soman injection. The arrow points to the time point that the animal behavior was consistent with stage 3 seizures. In rat (B), there was no evidence of seizure activity in any of the 4 electrodes at the same time point as in (A), or 30 min after administration of soman. (C), Diagrammatic presentation of electrode placement. The numbers 1, 2, 3, 4 refer to the electrodes/sites from where electrical activity was sampled (1, left frontal; 2, right frontal; 3, left parietal; 4, right parietal; the reference electrode is in the cerebellum).

In the control group, AChE activity in the BLA was approximately 2- and 2.5-fold higher than the AChE activity in the piriform cortex ($p = 0.001$) and hippocampus ($p < 0.001$), respectively (Figure 4). In the SE group, AChE activity was significantly reduced in all three brain regions ($p < 0.001$); in the BLA, AChE activity was reduced by $95.2 \pm 7.0\%$ (68.8 ± 10.2 nmol/min/ng in the SE group versus 1451.1 ± 101.2 nmol/min/ng in the control group), in the piriform cortex by $99.6 \pm 10.9\%$ (2.8 ± 0.8 nmol/min/ng in the SE group versus 660.2 ± 71.7 nmol/min/ng in the controls), and in the hippocampus by $99.3 \pm 5.7\%$ (4.1 ± 0.3 nmol/min/ng in the SE group versus 590.6 ± 33.4 nmol/min/ng in the controls) (Figure 4). In the no-SE group, the variability in AChE activity was high. This is not surprising since some of the animals in this group showed no behavioral changes, while others displayed chewing behaviors, consistent with Stage 1 seizures on the Racine scale, or head nodding, consistent with Stage 2 seizures. This

variability in the behavioral responses was probably due to the variability in the extent of AChE inhibition by soman, which was reflected in our measurements. AChE activity in the piriform cortex (85.9 ± 42.7 nmol/min/ng) of the no-SE group was reduced by $87.0 \pm 12.6\%$ in comparison to the control group, and in the hippocampus (46.7 ± 30.7 nmol/min/ng) it was reduced by $92.1 \pm 7.7\%$ ($p < 0.001$ for both regions). However, in the BLA of the no-SE group, AChE activity (1140.3 ± 260.7 nmol/min/ng) was reduced by only $21.4 \pm 19.3\%$ compared to the control group ($p = 0.535$; Figure 4). When AChE activity was compared between the SE group and the no-SE group, there was no significant difference in the piriform cortex ($p = 0.206$) or the hippocampus ($p = 0.404$), while in the BLA, AChE was significantly lower in the SE group ($p = 0.015$).

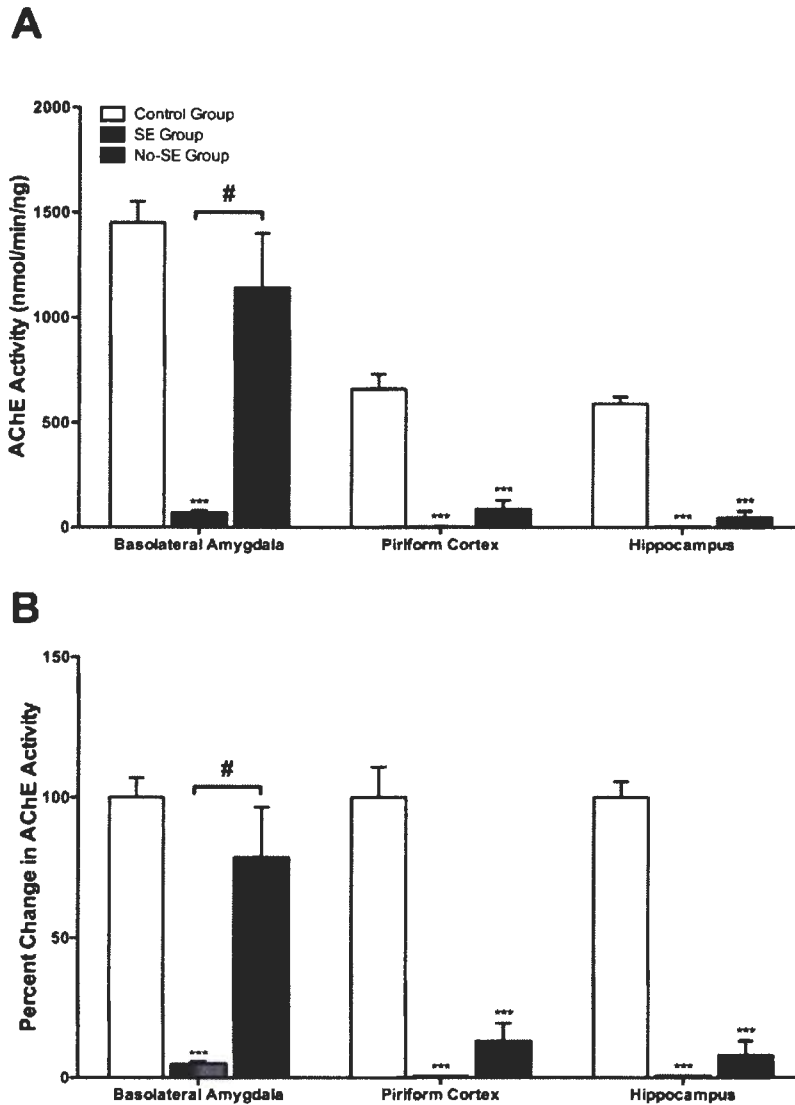


Figure 4 Reduction of brain AChE activity after exposure to soman. The “raw data” of AChE activity are shown in (A), while the data are expressed as percent of the control mean in (B). Soman-exposed rats that developed SE (SE group, $n = 7$) were sacrificed at the onset of Stage 3 seizures. These rats had significantly reduced AChE activity in all three regions examined, compared to controls ($n = 7$). Soman-exposed rats that did not develop SE (no-SE group, $n = 7$) were sacrificed at 30 min after soman exposure. These rats had significantly reduced AChE activity in the piriform cortex and hippocampus, but not in the BLA ($p = 0.535$). $***p < 0.001$ compared to the control group. $\#p < 0.05$ for the difference between the SE group and the no-SE group.

Seven days after soman administration, SE rats had significantly fewer neurons in the BLA ($77,122 \pm 1,417$) and CA1 ($348,986 \pm 16,427$) compared with the number of neurons in the BLA ($117,292 \pm 5,810$) and CA1 ($565,313 \pm 16,152$) of the no-SE rats. The number of neurons in the no-SE group did not differ from that of the controls (BLA, $115,108 \pm 4,043$; CA1 $556,603 \pm 14,559$), whereas SE rats had a 33% and 37% neuronal loss in the BLA and CA1, respectively, compared to the control group (Figure 5).

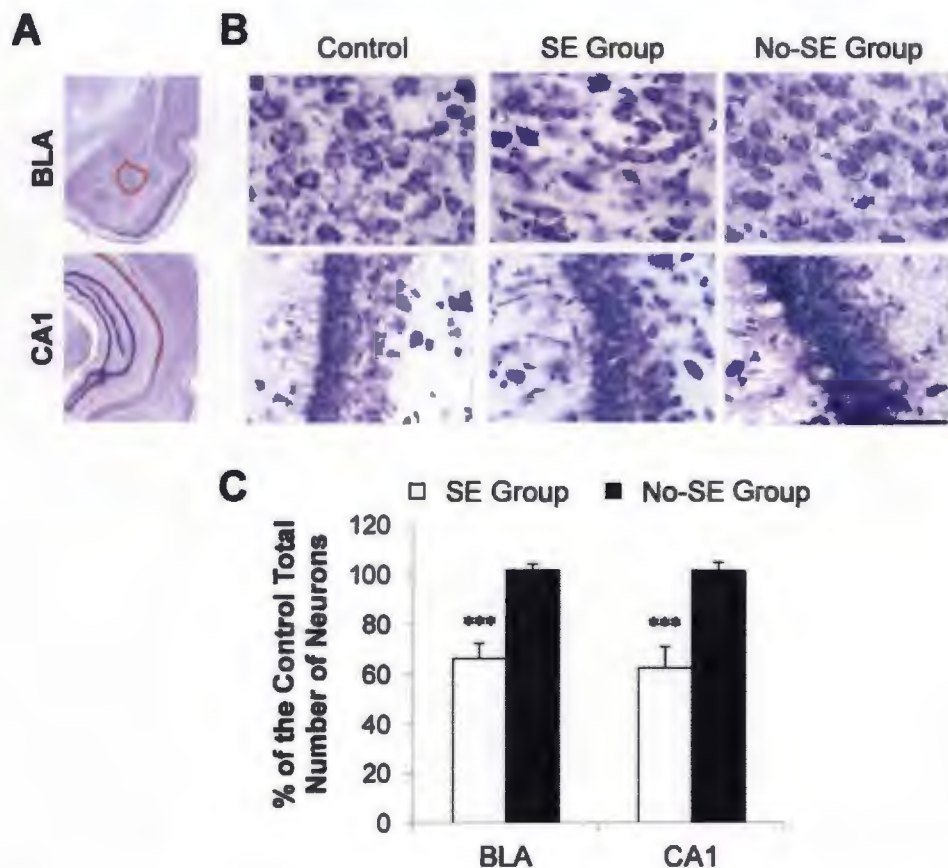


Figure 5 Neuronal loss in rats that developed SE versus rats that did not develop SE after soman exposure. (A) Panoramic photomicrographs of Nissl-stained sections of half hemispheres, outlining the BLA and the CA1 hippocampal subfield where stereological analysis was performed (red highlight). (B) Representative photomicrographs of Nissl-stained sections showing BLA and CA1 cells from a control rat, a SE rat, and a no-SE rat. Total magnification is 63x and scale bar is 50 μm . (C) Group data of stereological estimation of the total number of Nissl-stained neurons in the BLA (left) and CA1 (right), expressed as percent of the control ($n = 6$). Significant neuronal loss was present in SE rats ($n = 5$), while there was no neuronal loss in the no-SE rats ($n = 5$); $***p < 0.001$.

Neuronal degeneration in the SE group was moderate to severe in the amygdala (3.24 ± 0.3), piriform cortex (3.38 ± 0.2), and the hilus (3.26 ± 0.4) of the hippocampus, mild to moderate in neocortex (2.24 ± 0.13), CA1 hippocampal area (2.80 ± 0.4), and CA3 hippocampal area (2.10 ± 0.4), and mild in entorhinal cortex (1.7 ± 0.3). There were no degenerating neurons in the no-SE group and the controls (Figure 6).

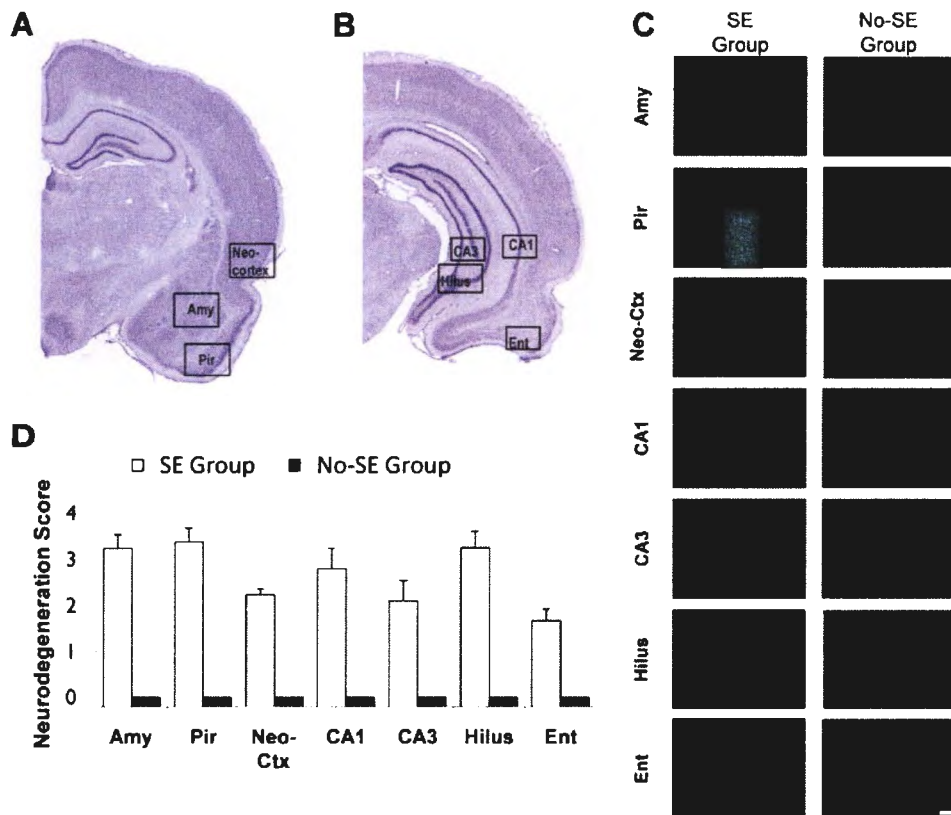


Figure 6 Neuronal degeneration in rats that developed SE versus rats that did not develop SE after soman exposure. (A) and (B) Panoramic photomicrographs of Nissl-stained sections showing the brain regions from where the FJC photomicrographs shown in C were taken. (C) Representative photomicrographs of FJC-stained sections from the brain regions where neuronal degeneration was evaluated, for the SE and the no-SE groups. Total magnification is 100x and scale bar is 50 μ m. (D) Neurodegeneration scores for the amygdala (Amy), piriform cortex (Pir), entorhinal cortex (Ent), CA1 and CA3 hippocampal subfields, hilus, and neocortex (neo-Ctx), in the SE group and the no-SE group ($n = 5$ for each group).

DISCUSSION

Previous studies have suggested that the amygdala plays a prominent role in the generation of seizures by nerve agent exposure (15; 17; 147; 175; 255). The present findings provide strong support for this view. We demonstrated that soman exposure dramatically reduces AChE activity in the hippocampus and piriform cortex, but SE develops only in rats where AChE is also reduced in the BLA. These results suggest that inhibition of AChE in the BLA after soman exposure is necessary to raise the hyperexcitability level to the point of seizure generation and propagation.

The results from the AChE activity measurements in the no-SE rats imply that AChE inhibition in the hippocampus and piriform cortex does not increase excitability sufficiently for seizure generation; or, even if some local seizure activity was induced in either region, it was not propagated to other brain areas to culminate in SE. These results are consistent with previous studies showing that the nerve agent VX, or soman in combination with carbachol or lithium chloride-pretreatment were not able to induce convulsions when microinjected into the piriform cortex, the hippocampus, or other brain regions. However, when these nerve agents were microinjected into the BLA, convulsions were elicited (175), suggesting that nerve agent-induced initiation of seizure activity in the BLA may be sufficient to trigger convulsive SE. The present study reinforces and complements these findings by showing that only when AChE activity in the BLA was significantly reduced by soman, SE developed. Taken together, the study of McDonough et al. (1987) and the present study suggest that AChE inhibition and initiation of seizures in the BLA may be both necessary and sufficient for seizure propagation and induction of SE.

The ability of the BLA to propagate seizures is well-known (20; 188; 287; 288). But it is also possible that the cholinergic system has a more significant role in the regulation of the excitability of the BLA, compared to the hippocampus and piriform cortex, and thus cholinergic hyperactivity in the BLA is more likely to produce hyperexcitability and seizures. The exceptionally dense cholinergic innervation of the BLA (183), its markedly high concentration of AChE ((31) and present study), and the high expression of muscarinic receptors – which play a primary role in seizure initiation by nerve agents (264) – on BLA pyramidal cells (173), may be attesting to the prominent role that the cholinergic system plays in the regulation of the BLA excitability. Why AChE activity in the BLA of the no-SE rats was not significantly inhibited remains to be determined. Perhaps these rats express greater amounts of the enzyme, or there may be other factors that make AChE in the BLA of the no-SE rats less susceptible to phosphorylation and inhibition by nerve agents.

The present findings do not imply that soman-induced inhibition of AChE in brain regions other than the BLA is unimportant for seizure initiation and the development of SE; most likely, inhibition of AChE simultaneously in many brain regions facilitates the development of SE. Our data also do not exclude the possibility that in the no-SE rats, soman failed to inhibit AChE activity in other brain regions – in addition to the BLA – which were not examined in this study, and may be important for the development of SE (see (195)). Nevertheless, along with previous studies (15; 17; 147; 175), the data presented here provide compelling evidence for a key role of the BLA in the initiation and spread of seizures after nerve agent exposure.

Soman reached the brain in the no-SE rats, as evidenced by the significant reduction of AChE in the piriform cortex and the hippocampus. However, there was no neuropathology present in these rats, as studied 7 days after soman exposure. Together with previous studies (117; 175; 178; 255), these data support the view that neuropathology is caused by the nerve agent-induced seizures, and not by a direct neurotoxic effect of the nerve agent, as thought initially (221). Nevertheless, others have found that after a subconvulsive dose of soman, brain lesions are present at 1 month, and become more pronounced at 3 months after exposure (131). Thus, more research is needed for a definitive conclusion regarding the long-term effects of soman on brain pathology that are independent of seizures.

The present study emphasizes the important role of the amygdala in seizure generation and propagation, as well as the important role of the cholinergic system in the regulation of amygdala's excitability. In addition, the knowledge that the amygdala is a key brain region for induction of SE by nerve agents, along with knowledge of amygdala's biochemistry and physiology, may contribute to the development of treatments or pretreatments that are designed to prevent AChE inhibition particularly in the amygdala, or to suppress primarily those mechanisms that play a prominent role in amygdala's excitability and hyperexcitability, in order to efficaciously prevent or limit seizures and the associated brain damage after nerve agent exposure.

ACKNOWLEDGMENTS

This work was supported by the CounterACT Program, National Institutes of Health, Office of the Director and the National Institute of Neurologic Disorders and Stroke [Grant Number 5U01NS058162-07], and the Defense Threat Reduction Agency-

Joint Science and Technology Office, Medical S&T Division [Grant Numbers
CBM.NEURO.01.10.US.18 and CBM.NEURO.01.10.US.15].

Conflicts of interest statement: None of the authors has any conflicts of interest
to disclose.

Chapter 3: The Recovery of Acetylcholinesterase Activity and the Progression of Neuropathological and Pathophysiological Alterations in the Rat Basolateral Amygdala After Soman-Induced Status Epilepticus: Relation to Anxiety-Like Behavior

Eric M. Prager^{1,3}, Vassiliki Aroniadou-Anderjaska^{1,2,3}, Camila P. Almeida-Suhett^{1,3},
Taiza H. Figueiredo¹, James P. Apland⁵, Franco Rossetti¹,
Cara H. Olsen⁴, Maria F.M. Braga^{1,2,3*}

¹Department of Anatomy, Physiology, and Genetics

² Department of Psychiatry

³ Program in Neuroscience

⁴Biostatistics Consulting Center

Uniformed Services University of the Health Sciences

4301 Jones Bridge Road

Bethesda, MD 20814, USA

⁵Neurotoxicology Branch

United States Army Medical Research Institute of Chemical Defense

Aberdeen Proving Ground, MD 21010, USA

*Corresponding Author:

Maria F.M. Braga, D.D.S., Ph.D.

Department of Anatomy, Physiology, and Genetics

Uniformed Services University of the Health Sciences

4301 Jones Bridge Road

Bethesda, MD 20814

Phone: (301) 295-3524

Fax: (301) 295-3566

Email: maria.braga@usuhs.edu

ABSTRACT

Organophosphorus nerve agents are powerful neurotoxins that irreversibly inhibit acetylcholinesterase (AChE) activity. One of the consequences of AChE inhibition is the generation of seizures and status epilepticus (SE), which cause brain damage, resulting in long-term neurological and behavioral deficits. Increased anxiety is the most common behavioral abnormality after nerve agent exposure. This is not surprising considering that the amygdala, and the basolateral nucleus of the amygdala (BLA) in particular, plays a central role in anxiety, and this structure suffers severe damage by nerve agent-induced seizures. In the present study, we exposed male rats to lethal doses of the nerve agent soman, and determined the time course of recovery of AChE activity, along with the progression of neuropathological and pathophysiological alterations in the BLA, during a 30-day period after exposure. Measurements were taken at 24 hours, 7 days, 14 days, and 30 days after exposure, and at 14 and 30 days, anxiety-like behavior was also evaluated. We found that more than 90% of AChE is inhibited at the onset of SE, and AChE inhibition remains at this level 24 hours later, in the BLA, as well as in the hippocampus, piriform cortex, and prelimbic cortex, which we analyzed for comparison. AChE activity recovered by day 7 in the BLA and day 14 in the other three regions. Significant neuronal loss and neurodegeneration were present in the BLA at 24 hours and throughout the 30-day period. There was no significant loss of GABAergic interneurons in the BLA at 24 hours post-exposure. However, by day 7, the number of GABAergic interneurons in the BLA was reduced, and at 14 and 30 days after soman, the ratio of GABAergic interneurons to the total number of neurons was lower compared to controls. Anxiety-like behavior in the open-field and the acoustic startle response tests was increased at 14 and 30 days post-exposure. Accompanying pathophysiological alterations in the BLA -

studied in *in vitro* brain slices – included a reduction in the amplitude of field potentials evoked by stimulation of the external capsule, along with prolongation of their time course and an increase in the paired-pulse ratio. Long-term potentiation was impaired at 24 hours, 7 days, and 14 days post-exposure. The loss of GABAergic interneurons in the BLA and the decreased interneuron to total number of neurons ratio may be the primary cause of the development of anxiety after nerve agent exposure.

Keywords: Soman, Status Epilepticus, Basolateral Amygdala, Acetylcholinesterase, Anxiety, Long-Term Potentiation

INTRODUCTION

Nerve agents are organophosphorus compounds that exert their toxic effects by rapidly and irreversibly inhibiting acetylcholinesterase (AChE) activity (24; 27; 110; 256; 263). In the brain, the resulting increase of acetylcholine and overstimulation of cholinergic receptors raises the excitation level to the point of seizure generation, and gives way to excessive activation of the glutamatergic system, which sustains and intensifies seizure activity (status epilepticus, SE), causing profound brain damage (177; 222). If death is prevented, long-term behavioral impairments may ensue due to brain pathologies (61; 91).

Five years after the attacks with the nerve agent sarin in Matsumoto and Tokyo, individuals exposed to sarin reported persistent increases in symptoms that characterize anxiety disorders, including irritability and restlessness, avoidance of places that triggered recollection of the trauma, tension, and insomnia (209; 296). Electrographic abnormalities indicative of epileptic activity were also present in exposed individuals (194; 205; 296). In animal models, exposure to nerve agents also results in long-term increases in anxiety and fear-like behaviors (61; 91; 150; 165; 187), as well as in the appearance of spontaneous recurrent seizures (68). The progression of pathological and pathophysiological alterations leading to these persistent behavioral and neurological abnormalities has not yet been elucidated. A better understanding of these alterations and the time course of their occurrence may allow for the development of treatment interventions that will prevent or minimize long-term neurological and behavioral deficits.

The amygdala is well recognized for its central role in emotional behavior (223), and the basolateral nucleus of the amygdala (BLA), in particular, is closely associated with the generation and expression of anxiety and fear (67; 82; 152); a common feature of anxiety disorders is hyperexcitability in the BLA (239; 282). In addition, evidence points to the BLA as a key brain region for seizure initiation and propagation after nerve agent poisoning (175), and we recently found that after exposure to the nerve agent soman, SE is induced only when AChE activity is sufficiently inhibited in the BLA (230). The BLA is also one of the most severely damaged regions after nerve agent-induced SE (17; 19; 23; 49; 90; 255).

Since inhibition of AChE is the primary mechanism of nerve agent poisoning, and sustained cholinergic dysregulation of the BLA may alter its excitability contributing to behavioral abnormalities, in the present study we examined the time course of recovery of AChE activity in the BLA; for comparison with other brain regions that may play an important role in seizure generation and propagation after nerve agent exposure (195), we also measured AChE activity in the piriform cortex, hippocampus, and prelimbic cortex. In addition, we investigated the progression of neuronal loss and degeneration in the BLA, during a 30-day period after soman exposure. To gain insight into the impact of the neuropathology on emotional behavior, we tested for the presence of increased anxiety at 14 and 30 days after soman-induced SE, and correlated the behavioral observations with synaptic alterations in the BLA, at the same time points.

MATERIALS AND METHODS

Animal Model

Experiments were performed using 6-week old (150-200 g) male, Sprague-Dawley rats (Taconic Farms, Derwood, MD). Animals were individually housed in an environmentally controlled room (20-23°C, ~44% humidity, 12-h light/12-h dark cycle [350-400 lux], lights on at 6:00 am), with food (Harlan Teklad Global Diet 2018, 18% protein rodent diet; Harlan Laboratories; Indianapolis, IN) and water available *ad libitum*. Cages were cleaned weekly and animal handling was minimized to reduce animal stress (232). All animal experiments were conducted following the Guide for the Care and Use of Laboratory Animals (Institute of Laboratory Animal Resources, National Research Council), and were approved by the U.S. Army Medical Research Institute of Chemical Defense and the Uniformed Services University of the Health Sciences Institutional Animal Care and Use Committees.

Soman administration and drug treatment

Soman (pinacolyl methylphosphonofluoridate; obtained from Edgewood Chemical Biological Center, Aberdeen Proving Ground, MD, USA) was diluted in cold saline and administered via a single subcutaneous injection (154 $\mu\text{g}/\text{kg}$), which, based on previous studies, is an approximate dose of 1.4 x LD₅₀ (89; 129). Following exposure to soman, rats were monitored for signs of seizure onset, and continuously rated for seizure severity according to the modified Racine Scale: Stage 0, no behavioral response; Stage 1, behavioral arrest, orofacial movements, chewing; Stage 2, head nodding/myoclonus; Stage 3, unilateral/bilateral forelimb clonus without rearing, straub tail, extended body posture; Stage 4, bilateral forelimb clonus plus rearing; Stage 5, rearing and falling; Stage

6, full tonic seizures (236; 237). Twenty minutes after injection of soman, rats received an intramuscular (i.m.) injection of 2 mg/kg atropine sulfate (Sigma, St. Louis MO), a muscarinic receptor antagonist, in order to control the peripheral effects of soman and prevent death from respiratory suppression. One group of animals was sacrificed at the onset of Stage 3 seizures, and therefore did not receive atropine sulfate. Stage 3 behavioral seizures have previously been found to coincide with the initiation of electrographically monitored SE (89; 150; 244). The control groups received saline instead of soman and were injected with atropine.

Acetylcholinesterase activity assay

Total AChE activity was measured using a previously established spectrophotometric protocol (77; 213), in animals randomly divided into control, seizure onset, 1-, 7-, 14-, and 30-day groups. Rats were anesthetized with 3-5% isoflurane and rapidly decapitated. The brain was removed and placed in ice-cold phosphate buffer (0.1 M, pH 8.0). Coronal brain slices (500 μ m-thick) containing the prelimbic cortex (Bregma 5.16 mm to 2.52 mm), BLA (Bregma -2.28 mm to -3.72 mm), piriform cortex (Bregma -1.72 mm to -3.00 mm), and hippocampus (Bregma -2.28 mm to -4.68 mm) were cut using a vibratome (series 1000; Technical Products International, St. Louis, MO). Structures were isolated by hand and placed in an Eppendorf tube containing 1:20 Triton + phosphate buffer, homogenized for 10 seconds and centrifuged at 14,000g for 5 min. The supernatant was removed and placed into a separate container. On the day of sampling, a glutathione curve was made by adding glutathione (1 – 10 μ L) to DTNB [5,5'-dithio-bis(2-nitrobenzoic acid)] (up to 200 μ L; (213). Glutathione supplies the sulfhydryl groups and is used to construct a standard curve. Tissue supernatants (10 μ L

per well) were added to either 10 μ L eserine (an all-purpose cholinesterase inhibitor that inhibits both butyrylcholinesterase and acetylcholinesterase) or ethoprozine (a specific butyrylcholinesterase inhibitor), all in the presence of acetylthiocholine (5 μ L) and 175 μ L DTNB (all purchased from Sigma-Aldrich, St. Louis, MO). Samples were read by the Softmax Pro 5.2 kinetics every 20 sec for 4 min. The total butyrylcholinesterase inhibition was subtracted from the absorbance sample to provide a difference score, which was multiplied by the slope and intercept of the standard curve to provide a total concentration of AChE activity. AChE specific activity was calculated by dividing the total activity by the calculated protein concentration assayed by the Bradford method (see (38), using a protein assay dye reagent (Bio-Rad, Hercules CA).

Neuropathology experiments

Fixation and tissue processing

1-, 7-, 14-, and 30-days after SE, rats were deeply anesthetized with pentobarbital (75-100 mg/kg, i.p.) and transcardially perfused with PBS (100 mL) followed by 4% paraformaldehyde (200 mL). Brains were removed and post-fixed in 4% paraformaldehyde overnight at 4°C, then transferred to a solution of 30% sucrose in PBS for 72 hours, and frozen with dry ice before storage at -80°C until sectioning. A 1-in-5 series of sections containing the amygdala was cut at 40 μ m on a sliding microtome (Leica Microsystems SM2000R). One series of sections was mounted on slides (Superfrost Plus, Daigger, Vernon Hills, IL) for Nissl staining with cresyl violet. Two adjacent series of sections were mounted on slides for Fluro-Jade-C staining or were stored at -20°C in a cryoprotectant solution for GAD-67 immunohistochemistry (90).

Fluoro-Jade C (FJC) staining

FJC (Histo-Chem, Jefferson, AR) was used to identify irreversibly degenerating neurons in the BLA. 2D-sample quantitative assessments were made from 3 brain sections (both hemispheres) per animal from AP -2.00 mm to - 3.96 mm. Mounted sections were treated and stained in a 0.0001% solution of FJC dissolved in 0.1% acetic acid for 10 min (234). Mosaics were made of the BLA from each hemisphere through a 20x lens, using Stereo Investigator Virtual Tissue tools (6 x 7 square; MicroBrightField, Williston, VT). Cells were counted using ImageJ (NIH Image, Bethesda, MD) with the cell counter tool. The reported number of degenerating cells is the total number counted in the three sections, in both hemispheres.

GAD-67 Immunohistochemistry

Free-floating sections were collected from the cryoprotectant solution, washed three times for 5 min each in 0.1 M PBS, and then incubated in a blocking solution containing 10% normal goat serum (Millipore Bioscience Research Reagents, Temecula, CA) and 0.5% Triton X-100 in PBS, for 1 hour at room temperature (90). The sections were then incubated with mouse anti-GAD-67 serum (1:1000, MAB5406; Millipore Bioscience Research Reagents), 5% normal goat serum, 0.3% Triton X-100, and 1% bovine serum albumin, overnight at 4°C. After rinsing three times for 10 min each in 0.1% Triton X-100 in PBS, sections were incubated with Cy3-conjugated goat anti-mouse antibody (1:1000; Jackson ImmunoResearch Laboratories Inc., West Grove, PA) and 0.0001% 4,6-diamidino-2-phenylindole dihydrochloride (Sigma-Aldrich, St. Louis, MO) in PBS for 1 hour at room temperature. Sections were given a final rinse in PBS for

10 min, then mounted on slides, air-dried for at least 30 min, and cover-slipped with ProLong Gold antifade reagent (Invitrogen, Carlsbad, CA).

Stereological quantification

Design-based stereology was used to determine total neuronal loss from Nissl-stained sections in the BLA, and interneuronal loss from GAD-67-immuno-stained sections in the BLA. Sections were viewed with a Zeiss (Oberkochen, Germany) Axioplan 2ie fluorescent microscope with a motorized stage, interfaced with a computer, running StereoInvestigator 8.0 (MicroBrightField, Williston, VT). The BLA was identified on slide-mounted sections under a 2.5x objective, based on the atlas of Paxinos and Watson (220). Sampling was performed under a 63x oil immersion objective. Nissl-stained neurons were distinguished from glial cells by their larger size and pale nuclei surrounded by darkly-stained cytoplasm containing Nissl bodies. The total number of Nissl-stained and GAD-67-immunostained neurons was estimated using the optical fractionator probe along with the coefficient of error (CE). Nissl-stained neurons were calculated using Stereo Investigator 9.0. The CE was calculated by the software according to Gundersen ($m = 1$; (108)) and Schmitz-Hof 2nd estimation (247) equations.

A 1-in-5 series of sections (~7 sections per rat) was analyzed for Nissl-stained neurons in the BLA. The counting frame was 35 x 35 μm , the counting grid was 190 x 190 μm , and the dissector height was 12 μm . Nuclei were counted when the cell body came into focus within the dissector, which was placed 2 μm below the section surface. An average of 235 neurons per rat was counted, and the average CE was 0.04 for both the Gundersen and Schmitz-Hof equations. Section thickness was measured at every counting site (averaging 20 μm for the BLA). For GABAergic interneurons immuno-

stained with GAD-67, a 1-in-10 series of sections was analyzed (on average five sections). The counting frame was 60 x 60 μm , the counting grid was 100 x 100 μm , and the dissector height was 20 μm . The average mounting section thickness of the BLA was 27.6 μm . An average of 239 neurons per rat was counted in the BLA, and the average CE was 0.07 for both the Gundersen et al., and Schmitz-hof equations. Nuclei were counted when the top of the nucleus came into focus within the dissector, which was placed 2 μm below the section surface. Section thickness was measured at every fifth counting site.

Behavioral Experiments

Open field test

Anxiety-like behavior was assessed using an open field apparatus (40 x 40 x 20 cm clear Plexiglas arena; (21; 83). One day prior to testing, animals were acclimated to the apparatus for 20 min. On the test day, rats were placed in the center of the open field and activity was measured and recorded for 20 min using an Accuscan Electronics infrared photocell system (Accuscan Instruments Inc., Columbus, OH). Data were automatically collected and transmitted to a computer equipped with "Fusion" software (from Accuscan Electronics, Columbus, OH). Locomotion (distance traveled in cm) and time spent in the center of the open field were analyzed. Anxiety behavior was measured as the ratio of the time spent in the center over the total movement time, expressed as a percentage of the total movement time.

Acoustic startle response test

Acoustic startle response (ASR) testing was conducted with the use of the Med Associates Acoustic Response Test System (Med Associates, Georgia, VT), which consists of weight-sensitive platforms inside individual sound-attenuating chambers. Rats

were individually placed in a ventilated holding cage, which is small enough to restrict extensive locomotion, but large enough to allow the subject to turn around and make other small movements (21). The chamber contained a ventilated fan to provide background noise. The cage was placed on a weight-sensitive platform; movements in response to stimuli were measured as a voltage change by a strain gauge inside each platform. Animals were acclimated to the apparatus in two sessions. A 3-min adaptation period was allowed, during which no startle stimuli were presented. Startle stimuli consisted of 110 or 120 dB sound pressure level noise bursts of 20-ms duration. Each stimulus had a 2-ms rise and decay time, such that the onset and offset were abrupt, which is a primary requirement for startle (84). Each trial type was presented eight times. Trial types were presented at random to avoid order effects and habituation, and inter-trial intervals ranged randomly from 15 to 25 s. Responses were recorded by an interfaced Pentium computer as the maximum response occurring during the no-stimulus periods, and during the startle period, and were assigned a value based on an arbitrary scale used by the software of the Test System.

Electrophysiological experiments

Animals were randomly divided into control, 1-, 7-, 14-, and 30-day groups and anesthetized with 3-5% isoflurane before decapitation. Coronal brain slices (400 μ m-thick) containing the amygdala (-2.64 to -3.36 from Bregma) were cut using a vibratome (series 1000; Technical Products International, St. Louis, MO), in ice-cold cutting solution consisting of (in mM): 115 sucrose, 70 NMDG, 1 KCl, 2 CaCl₂, 4 MgCl₂, 1.25 NaH₂PO₄, 30 NaHCO₃. Slices were transferred to a holding chamber, at room temperature, in a bath solution containing (in mM): 125 NaCl, 3 KCl, 1.25 NaH₂PO₄, 21

NaHCO₃, 2 CaCl₂ 1.5 MgCl₂, and 11 D-glucose (all purchased from Sigma-Aldrich, St. Louis, MO). Recording solution was the same as the holding bath solution. All solutions were saturated with 95% O₂, 5% CO₂ to achieve a pH near 7.4. Field potential recordings were obtained in an interface-type chamber, maintained at 32~33°C, with a flow rate of the ACSF at ~1.5 mL/min. Field potentials were evoked by stimulation of the external capsule at 0.05 Hz with a bipolar concentric stimulating electrode made of tungsten (World Precision Instruments, Sarasota, FL). For LTP experiments, a 20 min baseline was recorded; stimulus intensity was adjusted to elicit a response of about 70 to 80% of the maximum amplitude. High frequency stimulation (HFS) consisted of 3 trains of pulses at 100 Hz, each train lasted 1 s, and the interval between trains was 20 sec. Following HFS, field potential recordings resumed with stimulation at 0.05 Hz. Recording glass pipettes were filled with ACSF, and had a resistance of approximately 5 MΩ. Signals were digitized using the pClamp 10.2 software (Molecular Devices, Union City, CA), analyzed using AxoGraph (AxoGraph X, Berkley, CA), and final presentation was prepared using GraphPad Prism (GraphPad Software, La Jolla, CA).

Statistical analysis

All data are expressed as mean ± standard error. Welch F ANOVA and a Games-Howell post hoc were used to compare the results from the analysis of AChE activity, and the stereological estimation of the total number of GAD-67-positive interneurons. Welch F ANOVA was used due to heterogeneity of variance. Statistical results derived with the use of the Welch F ANOVA were confirmed with a Kruskal-Wallis non-parametric test, which does not assume a normal distribution. One-way ANOVA with a Tukey post hoc test was used to compare the cell count from degenerating neurons, and

to analyze the results from the behavioral tests. One-way ANOVA with a Dunnett's T post hoc test was used to compare the results from the stereological estimation of the total number of neurons and from the behavioral tests. Results from the electrophysiological experiments were analyzed using one-way ANOVA followed by a Dunnett's T post hoc test, paired-Student's t-test, or independent samples t-test. Statistical analyses were made using the software package PAWS SPSS 20 (IBM, Armonk, NY, USA). Differences were considered significant when $p < 0.05$. Sample size "n" refers to the number of animals except for electrophysiology experiments where "n" refers to the number of slices.

RESULTS

Soman was administered to 161 rats. The average latency to Stage 3 seizure onset (SE onset) was 8.7 ± 1.2 min. Of the surviving 104 rats that developed prolonged SE (see (16; 89; 90)), 51 rats were used to measure AChE activity, and 31 rats were used for electrophysiological experiments. From the remaining 22 soman-exposed rats, 5 rats were used for evaluation of neuropathology at 24-hours after soman exposure, 6 rats were used for evaluation of neuropathology at 7 days post-exposure, 5 rats were used for 14-day behavioral experiments followed by neuropathological studies, and 6 rats were used for 30-day behavioral tests followed by neuropathology assessments. Aged-matched rats that were not exposed to soman were used for control experiments.

Time course of recovery of AChE inhibition

The onset of SE induced by soman was associated with a dramatic reduction of AChE activity in the BLA ($91.9 \pm 4.0\%$), prelimbic cortex ($98.8 \pm 5.0\%$), piriform cortex ($99.2 \pm 8.3\%$), and hippocampus ($98.7 \pm 6.3\%$; all p 's < 0.001 ; Table 2 and Figure 7).

Twenty-four hours after SE, AChE activity was still reduced by at least 93% in all four brain regions (all p 's < 0.001). Seven days after SE, AChE activity in the BLA was no longer significantly lower than the control ($42.7 \pm 14.2\%$ lower; $p = 0.092$), while it remained significantly reduced in the prelimbic cortex ($52.1 \pm 10.3\%$ lower than control; $p = 0.001$), piriform cortex ($55.0 \pm 13.1\%$ lower; $p = 0.004$), and hippocampus ($46.6 \pm 11.7\%$ lower; $p = 0.009$). Within 14 days, AChE activity had recovered in all four brain regions; in the BLA, it was $116.3 \pm 18.8\%$ of the control activity, while in the prelimbic cortex, piriform cortex, and hippocampus it was $25.8 \pm 8.6\%$, $13.3 \pm 15.8\%$, and $15.1 \pm 14.5\%$ lower than the control values, respectively (all p 's > 0.05). Thirty days after SE, AChE activity was $118.8 \pm 10.7\%$ of control values in the BLA, while in the prelimbic cortex, piriform cortex, and hippocampus it was $144.8 \pm 18.4\%$, $147.4 \pm 18.2\%$, and $135.5 \pm 20.7\%$ of the control activity, respectively (all p 's > 0.05; Figure 7; Table 2).

Table 2: Reduction of AChE activity (in nmol/min/mg) and time course of recovery after soman-induced status epilepticus (SE)

Brain Region	Control	SE Onset	24-hours	7-days	14-days	30-days
Basolateral Amygdala	830.9 ± 33.6	68.8 ± 10.2	38.4 ± 6.1	488.2 ± 116.2	833.2 ± 114.2	1011.6 ± 84.2
Prelimbic Cortex	263.4 ± 13.2	3.0 ± 0.8	15.6 ± 4.3	130.2 ± 24.4	202.0 ± 19.1	393.9 ± 48.2
Piriform Cortex	351.9 ± 29.1	2.8 ± 0.8	11.4 ± 2.4	158.3 ± 35.4	274.1 ± 39.4	518.8 ± 57.0
Hippocampus	311.3 ± 19.7	4.1 ± 0.3	23.2 ± 5.3	166.2 ± 30.5	231.8 ± 26.9	421.8 ± 61.3

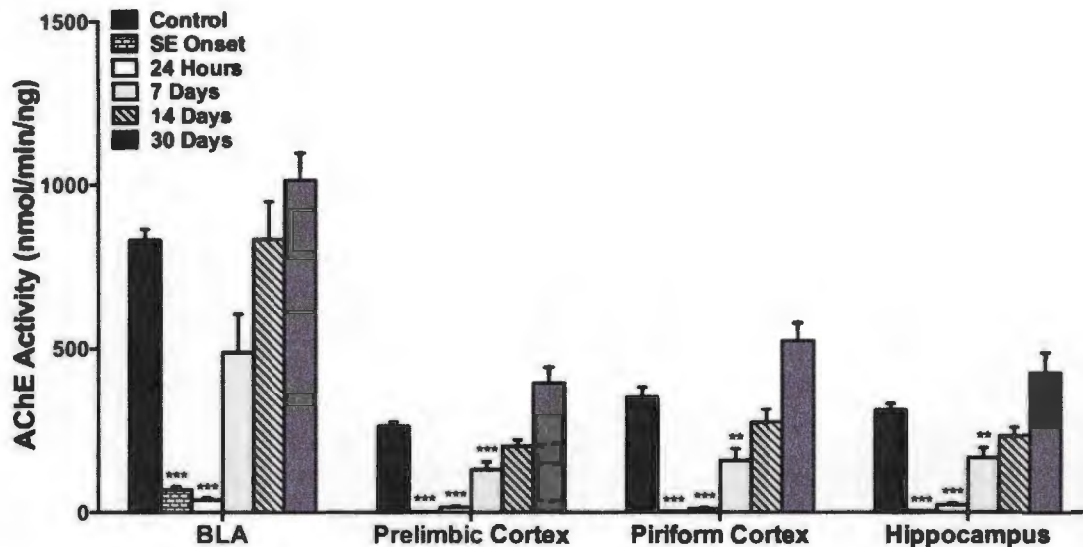


Figure 7 Time course of the recovery of AChE activity after soman-induced status epilepticus (SE). AChE activity was reduced by more than 90% in all four brain regions at the onset of SE ($n = 7$), as well as at 24 hours later ($n = 11$). At 7 days post-exposure ($n = 11$), AChE activity had recovered in the BLA, while at 14 days ($n = 10$) and 30 days ($n = 12$) post-exposure, it was not significantly different from the control levels in all 4 brain regions. $**p < 0.01$; $***p < 0.001$ compared to the controls (Welch F ANOVA with Games-Howell post hoc).

Time course of neurodegeneration and neuronal loss in the BLA

Twenty-four hours after exposure to soman, severe neurodegeneration was found in the BLA (Figure 8). The number of degenerating neurons was 928 ± 153 at 24 hours, 481 ± 35 at 7 days ($p = 0.003$), 305 ± 77 at 14 days ($p < 0.001$), and 133 ± 17 at 30 days ($p < 0.001$; all p values are in comparison to the 24-hour group). The number of degenerating neurons at 30 days was also significantly lower when compared to the 7-day group ($p = 0.014$; Figure 8).

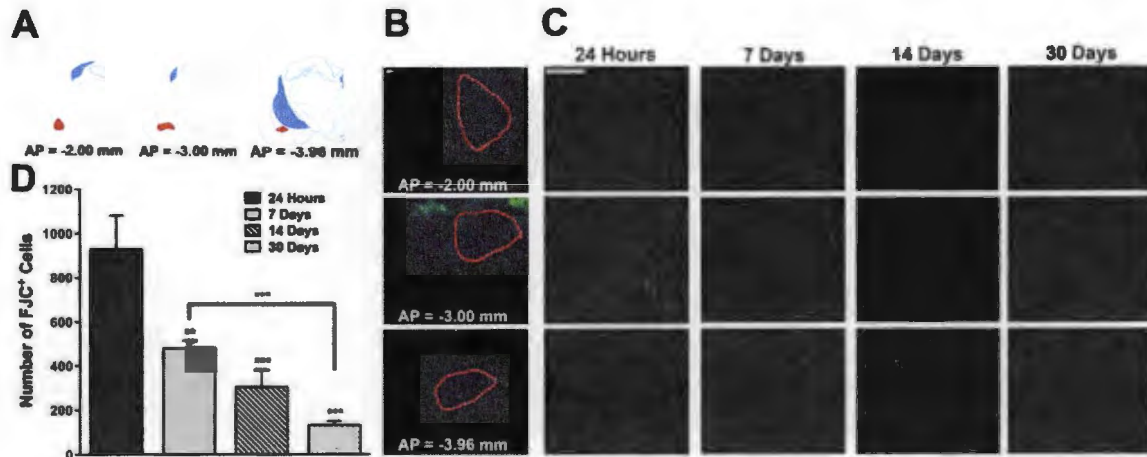


Figure 8 Time course of neuronal degeneration in the BLA after soman-induced SE. A, B. The BLA region where neuronal degeneration was assessed. In A, the drawings are from Paxinos and Watson (2005), while in B the BLA is outlined on FJC stained sections. C. Representative photomicrographs of FJC-stained sections, at 24-hours, 7-, 14-, and 30-days after soman exposure. Rows correspond to the coordinates shown in B. Total magnification is 20x. Scale bar, 250 μ m. D. Quantitative assessment of the extent of neurodegeneration at 24-hours (n = 4), 7- (n = 6), 14- (n = 4), and 30 days (n = 5) after soman exposure. Values are mean \pm SEM number of cells counted in the BLA from both hemispheres. ** p < 0.01, *** p < 0.001 (One-Way ANOVA with Tukey post hoc).

Estimation of the total number of neurons in the BLA (Figure 9A and B), using an unbiased stereological method in Nissl-stained sections, showed that animals exposed to soman had significantly fewer total number of neurons in the BLA at 24 hours ($71,003.5 \pm 1,198.1$), 7 days ($72,416.7 \pm 2,508.6$), 14 days ($72,499.4 \pm 1,713.8$) and 30-days ($71,412.1 \pm 2,731.8$) after exposure to soman, compared to the number of neurons in the control animals ($109,397.5 \pm 2,719.5$; all p 's < 0.05; Figure 9C). There was no significant difference between the number of neurons in the BLA at the different time points after soman exposure.

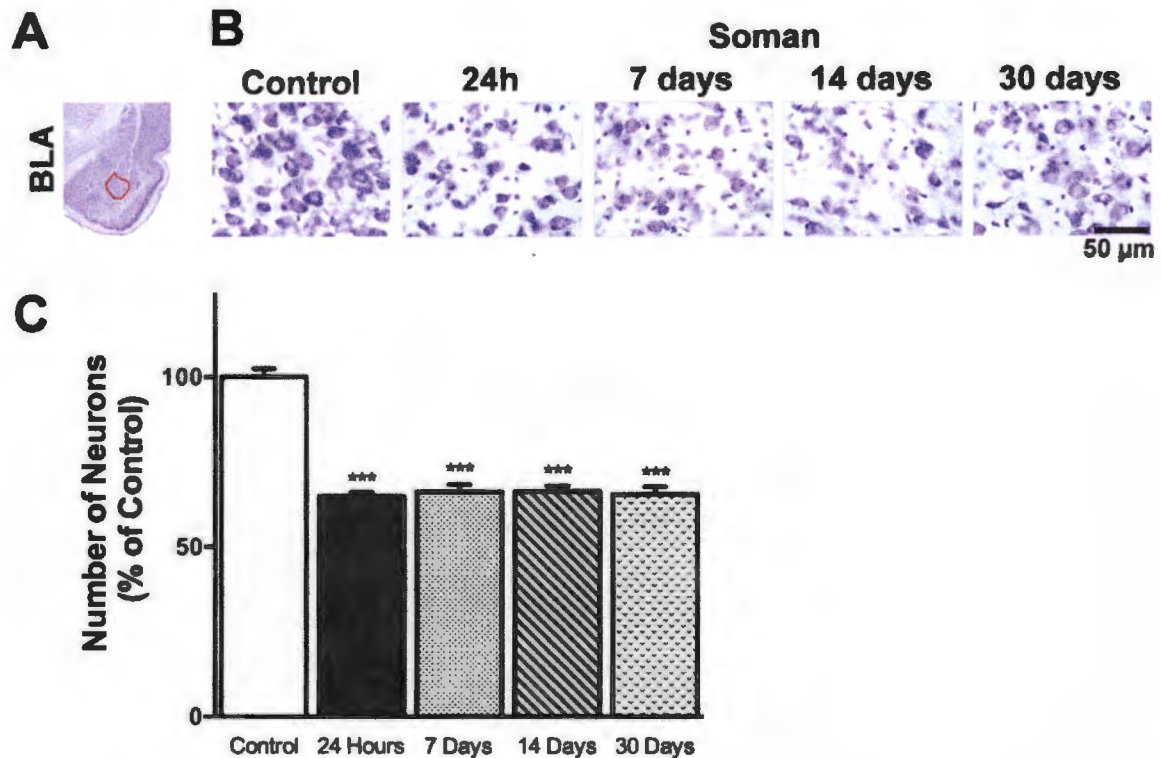


Figure 9 Time course of neuronal loss in the BLA after soman-induced SE. **A.** Panoramic photomicrograph of a Nissl-stained section from half hemisphere, outlining the BLA where stereological analysis was performed (red highlight). **B.** Representative photomicrographs of Nissl-stained sections showing BLA cells from a control rat and from soman-exposed rats, analyzed at 24-hours, 7-, 14- and 30-days after exposure. Total magnification is 63x and scale bar is 50 μ m. **C.** Group data of stereological estimation of the total number of Nissl-stained neurons in the BLA, expressed as percent of the control group (n = 11). Significant neuronal loss was present in rats at 24 hours (n = 5), 7 days (n = 6), 14 days (n = 5), and 30-days (n = 6) after soman exposure. There were no differences in the extent of neuronal loss among the 24-hour, 7-, 14-, and 30-day groups; *** $p < 0.001$ (One-Way ANOVA with Dunnett's T post hoc).

Estimation of the total number of GABAergic interneurons in the BLA, using an unbiased stereological method on GAD-67-immunostained sections, showed that 24-hours after exposure, the number of interneurons in the soman group ($10,539.1 \pm 575.1$; n = 5) did not differ significantly from the controls ($13,107.4 \pm 804.5$; $p = 0.129$; n = 10; Figure 10A, B). However, 7 days after soman exposure, the number of GABAergic interneurons in the soman-exposed group ($7,131.3 \pm 343.4$; n = 6) was significantly lower

than the number of GABAergic interneurons in the BLA of control animals ($p < 0.001$). No further loss of GABAergic interneurons was observed at 14 days ($6,745.5 \pm 315.4$; $n = 6$), or 30 days ($6,885.2 \pm 195.4$; $n = 5$) after SE, compared to the 7-day soman group ($p > 0.05$). The loss of GABAergic interneurons in the BLA was approximately 46%, 7-days after exposure. Moreover, the ratio of GABAergic interneurons to the total number of neurons in the BLA was altered after soman exposure. At 24 hours after SE, there was a significant increase in this ratio ($p = 0.006$). Seven days after exposure, the ratio of GABAergic interneurons to the total number of neurons was not significantly different from the control ($p = 0.175$), whereas it was significantly reduced at 14 days ($p = 0.006$) and 30 days ($p = 0.030$) after SE (Figure 10C).

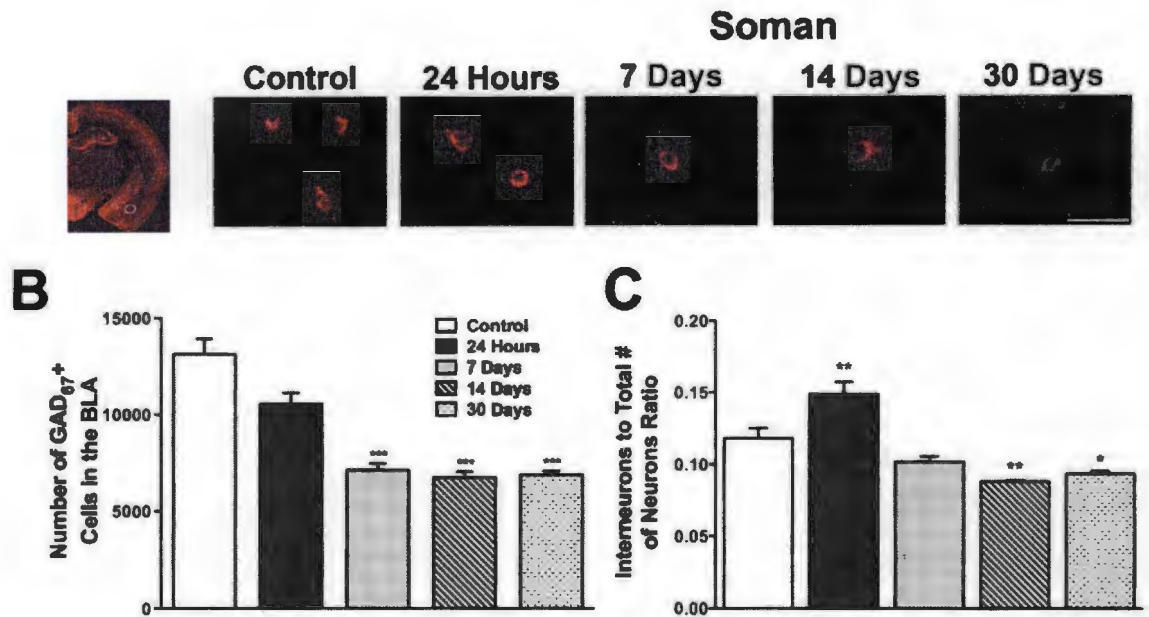


Figure 10 Delayed loss of GABAergic interneurons in the BLA after soman-induced SE. A. Panoramic photomicrograph of an immunohistochemically-stained section for GAD-67 (BLA is outlined in white). B. Representative photomicrographs of GABAergic interneurons in the BLA from a control rat and from soman-exposed rats, analyzed at 24-hours, 7-, 14- and 30-days after exposure. Total magnification is 630x; scale bar, 50 μ m. C. Group data showing the mean and standard error of the stereologically estimated total number of GAD-67-positive cells in the BLA. D. Group data showing the mean and standard error of the ratio of GABAergic interneurons to the total number of neurons. * $p < 0.05$, ** $p < 0.01$, *** $p < 0.001$ (Welch F ANOVA with Games-Howell post hoc and one-way ANOVA with Dunnett's T post hoc).

Anxiety-like behavior after soman exposure

The reduced ratio of the number of GABAergic interneurons to the total number of neurons in the BLA, on days 14 and 30 after soman-induced SE, suggests that GABAergic inhibition in the BLA may be impaired at these time points; the result could be a hyperexcitable amygdala, which can produced anxiety-related behavioral deficits. To determine if anxiety-like behavior was increased in the soman-exposed rats, we used the open field and the ASR tests. In the open field test, the more anxious an animal is, the

less time it spends in the center of the open field (233). Compared to the time the control group spent in the center of the open field ($14.2 \pm 2.1\%$ of the total movement time; $n = 6$), the soman-exposed rats spent significantly less time in the center, on day 14 post-exposure ($7.6 \pm 1.8\%$ of the total movement time; $n = 5$, $p = 0.046$) and on day 30 post-exposure ($5.3 \pm 1.6\%$ of the total movement time; $n = 6$, $p = 0.004$; Figure 11A). The difference between the 14-day and 30-day groups was not statistically significant ($p = 0.622$). The total movement time did not differ significantly among the three groups (695 ± 48 s for the control group, 718 ± 51 s for the 14-day group, and 793 ± 38 s for the 30-day group).

In the ASR test, the more anxious and fearful an animal is, the larger the amplitude of the startle in response to the acoustic stimulus (122; 156; 157). We measured the amplitude of the startle by averaging the amplitude of 8 trials, using two levels of acoustic stimuli (110 dB and 120 dB noise bursts). Compared to the amplitude of the ASR in the control group (11.5 ± 1.2 and 13.4 ± 2.2 in response to the 110 and 120 dB, respectively; $n = 6$), the ASR amplitude was increased in the soman-exposed rats, on day 14 (16.8 ± 1.9 in response to the 110 dB, $p = 0.42$, and 18.2 ± 1.1 in response to the 120 dB, $p = 0.010$; $n = 5$) and on day 30 after exposure (18.3 ± 2.2 in response to the 110 dB, $p = 0.017$, and 19.2 ± 0.9 in response to the 120 dB, $p = 0.001$; $n = 6$; Figure 11B). There was no significant difference in the amplitude of the ASR between the 14- and 30-day groups ($p > 0.05$).

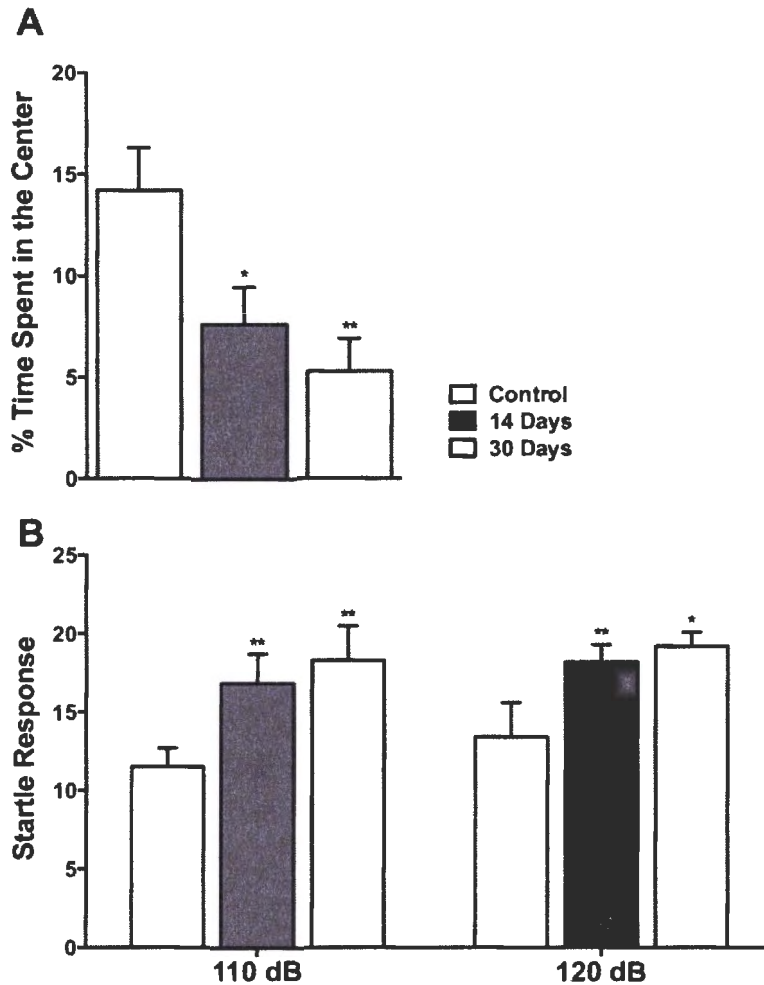


Figure 11 Exposure to soman causes long-lasting increases in anxiety-like behavior, as measured by the open field and acoustic startle response (ASR) tests. A. Soman-exposed rats spent significantly less time in the center of the open field, at 14 and 30 days after exposure, compared to control rats. B. Exposure to soman significantly increased the amplitude of the ASR to both the 110 and 120 dB startle stimuli, at 14 and 30 days after exposure, compared to controls. There were no significant differences between the 14- and 30-day groups. * $p < 0.05$, ** $p < 0.01$; $n = 17$ (One-Way ANOVA with Dunnett's T post hoc).

Time course of pathophysiological alterations in the BLA

The observed neuronal damage in the BLA of the soman-exposed rats, and the accompanying behavioral impairments in anxiety-like behavior suggest that impairments were probably also present in BLA physiology. To gain some insight into the

pathophysiological alterations in the BLA after soman exposure, we recorded BLA field potentials evoked by stimulation of the external capsule in brain slices obtained from soman-exposed rats, at 24 hours, 7 days, 14 days, and 30 days after soman administration.

Due to the non-laminar architecture of the amygdala, the activity of neuronal populations in this structure does not generate large extracellular electric dipoles, and, therefore, evoked field potentials have small amplitude. Nevertheless, field potentials of about 0.5 mV can be consistently evoked in the BLA, representing about 60 ~ 70% of the maximum evoked responses. In the soman-exposed rats, however, it was difficult to evoke field potentials, particularly at 24 hours and 7 days post-exposure. Stimulus intensities similar to those used in control slices would evoke field potentials in the BLA of soman-exposed rats that were about half the amplitude of the BLA field potentials in control rats. Notably, the BLA field potentials in the soman-exposed rats had a slow decay (Figure 12), which is probably indicative of reduced inhibition. To better assess if inhibitory activity in the BLA was impaired after soman exposure, we compared responses to paired-pulse stimulation in soman-exposed versus control rats. In the slices from the control rats, the ratio of the amplitude of the response to the second pulse over the amplitude of the response to the first pulse (paired-pulse ratio, or PPR) was 0.89 ± 0.07 ($n = 9$). In the slices from soman-exposed rats, the PPR was significantly higher compared to the controls, at 24 hours (PPR = 1.21 ± 0.03 , $n = 9$; $p = 0.008$), 7 days (PPR = 1.30 ± 0.06 , $n = 9$; $p = 0.001$), 14 days (PPR = 1.26 ± 0.09 , $n = 10$; $p = 0.002$), and 30 days (PPR = 1.23 ± 0.03 , $n = 11$; $p = 0.005$) after soman administration (Figure 12), suggesting that the inhibition which normally suppresses the amplitude of the synaptic

response to the second stimulus pulse (299) and limits contribution of spiking activity to the field potentials was reduced.

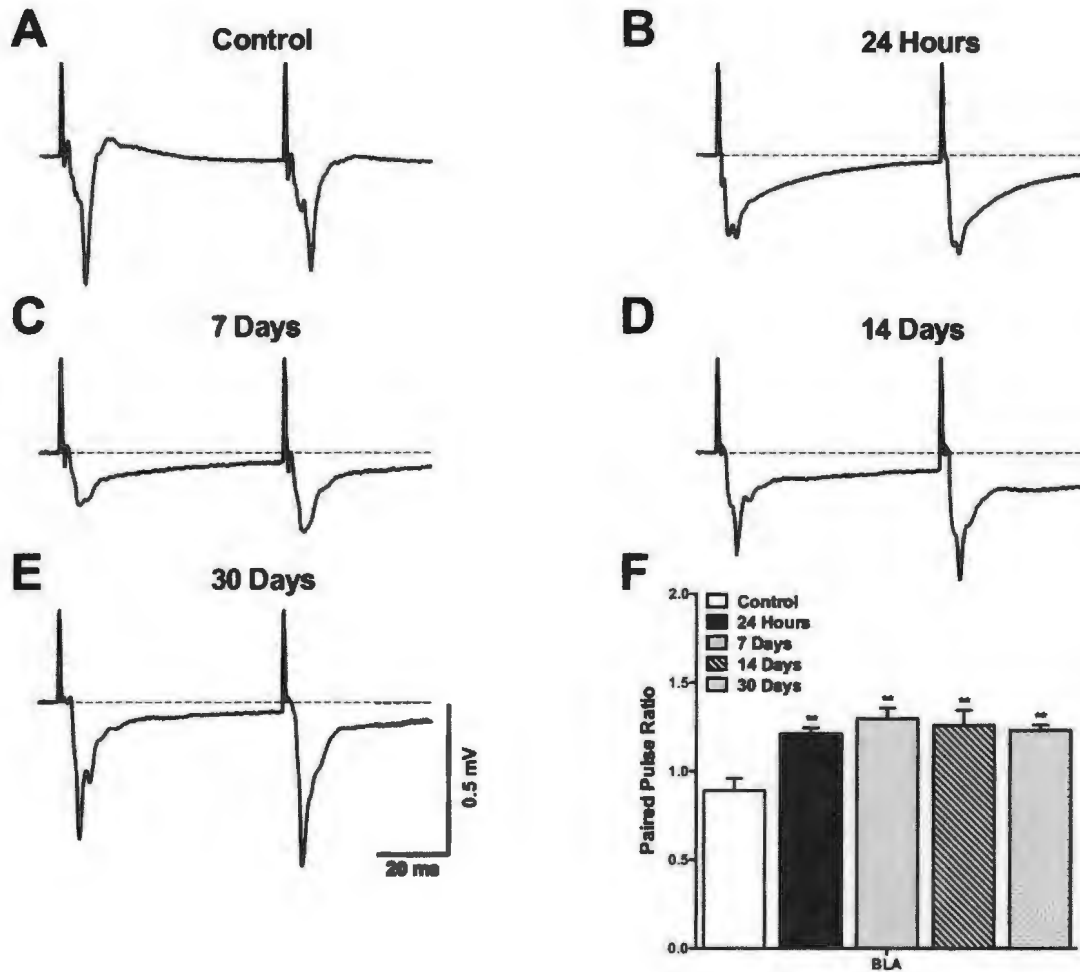


Figure 12 Alterations in the BLA field potentials after soman-induced SE. A to E show representative field potentials evoked in the BLA by paired-pulse stimulation of the external capsule, from control rats ($n = 9$) and soman-exposed rats, at 24-hours ($n = 9$), 7 days ($n = 9$), 14 days ($n = 10$), and 30 days ($n = 11$) after exposure; each trace is an average of 10 to 15 sweeps. In the soman-exposed rats, higher stimulus intensities were necessary to evoke field potentials compared to controls, the duration of the field potentials was prolonged (notice the decay of the waveforms), and the paired-pulse ratio was significantly increased (F). $**p < 0.01$ (One-Way ANOVA with Dunnett's T post hoc).

A synaptic property that is considered to be the cellular mechanism underlying learning and memory processes is the long-term potentiation (LTP) of synaptic transmission (164; 275). The amygdala plays a key role in fear-associated learning and memory formation (152; 215). The BLA, in particular, mediates the formation of fear memory and may also be the site, or one of the sites, where fear memory is stored (97). Therefore, we examined if the capacity of neuronal synapses in the BLA to express LTP had been altered after soman exposure. Potentiation of the evoked field potentials was measured by averaging the amplitude of the responses from 50 to 60 min after HFS, and expressing it as a percentage of the baseline response. Compared to the percent change in age-matched control animals ($158.0 \pm 8.4\%$, from 0.48 ± 0.03 mV at baseline to 0.74 ± 0.04 mV at 50 to 60 min after HFS, $n = 7$), the percent change in the 24-hours post-exposure group ($112.3 \pm 5.24\%$, from 0.27 ± 0.01 mV to 0.30 ± 0.02 mV, $n = 7$; Figure 13A), the 7-day post-exposure group ($122.3 \pm 8.53\%$, from 0.27 ± 0.06 mV to 0.34 ± 0.08 mV, $n = 8$; Figure 13B), and the 14-day post-exposure group ($126.9 \pm 10.6\%$, from 0.26 ± 0.02 mV to 0.35 ± 0.05 mV, $n = 10$; Figure 13C) were significantly lower ($p < 0.05$). At 30 days post-exposure, the time course of LTP was slower compared to the control group (Figure 13D), but the potentiation at 50 to 60 min post-HFS ($135.1 \pm 14.9\%$, from 0.40 ± 0.03 mV to 0.55 ± 0.07 mV, $n = 10$) was not significantly different from the controls ($p = 0.251$).

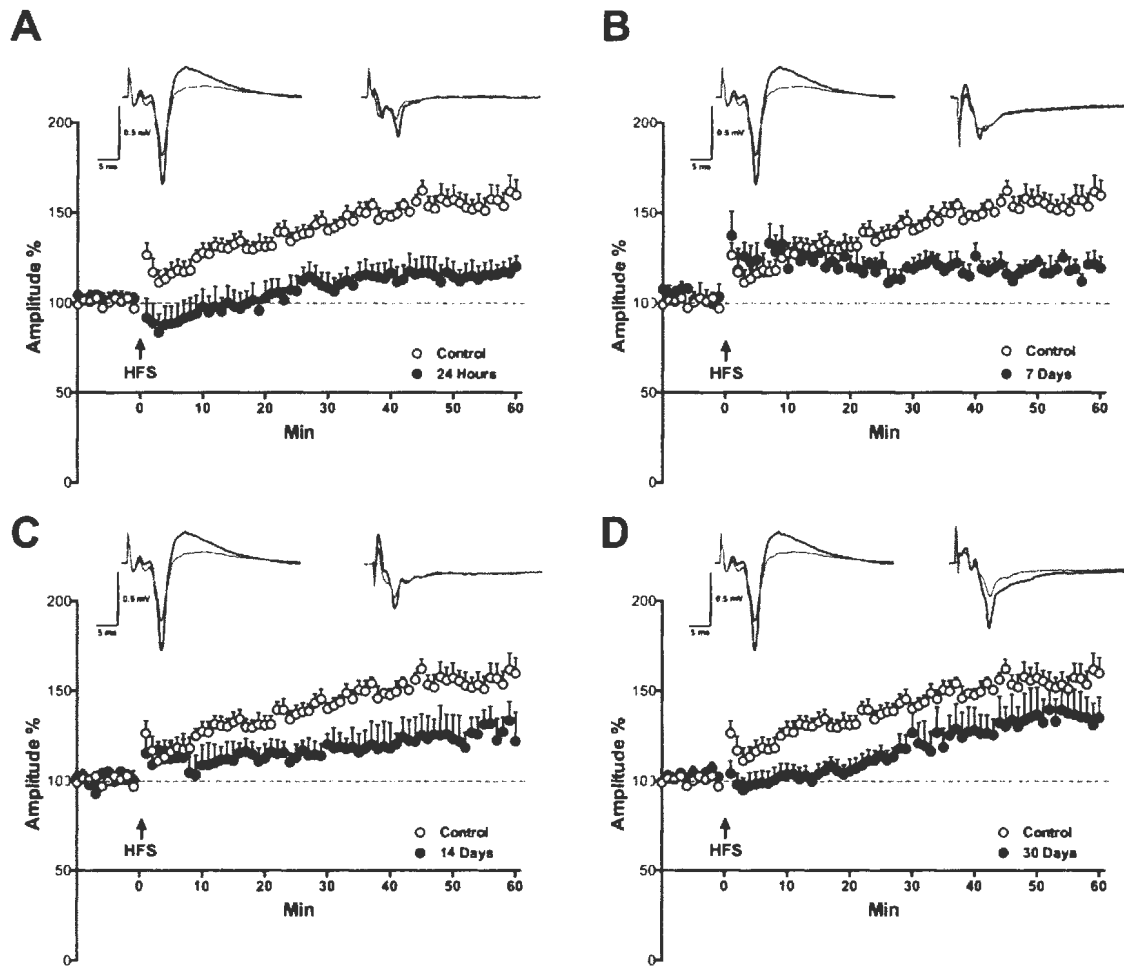


Figure 13 Effects of soman exposure on Long-Term Potentiation in the BLA. The plots show the time course of the changes in the amplitude of the field potentials after high-frequency stimulation (HFS). The amplitude of the 3 responses recorded in each min (stimulation at 0.05 Hz) was averaged, and each data point on the plots is the mean and standard error of these averages, from 7 to 10 slices (see sample sizes in the text). Traces over the plots are examples from a control rat and from soman-exposed rats studied at the indicated time-point after exposure; the superimposed field potentials are a baseline response and a response at 50 to 60 min after HFS (each trace is the average of 10 to 15 sweeps). Potentiation of the responses, measured at 50 to 60 min after HFS, was significantly lower – compared to the control group – at 24 hours, 7 days and 14 days post-exposure, but not at 30 days post-exposure.

DISCUSSION

After exposure of rats to lethal doses of soman, we found that more than 90% of AChE is inhibited at the onset of SE in brain regions that play a key role in seizure generation, and it takes up to two weeks for AChE activity to recover to normal levels. Significant neuronal loss and neurodegeneration was present in the BLA throughout the time period examined, from 24 hours to 30 days after soman exposure. Interestingly, at the 24-hour time point, there was no significant loss of GABAergic interneurons. However, by 7 days post-exposure, the number of GABAergic interneurons in the BLA was reduced, and by 14 and 30 days after soman, the ratio of GABAergic interneurons to the total number of neurons was lower compared to controls. At the same time points (14 and 30 days post-exposure), anxiety-like behavior was increased in the soman-exposed rats. Pathophysiological alterations accompanied the neuropathological damage and the behavioral deficits, namely a prolongation of evoked BLA field potentials and an increase in paired-pulse ratio, at all time points examined, as well as impaired synaptic plasticity at 24 hours, 7 days and 14 days post-exposure.

Inhibition and recovery of AChE

Nerve agents exert their toxic effects, including the induction of seizures, by inhibiting AChE (25; 115) via phosphorylation of the enzyme (263). It has been previously observed that during nerve agent-induced convulsions, brain AChE is inhibited dramatically (27; 145). In the present study, we found that at the onset of SE after administration of soman, AChE has been inhibited by more than 90% in the BLA, piriform cortex, hippocampus, and prelimbic cortex, regions that play an important role in seizure generation by nerve agent exposure (195; 230). It is noteworthy, in this regard,

that a reduction of AChE activity of about 91% in the hippocampus and 87% in the piriform cortex after soman exposure is not accompanied by seizures if AChE in the BLA is not inhibited significantly (230).

Previous studies have examined AChE inhibition after administration of organophosphorus pesticides (46; 135; 142), or nerve agents (55; 105; 158), however, there have been no systematic studies of the time course of AChE inhibition and the recovery of its activity after exposure to lethal doses of a nerve agent that induces prolonged status epilepticus. Here, we found that AChE was still inhibited by more than 90% at 24 hours post-exposure (Figure 7), when SE has stopped. This observation does not contradict the view that elevated acetylcholine (ACh) (due to inhibition of AChE) is the cause of seizures. First, it is well-understood that elevated ACh initiates seizures after nerve agent exposure, but seizures are sustained and reinforced by glutamatergic mechanisms (36; 176; 177); therefore, the duration and intensity of SE is not related to elevated ACh. Second, it appears that persistent inhibition of AChE does not necessarily correlate with persistent elevation of ACh at cholinergic synapses. Thus, Lallement et al. (1992) measured extracellular ACh levels for 90 min after soman-induced SE, in rats, and found that ACh returned to baseline concentrations within 50 min in septohippocampal areas, and within 90 min in the amygdala. The return of ACh to control levels – at a time when AChE remained inhibited – was attributed to negative feedback of the released ACh onto cholinergic terminals via muscarinic autoreceptors, and to the decreased availability of choline (145).

At 14 days after soman exposure, AChE had returned to control levels in the hippocampus, piriform, and prefrontal cortex, while in the BLA it recovered to nearly

basal levels in 7 days. The faster time course of recovery in the BLA may relate to the exceptionally dense cholinergic innervation of this region (183) – also reflected in the high basal level of AChE (31; 230) – which could result in a more efficient recovery of the enzyme. The recovery of AChE is probably the result of de novo AChE synthesis rather than dephosphorylation of the inhibited AChE, as the inhibition of AChE by nerve agents is irreversible, and the state of irreversibility is reached very fast after exposure to soman (263). The consequences of the prolonged AChE inhibition after soman exposure can be expected to include abnormal fluctuations of ACh concentrations at cholinergic synapses, with possible short-term and long-term effects on cholinergic receptor activity and expression.

Acute and delayed neuropathology

Significant neuronal death had occurred by 24 hours, and the extent of neuronal loss did not increase over time, despite ongoing neurodegeneration. The initial neuronal death was probably a process of excitotoxicity-induced necrosis, whereas the slow death of the degenerating neurons may result from simultaneous influences and competition of survival- and death-inducing factors (57; 96; 125). It has been shown previously that excitotoxic damage can induce either an immediate, necrotic death or a slow apoptotic death to the same neuronal population, where necrosis is associated with immediate loss of mitochondrial function, while apoptosis ensues in neurons that recover their mitochondrial function and energy levels, yet the excitotoxic insult has activated an endogenous cell death program (14). Our data suggest that BLA principal cells can undergo immediate, necrotic death (cell loss by 24 hours after exposure) or slow, apoptotic-like death (since neurodegeneration continues after the 24 hours). The relative

stability of the level of neuronal loss from 24 hours to 30 days post-exposure, in the presence of degenerating neurons and loss of interneurons, may be explained by a concomitant process of neuronal regeneration (59; 60).

As we have observed previously (90), at 24 hours post-exposure there was no loss of GABAergic interneurons, while by day 7, significant loss had occurred. Thus, GABAergic interneurons in the BLA appear to undergo only the apoptotic type of slow death. This does not imply that they are less vulnerable, as the interneuron to total number of neurons ratio decreased over time. However, it implies that they are less susceptible to necrosis and more susceptible to apoptosis, for reasons that remain to be determined. Delayed death of GABAergic interneurons has also been observed after pilocarpine-induced SE, as the majority of chronically degenerating FJC-positive neurons exhibited GAD-immunoreactivity (285). One factor contributing to the death of GABAergic interneurons may involve NMDA receptor-mediated excitotoxicity due to a gradual upregulation of D-serine (160), a positive NMDA receptor modulator (160; 191; 291).

By investigating the time course of neuronal loss beyond one week after soman exposure, in the present study, we found that although there was no significant further decrease of either the number of interneurons or the total number of neurons up to 30 days post-exposure, the small changes that occurred were sufficient to decrease the ratio of interneuron number to the total neuronal number. GABAergic interneurons account for only 15-20% of the neuronal population in the BLA (172; 245; 268) and tightly regulate principal cell excitability (149; 268; 293). Therefore, the reduction in the interneuronal population by about 46% by day 7 after soman exposure and the subsequent decrease of

the interneuronal to the total number of neurons ratio can be expected to have a significant impact on the excitability of the BLA network, contributing to the development of spontaneous recurrent seizures (68) and behavioral deficits.

Increased anxiety-like behavior and pathophysiological alterations

At 14 and 30 days after exposure to soman, the animals displayed increased anxiety-like behavior, assessed using the open field (233) and the ASR (122; 156; 157) tests. Increased anxiety has been observed previously after nerve agent exposure in animals (61; 165) and humans. Some of the victims of the Tokyo sarin attacks, for example, presented posttraumatic stress disorder, five or seven years after the events (124). Hyperexcitability of the amygdala, and the BLA in particular, is a characteristic feature of anxiety-like behavior in animals (44; 67; 246) and anxiety disorders in humans (143; 240; 282). Therefore, the increased anxiety in animals and humans after nerve agent exposure is likely to be due to neuropathological and pathophysiological alterations that have increased the excitability of the BLA network.

A number of factors may have contributed to increased BLA excitability, including damage to afferents from other brain regions (such as the prefrontal cortex) that, normally, suppress activity and excitability of the BLA. Alterations in the cholinergic regulation of the BLA can potentially contribute to BLA hyperexcitability, despite that AChE has recovered at the time that increased anxiety was observed. For example, we have found that the net effect of the α_7 -containing nicotinic acetylcholine receptor (α_7 -nAChR) activation in the BLA is an increase in GABAergic inhibition (225). Since the activity and expression of the α_7 -nAChR is sensitive to ACh exposure (98; 141), desensitization or downregulation of these receptors could increase BLA

excitability. Nevertheless, the present data suggest that the primary cause of an increased BLA excitability is probably the loss of GABAergic interneurons and the decreased ratio of the interneurons to the total number of neurons.

The pathophysiological significance of the interneuronal death was reflected in the increased duration of the field potentials evoked in the BLA and the increased PPR. In the soman-exposed rats, the field potentials were smaller and difficult to evoke, as it can be expected considering the significant neuropathological damage (neuronal loss and degeneration). At the same time, the decay of the field potentials was slower compared to controls; this suggests reduced GABAergic inhibition, resulting in the appearance of polysynaptic inputs and/or increased contribution of NMDA receptor-mediated synaptic activity to the evoked response. An increased PPR implies either that the probability of neurotransmitter release in response to the first pulse has been reduced, or that the evoked inhibition that normally suppresses the response to the second pulse is impaired. We do not know if there are alterations in the presynaptic release of glutamate, but considering the interneuronal loss and the prolongation of the field potentials, it is reasonable to suggest that the increased PPR reflects, at least in part, reduction of evoked GABAergic inhibition. Because the BLA does not have the discrete laminar architecture that other brain regions have, it cannot be ascertained if purely synaptic activity or population spikes contribute to the field potentials; the waveforms, however, suggest the presence of spiking activity in the evoked responses. When inhibition is reduced in the BLA, both the synaptic- (299) and the spiking component of the response to the second stimulus pulse can be expected to increase, producing an increased PPR.

The reduced inhibition may have facilitated the induction of LTP, despite the presence of severe neuronal damage. At 24 hours, 7 days, and 14 days after exposure, synaptic plasticity (as reflected in the synaptic capacity for LTP expression) was significantly impaired, but recovered by 30 days post-exposure. These results are consistent with previous behavioral data indicating severely impaired fear-conditioning at 8 days after soman exposure (187). The recovery of synaptic plasticity over time after soman-induced SE could be related to synaptic re-organization (182; 265).

The present study described the time course of AChE recovery in the brain, as well as neuropathological, behavioral, and pathophysiological alterations during 30 days after exposure of rats to soman, which corresponds, approximately, to 3 years of human life (250). We show that recovery of AChE is slow, which can have both acute and long-term consequences on the cholinergic modulation of neuronal excitability. The death of GABAergic interneurons is slow, which may provide an opportunity for pharmacological intervention to prevent it, if the mechanisms of this slow death become well-understood. Such intervention could have an impact in preventing long-term behavioral deficits, such as increased anxiety, which we found to persist at 30 days post-exposure. The apparent recovery of synaptic plasticity in the BLA by 30 days after exposure may suggest that at least certain aspects of fear-related learning may be normalized at this time, despite the persistence of increased BLA excitability, which may impact amygdala's modulation of cognitive processes.

ACKNOWLEDGMENTS

This work was supported by the CounterACT Program, National Institutes of Health, Office of the Director and the National Institute of Neurologic Disorders and

Stroke [Grant Number 5U01NS058162-07], and the Defense Threat Reduction Agency-Joint Science and Technology Office, Medical S&T Division [Grant Numbers CBM.NEURO.01.10.US.18 and CBM.NEURO.01.10.US.15].

Conflict of interest: The authors declare no conflict of interest.

Chapter 4: Pathophysiological Mechanisms Underlying Increased Anxiety After Soman Exposure: Reduced GABAergic Inhibition in the Basolateral Amygdala

Eric M. Prager^{1,3}, Volodymyr I. Pidoplichko¹, Vassiliki Aroniadou-Anderjaska^{1,2,3},
James P. Apland⁴, Maria F.M. Braga^{1,2,3*}

¹Department of Anatomy, Physiology, and Genetics

²Department of Psychiatry

³Program in Neuroscience

Uniformed Services University of the Health Sciences

4301 Jones Bridge Road

Bethesda, MD 20814, USA

⁴Neurotoxicology Branch

United States Army Medical Research Institute of Chemical Defense

Aberdeen Proving Ground, MD 21010, USA

Abbreviated title: Impaired Inhibition after Nerve Agent Exposure

Classification: Biological Sciences, Neuroscience

*Corresponding Author:

Maria F.M. Braga, D.D.S., Ph.D.

Department of Anatomy, Physiology, and Genetics

Uniformed Services University of the Health Sciences

4301 Jones Bridge Road

Bethesda, MD 20814

Phone: (301) 295-3524

Fax: (301) 295-3566

Email: maria.braga@usuhs.edu

ABSTRACT

The recent sarin attack in Syria killed 1,429 people, including 426 children, and left countless more to deal with the health consequences of the exposure. Prior to Syria, the nerve agent attacks in Japan have left many victims suffering from neuropsychiatric illnesses, particularly anxiety disorders, more than a decade later. Uncovering the neuro-pathophysiological mechanisms underlying the development of anxiety after nerve agent exposure is necessary for successful treatment. Anxiety is associated with hyperexcitability of the basolateral amygdala (BLA). The present study sought to determine the nature of the nerve agent-induced alterations in the BLA, which could explain the development of anxiety. At 24 hours and 14 days after exposure of rats to soman, at a dose that induced prolonged status epilepticus, spontaneous IPSCs (sIPSCs) in the BLA were reduced, along with reduction in the frequency but not amplitude of miniature IPSCs. In addition, activation of α_7 -nicotinic acetylcholine receptors, a cholinergic receptor that participates in the regulation of BLA excitability and is involved in anxiety, increased sEPSCs in both the soman-exposed rats and the controls, but was less effective in increasing sIPSCs in the soman-exposed rats. Despite the loss of both interneurons and principal cells after soman-induced status epilepticus, the frequency of sEPSCs was increased in the soman-exposed rats. Impaired function and cholinergic modulation of GABAergic inhibition in the BLA may underlie anxiety disorders that develop after nerve agent exposure.

Keywords: soman, basolateral amygdala, anxiety, GABA_A receptors, inhibition, alpha7 nicotinic receptors

SIGNIFICANCE STATEMENT

The recent sarin attack in Syria killed 1,429 people, including 426 children, and left countless more to deal with the health consequences of the exposure. Prior to Syria, the nerve agent attacks in Japan have left many victims suffering from neuropsychiatric illnesses, particularly anxiety disorders, more than a decade later. The biological mechanisms underlying the development of anxiety after nerve agent exposure are not known; uncovering these mechanisms is necessary for successful treatment. Our study suggests that a dramatic impairment in the function of the GABAergic system in the basolateral amygdala, including reduced tonic inhibition and impaired modulation by α_7 -nicotinic acetylcholine receptors, along with an increase in excitatory neurotransmission, may explain the development of anxiety disorders after nerve agent exposure.

INTRODUCTION

Many survivors of the August 2013 chemical nerve agent attack, which killed 1,429 Syrians including 426 children, will have to deal with the health consequences of the exposure (72). Nerve agents are organophosphorus compounds that irreversibly inhibit acetylcholinesterase (AChE), causing an accumulation of acetylcholine (ACh) at cholinergic synapses; hyperstimulation of cholinergic receptors raises the excitation level to the point of seizure generation. If pharmacological intervention is not immediately administered, cholinergic receptor hyperstimulation gives way to excessive activation of the glutamatergic system, which sustains and intensifies seizure activity (status epilepticus, SE), causing profound brain damage (174; 177; 222; 255) and long-term behavioral deficits (61; 91).

Currently approved antidotes can be effective in suppressing seizure activity if given immediately after an exposure (72). However, civilians are unequipped to self-administer antidotes after an attack, and delays of at least 30 min may occur before emergency personnel can safely assess victims to provide initial treatments (196; 296). Delaying treatment increases the incidence of neuropathology, as it has been observed in animal models of nerve agent exposure; seizures lasting 20 min cause brain damage in approximately 10% of animals, whereas 40 min of continuous seizures causes damage in approximately 79% of animals (174). If seizures are not controlled, 98% of surviving animals suffer moderate to severe neuropathology within 24 hours of nerve agent exposure (90; 174; 230; 231), and go on to develop long-term neurological and behavioral impairments. Victims of the Tokyo and Matsumoto sarin attacks, for example, reported symptoms associated with anxiety disorders over a decade after the attacks (124; 209). Similarly, animals display enduring anxiety- and fear-like behaviors after exposure

to soman (61; 91; 150; 187; 231). The mechanisms underlying the development of anxiety after nerve agent exposure are unknown. Knowledge of these mechanisms is necessary for successfully treating these behavioral impairments.

Anxiety disorders and, in particular, posttraumatic stress disorder (PTSD) were the most documented neuropsychiatric deficits observed after the Japan sarin attacks (296). PTSD and other anxiety disorders are associated with amygdalar hyperactivity (143) and volumetric loss (243). The basolateral amygdala (BLA), in particular, is recognized for its central role in the generation and expression of anxiety and fear (67; 82; 152; 223; 240; 252; 269). Because GABAergic inhibition in the BLA plays a central role in regulating network excitability (149; 268; 293) and anxiety-like behavior (277), we examined how GABAergic inhibition is altered 24 hours and 14 days after soman exposure in rats. In addition, we examined whether soman exposure alters the function of α_7 -nicotinic acetylcholine receptors (α_7 -nAChRs), which are involved in anxiety-like behavior (88), and were recently shown to modulate GABAergic inhibition in the BLA (225). Our results revealed deficits in GABAergic inhibitory synaptic transmission, diminished α_7 -nAChR-mediated enhancement of GABAergic activity, and increased spontaneous excitatory activity in the BLA after soman exposure.

RESULTS

Soman was administered to 78 rats. The average latency to Stage 3 seizure onset, which corresponds to the initiation of SE, was 5.76 ± 1.37 min. Of the surviving 19 rats, 12 rats developed prolonged SE (16; 89; 90) and were subsequently used for electrophysiological experiments. Aged-matched rats that were not exposed to soman served as controls.

Diminished GABAergic Inhibition after Soman-Induced SE

To determine whether GABAergic inhibition was reduced after SE, we recorded GABA_A receptor-mediated spontaneous inhibitory postsynaptic currents (sIPSCs) from principal neurons in the BLA, in the presence of α -conotoxin AulB (1 μ M), DH β E (10 μ M), atropine sulfate (0.5 μ M), D-AP5 (50 μ M), CNQX (20 μ M), SCH50911 (10 μ M), and LY 3414953 (3 μ M) at a holding potential of +30 mV. Principal neurons were identified based on their firing pattern in response to depolarizing current pulses in the current clamp mode, and the presence of the I_h current activated by hyperpolarizing voltage-steps, in the voltage-clamp mode (21; 218; 225; 245). The mean frequency of sIPSCs was reduced from 11.35 ± 0.61 Hz in the control rats (n = 20), to 6.63 ± 0.88 Hz (n = 18; $P < 0.001$) at 24 hours after soman exposure, and 7.78 ± 0.58 Hz (n = 24; $P = 0.001$) at 14 days after exposure, reflecting a $41.5 \pm 7.7\%$ and $32.3 \pm 5.2\%$ reduction at the 24 hour and the 14 day time points, respectively (Figure 14A and B). The mean amplitude of sIPSCs in the soman-exposed rats was also reduced compared to controls (75.5 ± 9.2 pA), by $37.2 \pm 3.9\%$ (47.4 ± 2.9 pA; $P = 0.005$) at 24 hours, and $35.0 \pm 4.7\%$ (49.1 ± 3.5 pA; $P = 0.005$) at 14 days after exposure (Figure 14A and C). There were no significant differences between soman-exposed rats and control rats in the rise time and the decay time constant of the sIPSCs. These results suggest a reduced inhibitory tone of BLA pyramidal cells at 24 hours and 14 days after SE.

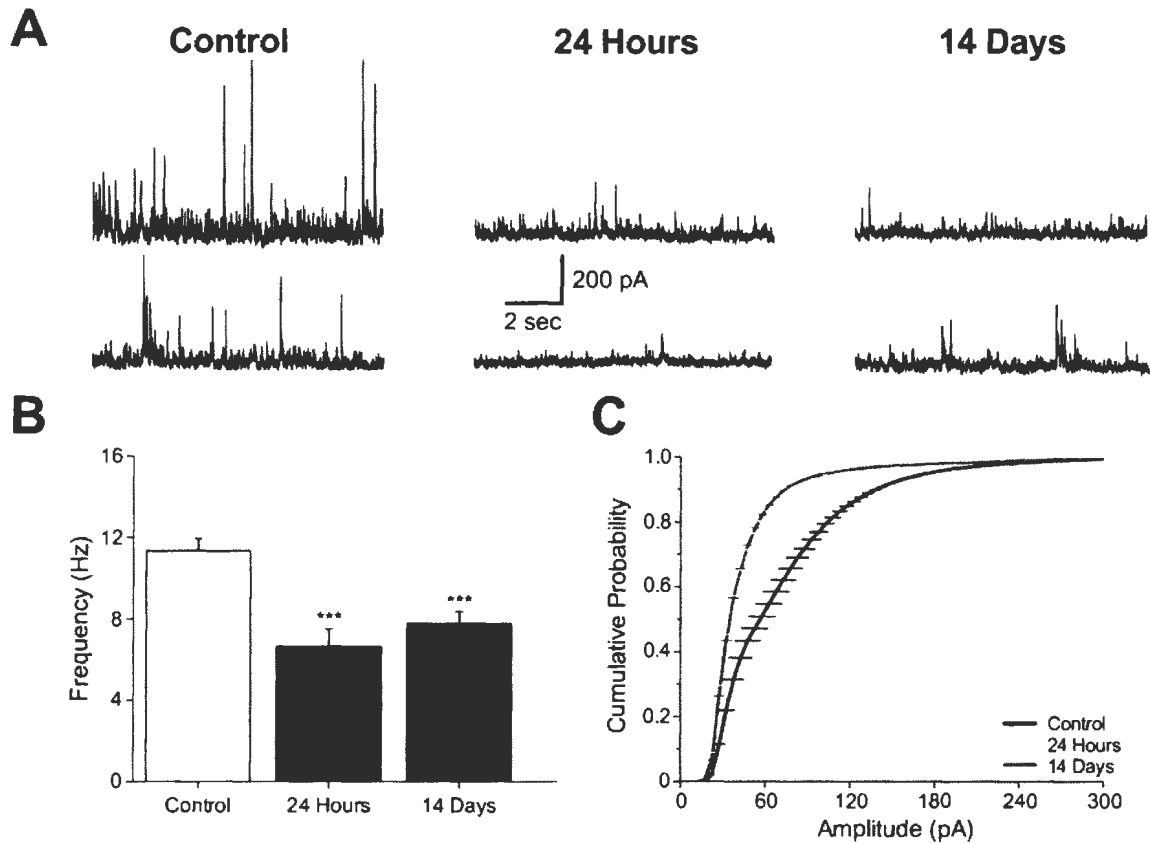


Figure 14 Exposure to soman reduces the frequency and amplitude of GABA_A receptor mediated spontaneous IPSCs. Recordings are from BLA principal cells at a holding potential of +30 mV and internal chloride concentration of 10 mM. (A) Representative traces of sIPSCs recorded from BLA pyramidal cells in slices obtained from control animals and from animals at 24 hours and 14 days after soman exposure. (B) Significant decreases in the frequency of sIPSCs was observed at 24 hours ($n = 18$; 6.63 ± 0.88 Hz; $P < 0.001$) and 14 days ($n = 24$; 7.78 ± 0.58 Hz; $P = 0.001$) after soman exposure compared to controls ($n = 20$; 11.35 ± 0.61 Hz). (C) Cumulative probability amplitude distributions of sIPSCs. The mean amplitude of sIPSCs was significantly reduced at 24 hours (47.39 ± 2.91 pA; $P = 0.005$) and 14 days (49.06 ± 3.52 pA; $P = 0.005$) after exposure compared to controls (75.51 ± 9.20 pA). *** $P < 0.001$ (One-way ANOVA with Tukey post hoc).

To determine whether the reduction of sIPSCs was associated with a decreased responsiveness of postsynaptic GABA_A receptors or reduced presynaptic GABA release, we recorded action potential-independent, miniature IPSCs (mIPSCs) from BLA pyramidal neurons of soman-exposed and control rats. mIPSCs were recorded at a

holding potential of +30 mV in the presence of α -conotoxin Au1B (1 μ M), DH β E (10 μ M), atropine sulfate (0.5 μ M), D-AP5 (50 μ M), CNQX (20 μ M), SCH50911 (10 μ M), LY 3414953 (3 μ M), and TTX (0.5 μ M). The mean frequency of mIPSCs was reduced from 7.41 ± 0.47 Hz in control rats ($n = 20$) to 3.19 ± 0.24 Hz ($n = 17$; $P < 0.001$) at 24 hours, and 4.75 ± 0.28 Hz ($n = 24$; $P < 0.001$) at 14 days after exposure, reflecting a $57.0 \pm 3.2\%$ and $36.0 \pm 3.8\%$ reduction at the two time points, respectively (Figure 15A and B). There were no significant differences in mIPSC amplitude between the SE groups (24-hour, 34.9 ± 0.76 pA; 14 day, 37.6 ± 1.4 pA) and the controls (35.9 ± 1.3 pA; P 's > 0.05) (Figure 15C). In addition, there were no significant differences between rats exposed to soman and control rats in the rise time and the decay time constant of the mIPSCs. Thus, the reduced frequency and amplitude of sIPSCs (Figure 14) did not involve a decrease in the responsiveness of postsynaptic GABA_A receptors.

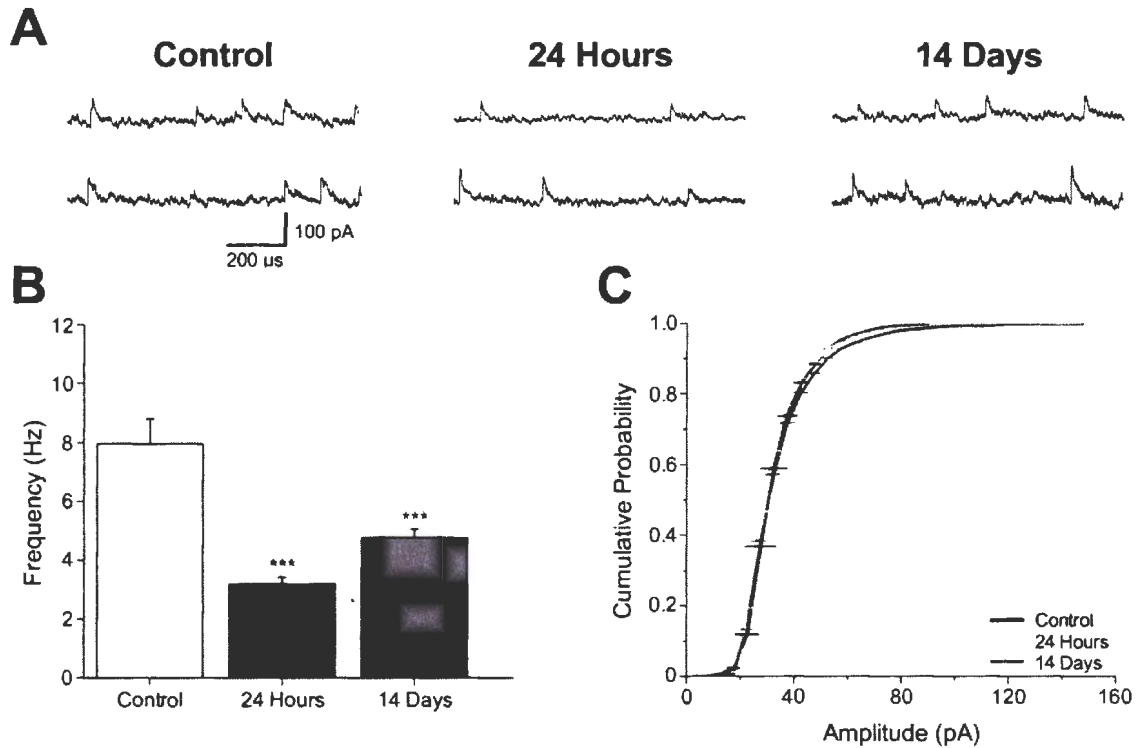


Figure 15 Exposure to soman reduces the frequency but not the amplitude of GABA_A receptor mediated miniature IPSCs. Recordings are from BLA principal cells at a holding potential of +30 mV and internal chloride concentration of 10 mM. (A) Representative traces of mIPSCs recorded from BLA pyramidal cells, in slices obtained from control animals and from animals at 24 hours and 14 days after soman exposure. (B) A significantly lower frequency of mIPSCs was observed at 24 hours ($n = 17$; 3.19 ± 0.24 Hz; $P < 0.001$) and 14 days ($n = 24$; 4.75 ± 0.28 Hz; $P < 0.001$) after exposure, compared to controls ($n = 20$; 7.41 ± 0.47 Hz). (C) Cumulative probability amplitude distributions of mIPSCs. *** $P < 0.001$ (One-way ANOVA with Tukey post hoc).

Impaired α_7 -nAChR Mediated Enhancement of Inhibitory Synaptic Transmission after Soman-Induced SE

The α_7 -nAChRs are expressed on both GABAergic interneurons and glutamatergic neurons in the BLA (141; 225); activation of these receptors enhance both spontaneous excitatory postsynaptic currents (sEPSCs) and sIPSCs, but the increase of sIPSCs is significantly greater than the increase of sEPSCs (225). To determine if the

modulation of GABAergic transmission by α_7 -nAChRs had been altered in the soman-exposed rats, we bath applied choline chloride while recording from principal neurons, in the presence of α -conotoxin AulB (1 μ M), DH β E (10 μ M), atropine sulfate (0.5 μ M), D-AP5 (50 μ M), CNQX (20 μ M), SCH50911 (10 μ M), and LY 3414953 (3 μ M), at a +30 mV holding potential. Choline chloride (5 mM) was bath-applied at a flow rate of ~8 ml/min. The effect was immediate and consisted of the transient appearance of a barrage of sIPSCs (Figure 16A), as we have observed previously (225). To quantify the effects, we calculated the total charge transferred during choline application. The charge, in pico Coulombs (pC), was calculated as the area delimited by the inhibitory current and the baseline (225). The measurement of the charge transferred was made using a 30 second time window from the peak of the effect. In the control slices, choline application increased the charge transferred increased to $8,872.3 \pm 809.8$ pC (from a baseline of 224.4 ± 48.5 pC; $P < 0.001$; paired t-test; $n = 17$). Twenty-four hours and 14 days after soman exposure, the charge transferred in the presence of choline chloride increased from 58.4 ± 10.6 pC to $3,986.4 \pm 671.6$ pC ($n = 16$) and from 73.7 ± 10.1 pC to $6,262.2 \pm 684.3$ pC ($n = 22$; P 's < 0.001 ; paired t-test), at the two time points, respectively. The total charge transferred by GABA_A current in the presence of choline was significantly smaller in the 24-hour soman ($P < 0.001$) and the 14-day soman group ($P = 0.032$) compared to the controls (Figure 16B). In addition, the mean amplitude of the sIPSCs recorded in the presence of choline was significantly reduced at 24 hours (95.7 ± 6.9 pA; $P = 0.037$) but not at 14 days (121.6 ± 7.8 pA; $P = 0.938$) after exposure, compared to controls (125.3 ± 8.2 pA) (Figure 16C). These results suggest that the α_7 -nAChR mediated enhancement of GABAergic inhibition is impaired after soman exposure.

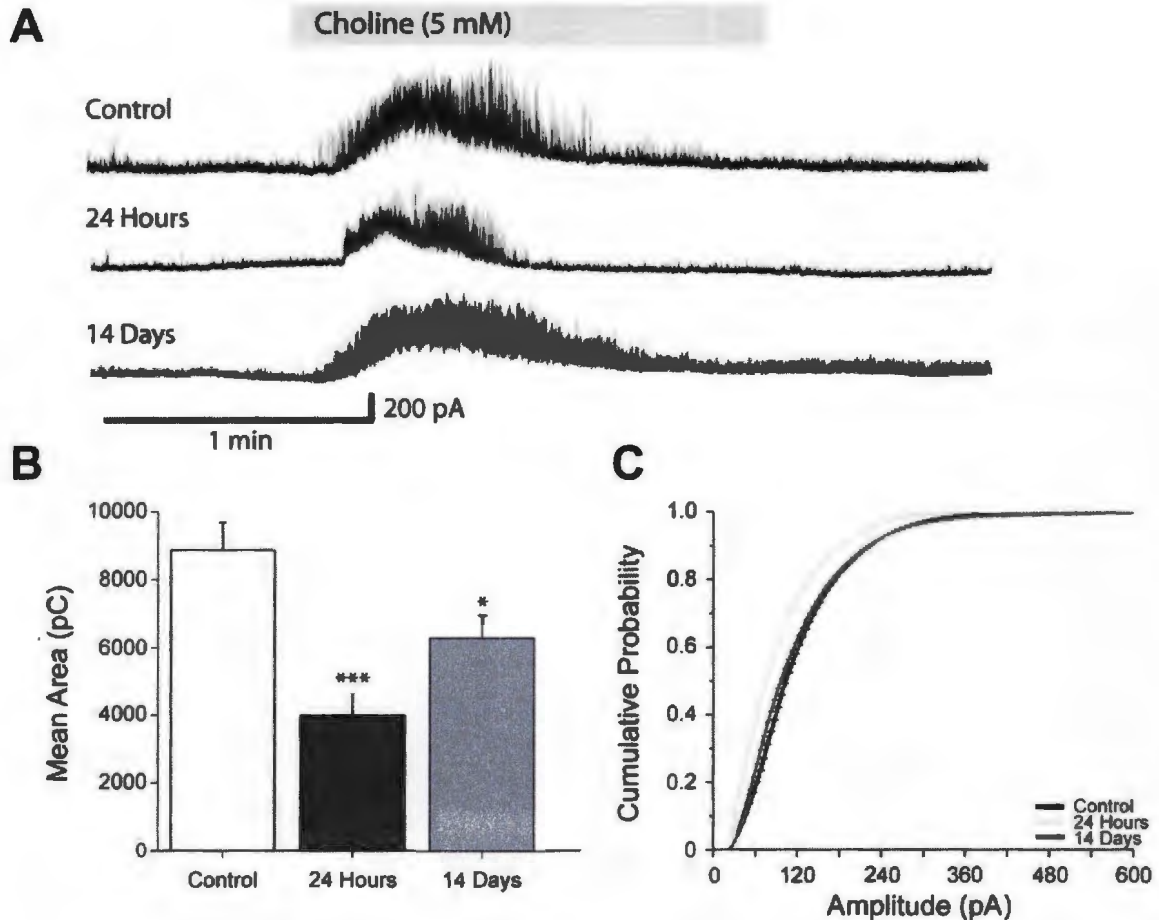


Figure 16 Exposure to soman impairs the α_7 -nAChR-mediated enhancement of spontaneous inhibitory synaptic transmission. Recordings are from BLA principal cells at a holding potential of +30 mV and internal chloride concentration of 10 mM. (A) Bath application of choline chloride (5 mM) increased the frequency and amplitude of sIPSCs in control slices, as well as in slices obtained from animals at 24 hours and 14 days after soman exposure. (B) The increase in the charge transferred by sIPSCs upon application of choline chloride was significantly lower at 24 hours after soman exposure ($n = 16$, $P < 0.001$) and 14 days after exposure ($n = 22$, $P = 0.032$) compared to the controls ($n = 17$). (C) Cumulative probability amplitude distributions of sIPSCs in the presence of choline. The mean amplitude of sIPSCs was significantly reduced at 24 hours ($P = 0.037$), but not at 14 days ($P = 0.938$) after exposure, compared to controls. * $P < 0.05$; *** $P < 0.001$ (One-way ANOVA with Dunnett T post hoc).

To determine if the α_7 -nAChR-mediated enhancement of excitatory activity was also impaired in the soman exposed rats, we recorded sEPSCs and sIPSCs simultaneously

from principal neurons in the presence of α -conotoxin Au1B (1 μ M), DHBE (10 μ M), atropine sulfate (0.5 μ M), D-AP5 (50 μ M), SCH50911 (10 μ M), and LY 3414953 (3 μ M), at a holding potential of -58 mV and internal chloride concentration of 1 mM. Bath application of choline chloride (5 mM) increased both sIPSCs and sEPSCs (Figure 17). The current areas were analyzed for a time period of 5 seconds from the start of the response. The increase in charge transferred by sEPSCs in control slices (from 4.0 ± 0.6 pC to 15.5 ± 1.9 pC), was not significantly different from the increase in the 24-hour soman group (from 3.9 ± 0.5 pC to 14.3 ± 1.7 pC), or the 14-day soman group (from 3.1 ± 0.5 pC to 11.7 ± 1.4 pC; P 's > 0.05 , Figure 17D). On the other hand, the charge transferred by sIPSCs in the presence of choline chloride was increased from 3.3 ± 0.7 pC to 137.9 ± 28.9 pC in the control rats ($n = 12$), from 3.0 ± 0.5 pC to 70.2 ± 10.5 pC in the 24 hour soman group ($n = 16$, $P = 0.017$ compared to controls), and from 1.1 ± 0.3 pC to 47.4 ± 7.3 pC in the 14 day soman group ($n = 14$, $P = 0.002$ compared to controls; Figure 17E). Thus, soman exposure does not impair the α_7 -nAChR-mediated enhancement of excitatory activity in the BLA.

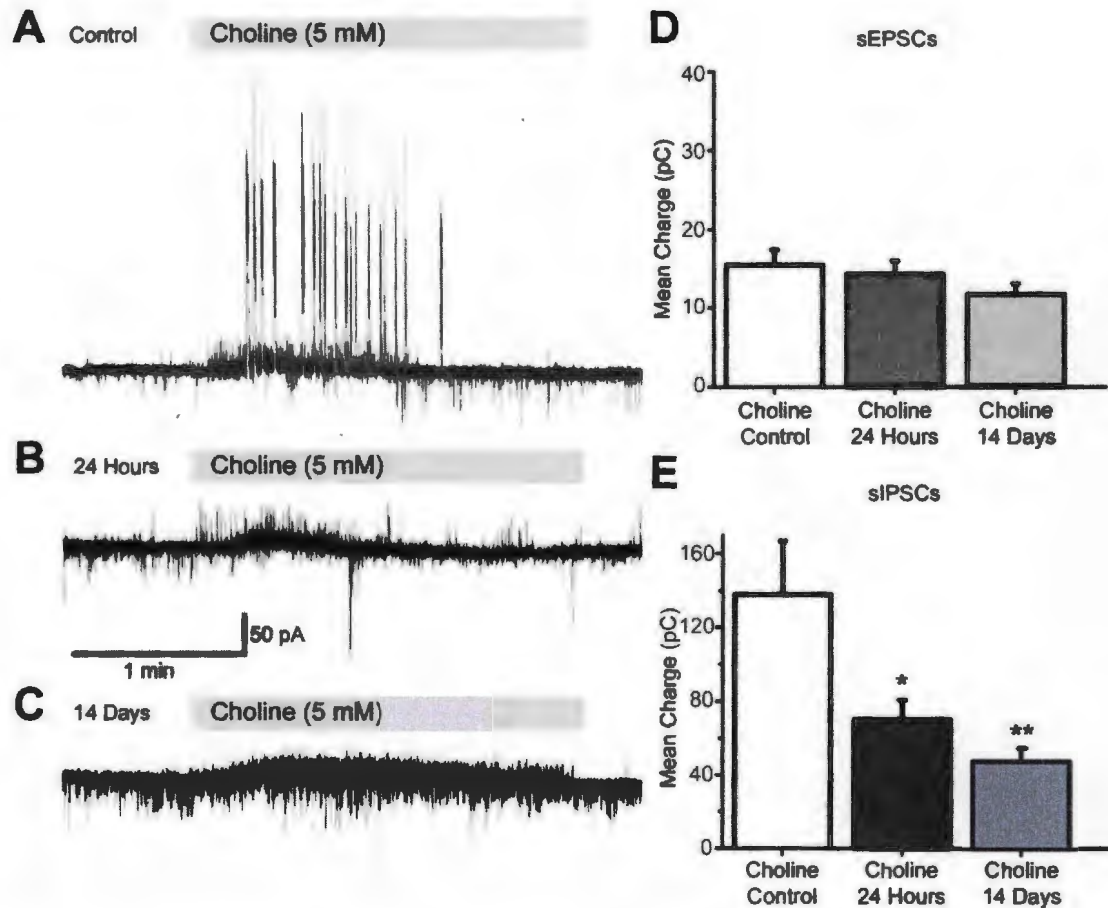


Figure 17 The α_7 -nAChR-mediated enhancement of spontaneous excitatory synaptic transmission is not impaired after soman exposure. Recordings were obtained from principal neurons at a holding potential of -58 mV and internal chloride concentration of 1 mM. (A-C) Bath application of choline chloride (5 mM) induced a transient increase in the frequency and amplitude of both sIPSCs (outward currents) and sEPSCs (inward currents). (D) The charge transferred by sEPSCs during choline application was not significantly altered at 24 hours or 14 days after soman exposure compared to controls. (E) The charge transferred by sIPSCs was significantly reduced at 24 hours ($n = 16$; $P = 0.017$) and 14 days ($n = 14$; $P = 0.002$) after soman exposure compared to controls ($n = 12$). * $P < 0.05$; ** $P < 0.01$ (One-way ANOVA with Dunnett T post hoc).

Increased Spontaneous Excitatory Activity after Soman-Induced SE

After soman-induced SE, the BLA suffers significant loss of both principal cells and interneurons (90; 231). The loss of principal neurons could produce a reduction in tonic glutamatergic activity. However, this could be compensated by the concomitant loss

of interneurons and the decreased tonic inhibition (Figure 14 and 15). To determine whether there are alterations in the tonic glutamatergic activity in the BLA after soman exposure, we recorded sEPSCs from principal neurons in the presence of α -conotoxin Au1B (1 μ M), DH β E (10 μ M), atropine sulfate (0.5 μ M), D-AP5 (50 μ M), SCH50911 (10 μ M), and LY 3414953 (3 μ M), at a holding potential of -58 mV and internal chloride concentration of 1 mM. The mean frequency of sEPSCs was 6.3 ± 0.5 Hz in the control rats, 11.9 ± 1.3 Hz in the 24 hour soman group ($P < 0.001$ compared to controls), and 9.7 ± 1.6 Hz in the 14 day soman group ($P = 0.040$ compared to controls), reflecting a $87.7 \pm 21.0\%$ and $54.0 \pm 25.4\%$ increase after soman exposure, at 24 hours and 14 days, respectively (Figure 18A). There were also differences between the control group and the soman-exposed rats in the amplitude of the sEPSCs. The mean amplitude of sEPSCs was 12.8 ± 0.3 pA in control rats ($n = 28$), 14.1 ± 0.6 pA in the 24 hour soman group ($n = 16$; $P = 0.172$) and 14.8 ± 1.0 pA in the 14 day soman group ($n = 14$; $P = 0.031$). The amplitude distribution in the three groups is shown in Figure 18B.

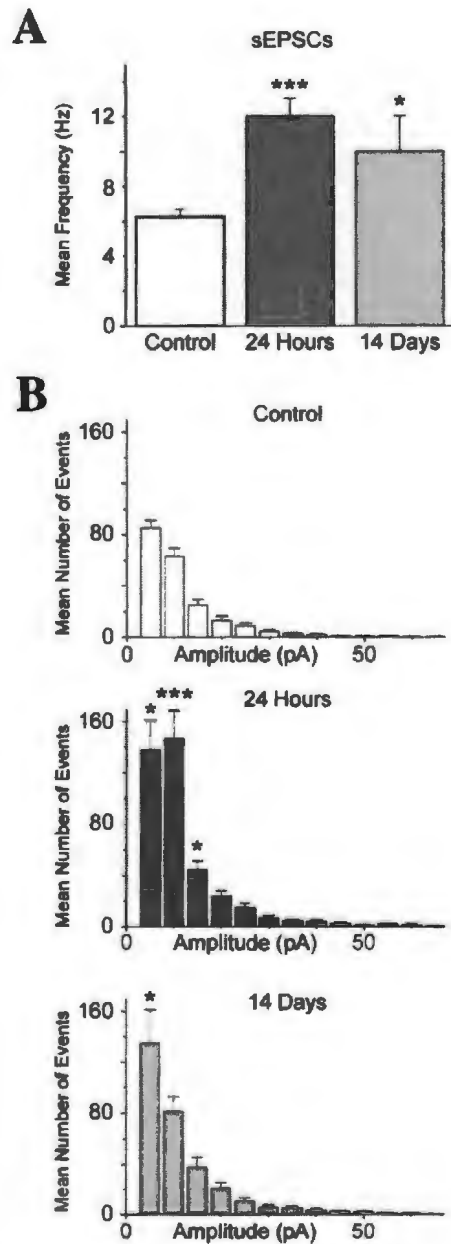


Figure 18 Spontaneous excitatory synaptic transmission is increased after soman exposure. Recordings were obtained from principal neurons at a holding potential of -58 mV and internal chloride concentration of 1 mM. (A) The frequency of sEPSCs was greater at 24 hours ($P < 0.001$; $n = 16$) and 14 days ($P = 0.04$; $n = 14$) after soman exposure, compared to controls ($n = 28$). (B) Amplitude-frequency histograms showing the effects of soman on sEPSCs, at 24 hours ($n = 16$) and 14 days ($n = 14$) after exposure, compared to controls ($n = 28$). * $P < 0.05$; ** $P < 0.01$; *** $P < 0.001$ (One-way ANOVA with Dunnett T post hoc).

DISCUSSION

The most debilitating neuropsychiatric symptoms reported by victims of the Japan sarin attack, more than a decade later, were indicative of anxiety disorders, including PTSD (296). However, the pathophysiological mechanisms underlying these enduring emotional deficits have been unknown. This is the first study to provide evidence that anxiety disorders caused by nerve agent exposure are due to reduced GABAergic inhibition in the BLA and increases in spontaneous excitatory activity. The observed decrease in spontaneous inhibitory synaptic transmission after soman exposure was not due to postsynaptic alterations in GABA_A receptor function, as there was no significant decrease in the amplitude of GABA_A receptor-mediated mIPSCs. We also found that activation of α_7 -nAChRs by choline chloride was less effective in enhancing inhibitory activity in the soman-exposed rats compared to controls, while there was no significant difference between the groups in the enhancement of sEPSCs upon α_7 -nAChR activation. Spontaneous glutamatergic activity was enhanced in the BLA of the soman-exposed rats, which was probably a result of the decreased inhibitory tone. As anxiety disorders are associated with increased excitatory activity and excitability in the BLA (82; 143; 223) the data presented here explain the development of anxiety after nerve agent exposure.

The presence of anxiety disorders that ensued in the Japan sarin-attack victims (124; 209) was accompanied by reduced regional gray matter volumes in the amygdala (243). Similar observations have been made in animals, where exposure to soman has caused amygdalar atrophy (50; 107) and enduring increases in anxiety- and fear-like behaviors (61; 91; 150; 187; 231). The decreases in gray matter volume after nerve agent exposure reflect the death of principal neurons and GABAergic interneurons (90; 174;

231; 255). GABAergic interneurons in the BLA account for approximately 15-20% of the total neuronal population (172; 245; 268), and tightly regulate principal neuron excitability (148; 214; 228; 266). Our results suggest that the dramatic reduction in spontaneous GABAergic activity after soman exposure, due to deficits in GABA release or the loss of GABAergic interneurons (90; 231), disrupts the capability of inhibitory inputs to regulate excitatory neurons in the BLA, causing a significant increase in glutamatergic activity; this can promote hyperactivity in the BLA network and ultimately result in the development of anxiety (67; 82; 152; 239; 282). In consistency with this view, it has been previously shown that damage to GABAergic interneurons in the BLA leads to anxiety-like behavior (277).

Interestingly, after soman-induced SE, there is a significant loss of principal BLA neurons already at 24 hours after the exposure, but the number of GABAergic interneurons is not reduced at this early time point; when examined 7 days later, interneurons are also significantly reduced, and by 14 days after exposure, the ratio of the number of GABAergic interneurons to the total number of neurons in the BLA is significantly decreased (231). The results presented here indicate that tonic GABAergic activity is already dramatically decreased at 24 hours after exposure, despite that there is no evidence of interneuronal death at this time point, suggesting that the function of interneurons is already compromised. Assuming that the interneurons maintain the viability of all of their inhibitory presynaptic terminals, at 24 hours post-exposure, the reduced frequency of the mIPSCs at that time point would suggest deficits in quantal release of GABA, as it has been observed in models of temporal lobe epilepsy (121).

A number of modulatory systems are involved in regulating BLA excitability, mainly by affecting the excitability state of the principal cells and/or the GABAergic interneurons. The cholinergic input to the amygdala from the basal forebrain appears to be of major importance in this regard, as suggested by the remarkably dense cholinergic innervation of the BLA (183), its exceptionally high AChE activity (31; 230; 231), as well as the increase in anxiety-like behavior when the function of the basal forebrain is disrupted (169). The most well known behavioral evidence for the importance of the cholinergic system in the regulation of amygdalar function comes from the symptoms of Alzheimer's disease, where anxiety is prevalent (80; 87). In the case of anxiety that develops after nerve agent exposure, its association with impairments in the cholinergic modulation of the BLA would not be surprising, particularly considering that inhibition of AChE is the primary effect of nerve agents, and AChE in the BLA remains inhibited for about a week (230); the resulting long-term derangements in cholinergic activity are likely to affect the function of the cholinergic system. From the different types of cholinergic receptors, the α_7 -nAChRs have been shown to play an anxiolytic role (32; 88), and we recently demonstrated that in the rat BLA α_7 -nAChR activation increases both sIPSCs and sEPSCs, but the net effect is a transient, dramatic increase of GABAergic activity (225). Here, we found that after exposure to soman, the α_7 -nAChR-mediated enhancement of inhibitory activity – but not the excitatory activity – is impaired. The most plausible explanation of these results is that the loss of principal BLA neurons in the soman-exposed rats (231) is not high enough to significantly impair the increase of excitatory activity upon α_7 -nAChR activation, while the 46% loss of interneurons (231) has more profound consequences, including an impaired enhancement

of inhibitory activity when α_7 -nAChRs are activated in the BLA network. The involvement of other mechanisms, such as differential alterations in the function or density of α_7 -nAChRs on BLA interneurons versus principal cells cannot be excluded. The impaired modulation of GABAergic inhibition by α_7 -nAChRs after soman exposure may contribute to BLA hyperexcitability and the development of anxiety.

A major health concern for survivors of the Syrian nerve agent attack is the development of anxiety disorders. Thus far, no effective treatments against chronic neuropsychiatric and neurological symptoms caused by nerve agent exposure have been developed (53; 72). Individuals with anxiety disorders are often treated with pharmacological agents that target the GABAergic system to enhance inhibitory transmission and thus reduce anxiety (65; 241). Epidemiological studies have shown that treatments targeting the GABAergic system have repeatedly failed to alleviate symptoms associated with PTSD (41; 51; 65; 241). While unclear why these drugs fail to mitigate the majority of symptoms associated with PTSD, our study suggests that a severely impaired inhibitory function in the BLA may be a reason for the lack of effectiveness of these compounds. Our results also suggest that targeting excitatory synaptic transmission may be a more direct and efficacious therapeutic strategy to reduce BLA hyperexcitability and the expression of anxiety in PTSD patients after nerve agent exposure. Following this strategy, a new class of therapeutic options can become available. For example, antagonists of kainate receptors containing the GluK1 subunit are not effective only against nerve agent-induced seizures and brain damage (90), but they also have anxiolytic effects (21).

The present study showed that exposure to a nerve agent, at a dose that induces prolonged SE, damages the function of the GABAergic system in the BLA, resulting in significantly increased tonic excitatory activity. This is evidence of BLA hyperexcitability, which is a characteristic feature of anxiety disorders (82; 240; 252; 269). These findings, therefore, suggest that the development of anxiety disorders after nerve agent exposure, as seen in the victims of the sarin attacks in Japan, is not necessarily due to the stress component of the experience, but rather it can be due to the damage of the GABAergic system by the seizures induced by the nerve agent. It is conceivable that any brain insult that produces long-term hyperexcitability in the BLA, by impairing GABAergic inhibition and/or by other mechanisms, can have the potential to culminate in development of anxiety. Our findings also suggest that because GABAergic inhibition in the BLA can be severely damaged after nerve agent exposure, a more efficacious approach to treating anxiety in exposure victims may be to suppress glutamatergic excitatory activity.

MATERIALS AND METHODS

Animals

Experiments were performed using 27-30 day old (~75 g) male, Sprague-Dawley rats (Charles River Laboratories, Inc., Wilmington, MA). Animals were individually housed in an environmentally controlled room (20-23°C, ~44% humidity, 12-h light/12-h dark cycle [350-400 lux], lights on at 6:00 am), with food (Harlan Teklad Global Diet 2018, 18% protein rodent diet; Harlan Laboratories; Indianapolis, IN) and water available *ad libitum*. Cages were cleaned weekly and animal handling was minimized to reduce animal stress (232). All animal experiments were conducted following the Guide for the

Care and Use of Laboratory Animals (Institute of Laboratory Animal Resources, National Research Council), and were approved by the U.S. Army Medical Research Institute of Chemical Defense and the Uniformed Services University of the Health Sciences Institutional Animal Care and Use Committees.

Experimental Procedures

Soman Administration and Drug Treatment

Soman (pinacolyl methylphosphonofluoridate) obtained from Edgewood Chemical Biological Center (Aberdeen Proving Ground, MD, USA) was diluted in cold saline and administered via a single subcutaneous injection (149 $\mu\text{g}/\text{kg}$), which, based on previous studies, is an approximate dose of $1.35 \times \text{LD}_{50}$ (90; 129). To increase survival rate, rats were administered 2 mg/kg atropine sulfate (Sigma, St. Louis MO) 20 minutes after injection of soman. Rats were monitored for signs of seizure onset, and continuously rated for seizure severity according to the modified Racine Scale: Stage 0, no behavioral response; Stage 1, behavioral arrest, orofacial movements, chewing; Stage 2, head nodding/myoclonus; Stage 3, unilateral/bilateral forelimb clonus without rearing, straub tail, extended body posture; Stage 4, bilateral forelimb clonus plus rearing; Stage 5, rearing and falling; Stage 6, full tonic seizures (236; 237). Control animals received atropine sulfate, and were injected with saline instead of soman.

Electrophysiological Experiments

Twenty-four hours or 14 days after soman exposure, animals were anesthetized with 3-5% isoflurane before decapitation. Coronal brain slices (400 μm -thick) containing the amygdala (-2.64 to -3.36 from Bregma) were cut using a vibratome (Leica VT 1200 S; Leica Microsystems, Buffalo Grove, IL), in ice-cold cutting solution consisting of (in

mM): 115 sucrose, 70 NMDG, 1 KCl, 2 CaCl₂, 4 MgCl₂, 1.25 NaH₂PO₄, 30 NaHCO₃.

The slices were transferred to a holding chamber, at room temperature, in a bath solution containing (in mM): 125 NaCl, 2.5 KCl, 1.25 NaH₂PO₄, 21 NaHCO₃, 2 CaCl₂, 1 MgCl₂, and 11 D-glucose. Recording solution was the same as the holding bath solution. All solutions were saturated with 95% O₂ / 5% CO₂ to achieve a pH near 7.4. The recording chamber (0.7 mL capacity) had continuously flowing ACSF (~6-8 mL/min) at temperature 32~33°C. The osmolarity of this external solution was adjusted to 325 mOsm with D-glucose.

Whole-cell recordings were obtained from neurons visualized under infrared light using Nomarski optics of an upright microscope (Zeiss Axioskop 2, Thornwood, NY) through a 40x water immersion objective, equipped with a CCD-100 camera (Dage-MTI, Michigan City, IN(90)). The patch electrodes had resistances of 3.5–4.5 MΩ when filled with the internal solution (in mM): 60 CsCH₃SO₃, 60 KCH₃SO₃, 10 KCl, 10 EGTA, 10 HEPES, 5 Mg-ATP, 0.3 Na₃GTP (pH 7.2), 290 mOsm (225). When sIPSCs and sEPSCs were recorded simultaneously, the internal chloride concentration was 1 mM, and osmolarity was adjusted with potassium gluconate. Tight-seal (over 1 GΩ) whole-cell recordings were obtained from the cell body of pyramidal neurons in the BLA region and were identified on the basis of their electrophysiological properties (218; 245). Access resistance (15–24 MΩ) was regularly monitored during recordings, and cells were rejected if the resistance changed by more than 15% during the experiment. Ionic currents and action potentials were amplified and filtered (1 kHz) using the Axopatch 200B amplifier (Axon Instruments, Foster City, CA) with a four-pole, low-pass Bessel filter, were digitally sampled (up to 2 kHz) using the pClamp 10.2 software (Molecular

Devices, Sunnyvale, CA), and analyzed using the Mini Analysis program (Synaptosoft Inc., Fort Lee, NJ), Origin (OriginLab Corporation, Northampton, MA), or GraphPad Prism (GraphPad Software, La Jolla, CA). In some experiments, the charge transferred by postsynaptic currents was calculated, using the Mini60 software by Synaptosoft (Synaptosoft Inc., Fort Lee, NJ).

Drugs used were as follows: bicuculline methiodide, a GABA_A receptor antagonist, atropine sulfate, a muscarinic AChR antagonist, dihydro- β -erythroidine (DH β E), an $\alpha_4\beta_2$ nicotinic receptor antagonist, choline chloride, an α_7 agonist, and CNQX, an AMPA/kainate receptor antagonist (all purchased from Sigma-Aldrich, St. Louis; MO). We also used D-AP5, an NMDA receptor antagonist, SCH50911, a GABA_B receptor antagonist, α -conotoxin Au1B, an $\alpha_3\beta_4$ nicotinic receptor antagonist, and LY 341495, a metabotropic glutamate group II/III receptor antagonist (all purchased from Tocris, Ellisville, MO).

Statistical Analysis

Statistical values are presented as mean \pm standard error (SE). Analyses were conducted using a one-way ANOVA followed by Tukey or Dunnett T post-hoc tests. Results were considered statistically significant when $P < 0.05$. Sample size “ n ” refers to the number of recorded neurons.

Conflict of Interest: The authors declare no conflict of interest.

ACKNOWLEDGEMENTS

This work was supported by the CounterACT program, National Institutes of Health, Office of the Director and the National Institute of Neurologic Disorders and Stroke [Grant Number 5U01NS058162-07], and the Defense Threat Reduction Agency-Joint Science and Technology Office, Medical S&T Division [Grant Numbers CBM.NEURO.01.10.US.18 and CBM.NEURO.01.10.US.15].

Author Contributions: E.M.P, V.A-A, M.F.M.B designed research; E.M.P, V.I.P, J.P.A performed research; E.M.P, V.I.P analyzed data; and E.M.P, V.A-A, M.F.M.B wrote the paper

CHAPTER 5: Discussion

The purpose of this dissertation is to identify the brain regions responsible for seizure onset after exposure to a nerve agent and the underlying pathological and pathophysiological alterations responsible for the development of anxiety disorders after a nerve agent exposure. Revealing these mechanisms allows for new and efficacious treatments to be developed to mitigate the neuropsychiatric symptoms and increase recovery in exposed victims. We found that exposure to soman rapidly and irreversibly inhibits AChE in multiple brain regions, including the BLA, hippocampus, and piriform cortex (230). If AChE activity is not sufficiently inhibited in the BLA, animals do not develop seizures and no neuronal loss or neurodegeneration occurs, at least up to 7 days after exposure. However, if AChE is sufficiently inhibited in the BLA and seizures ensue, severe neuropathology and pathophysiological alterations occur.

Because the BLA plays a central role in seizure generation and hyperactivity within the BLA is associated with anxiety disorders, we examined the morphological and pathophysiological alterations that occur within the BLA and related this to the long-lasting increases in anxiety-like behavior observed within 14 days of soman exposure. Approximately 35% of the total population of neurons in the BLA die within 24 hours and neurodegeneration is ongoing up to 30 days after the exposure. In addition, GABAergic interneurons die within 7 days of nerve agent exposure and the ratio of GABAergic interneurons to total number of neurons is reduced 14 and 30 days after exposure (231). The loss of GABAergic interneurons and the presumptive deficits to GABAergic inhibition, led to an increase in the duration of BLA field potentials and an increase in the paired pulse ratio at all time points after exposure. In addition, synaptic

plasticity was also impaired up to 14 days after SE (231). To more closely assess the mechanisms underlying hyperactivity and subsequent anxiety-like behavior in animals, we examined whether soman exposure disrupted GABAergic inhibition. We found that exposure to soman dramatically impaired the function of the GABAergic system in the BLA, including reduced inhibition and impaired modulation by α_7 -nAChRs. The loss of inhibition led to long-lasting increases in glutamatergic activity. Thus, the decrease in inhibitory tone and subsequent increases in glutamatergic activity may be an underlying mechanism responsible for the development of anxiety after a nerve agent exposure.

ACHE INHIBITION AND RECOVERY AFTER NERVE AGENT EXPOSURE

Following exposure to a nerve agent, AChE activity is rapidly and irreversibly inhibited, causing an accumulation of ACh at cholinergic synapses. The reduction in AChE activity was observed in victims from both the Japan and Syria attacks. Civilians immediately killed by sarin exposure in Japan, for example, had severely reduced blood and brain AChE concentrations (198). Similarly, surviving victims severely intoxicated by sarin had significantly reduced serum AChE as well as reduced AChE in erythrocytes (189; 296). Although AChE concentrations remained reduced 3 weeks after exposure, blood concentrations of AChE returned to normal 3 months after the exposure (189). We found that AChE was inhibited by more than 90% in brain regions responsible for seizure generation after nerve agent exposure, but for seizure induction, AChE must be significantly inhibited in the BLA (230). The results imply that AChE inhibition in the piriform cortex and hippocampus, regions previously thought to be essential in the generation of seizures after nerve agent exposure (195), does not sufficiently increase excitability for seizure generation, nor is the increase in excitability from these two

regions propagated to other brain regions and culminate in seizure onset (230). While no significant recovery of AChE activity occurs within the first 24 hours, AChE recovers in a region dependent manner, with AChE activity recovering more quickly in the BLA than the piriform cortex, hippocampus, and prelimbic cortex (231).

The role of the BLA in seizure generation has been well documented (19; 230). Microinjection of VX or soman (in combination with carbachol or lithium chloride), for example, only induces convulsive activity when injected into the amygdala as compared to injections in the piriform cortex and hippocampus (175). Similarly, microinjection of scopolamine, a mAChR antagonist, into the BLA, is more potent in blocking seizures than injections to any other brain region (264). The data in Chapter 2 and 3 demonstrate, for the first time, that the generation of seizures only occurs when AChE is inhibited by more than 90% in the BLA (230). No recovery of AChE activity occurs within the first 24 hours, but AChE activity recovers within 7 days in the BLA and 14 days in other brain regions. The results imply that the BLA is a necessary brain region for seizure generation, but also suggests that the long-lasting behavioral alterations may not be a result of cholinergic receptor hyperstimulation since AChE completely recovers.

Early studies demonstrated that inhibition of AChE by soman causes an increase in ACh concentrations (145; 177). The generation of seizures is associated with hyperactivity of cholinergic receptors, whereas glutamatergic receptor hyperstimulation sustains and reinforces seizures (176). However, because seizures continue for many hours after the initial exposure (16; 89; 90), if left untreated, it is unlikely that the cholinergic system sustains the seizures. Evidence in favor of this hypothesis includes: 1) generation of seizures does not occur unless AChE is sufficiently inhibited and there is an

accumulation of ACh in the BLA (230); 2) ACh concentrations rapidly increase and peak within 90 min of SE onset in the amygdala and 50 min in septohippocampal areas before returning to baseline values, whereas glutamate concentrations remain elevated after soman exposure (145); 3) AChE concentrations remain reduced up to 7 days after SE in the BLA, yet animals do not display seizure activity during the latency period after the initial SE but before the occurrence of spontaneous seizures (68); and 4) mAChR autoreceptors at cholinergic terminals inhibit ACh release (145). In addition, it would be expected that with AChE inhibition, choline levels should decrease, as has been demonstrated after administration of the organophosphates dichlorvos or diisopropyl phosphorofluoridate (94; 186). However, choline concentrations remain elevated between 40 min and 4 hours after soman exposure before returning to baseline concentrations (94). The increase in choline concentrations after soman exposure may result from deficits in choline acetyltransferase activity, which has previously been found to facilitate the transfer of acetate to the choline, producing ACh (74); alternatively, increased choline concentrations may be a product of enzymatic degradation of the phospholipid phosphoglyceride by phospholipase (43; 254). Thus, while choline levels remain elevated, ACh concentrations decrease over time, whereas glutamate levels remain elevated. This suggests that AChE inhibition is necessary for SE onset but not for sustaining and reinforcing seizures.

The evidence provided in Chapter 2 suggests that in the no-SE animals, soman readily crosses the blood brain barrier and inhibits AChE activity in the piriform cortex and hippocampus, but AChE was not sufficiently reduced in the BLA. An important question is why AChE is not inhibited in the BLA of the no-SE animals while AChE was

sufficiently inhibited in the SE animals. Initial hypotheses may be that there are mutations to AChE in the amygdala versus other brain regions. In agreement, point mutations near the catalytic triad Ser302 have been found to reduce sensitivity of AChE to organophosphate pesticides (284), thus leading to AChE resistance to inhibition by an organophosphorus agent. In addition, the human butyrylcholinesterase (BChE) mutant G117H leads to increased resistance to organophosphorus toxicity by either hydrolyzing the agent or by hydrolyzing ACh after AChE inhibition (286). It is unlikely, however, that mutations would be specific to the BLA; rather, these mutations would likely take on a global effect. In addition, if AChE hydrolyzes ACh more efficiently, as occurs with the BChE mutant G117H, then binding of thiochoine to the DTNB chromogen would have generated a more pronounced yellow color as read by the spectrophotometer. Other hypotheses for increased resistance may be that AChE is in a phosphorylated state, which can subsequently enhance hydrolysis of ACh (104). While phosphorylation of AChE would leave the enzyme's affinity for ACh unaltered, phosphorylation of AChE has been found to enhance acetylthiocholine hydrolysis near 10-fold (104), and would then be observed as a much larger increase in AChE activity in our assay. Whether AChE being in a phosphorylated state prevents nerve agents from binding to the enzyme remains unknown.

A more likely contributor to the resistance of AChE inhibition by nerve agents may be alterations to microRNA (miR). Stress has been found to differentially alter miR in both the CA1 hippocampal region and in the amygdala (181). miR-134 and miR-183 encodes the splicing factor SC35, which in turn promotes alternative splicing of AChE from the synapse-associated isoform to the rare soluble protein (181). Chronic stress has

been found to decrease miR-134 in the amygdala, while leaving miR-183 unaltered in the CA1 and amygdala. The reduced miR-134 in the amygdala increases the expression of SC35 protein and the alternative splicing of AChE (181). Perhaps, baseline alterations to miR-134 in the amygdala may contribute to increased resistance of AChE from being inhibited by soman as it may be in a different molecular form. Indeed, while the G₄ isoform is the most widely expressed molecular form of AChE in the brain, regional differences in AChE isoforms have been observed. Patients with Alzheimer's disease, for example, have been shown to have a marked decrease of the G₄/G₁ ratio in the amygdala compared to the hippocampus (92; 260). Thus, future studies must be undertaken to examine whether the different AChE isoforms in the brain react differently to AChE inhibition by nerve agents. By understanding the molecular differences of AChE in the BLA, hippocampus, and piriform cortex, there is a potential for more effective options to lessen the deleterious consequences following a nerve agent exposure.

Examining the recovery of AChE activity is essential for the development of effective therapeutics. Within 3 months of exposure, AChE completely recovered in victims of the Japan terrorist attacks (189). Our data demonstrate that the recovery of AChE activity in rats occurs within 7-14 days of soman exposure in brain regions critical to seizure generation and anxiety. Our data are in line with previous studies finding that the recovery of AChE activity occurs within 16 and 32 days (55; 105; 126; 158; 184). However, these studies had methodological differences that prevent a comparison between our data and the data from these studies. Moreover, no study, prior to ours, examined whether AChE inhibition was necessary for SE onset. We demonstrated that not only was inhibition of AChE activity in the BLA necessary for seizure generation, but

it was also the first structure where AChE recovers after soman induced SE. The more rapid recovery of AChE activity in the BLA as compared to the other brain regions may be due to the density of cholinergic innervation. Cholinergic fibers innervate the BLA from the nucleus basalis magnocellularis more densely than the hippocampus or piriform cortex (183). The dense innervation may lead to exceptionally high concentrations of AChE and a more efficient recovery of AChE (31; 230; 231) by promoting an increase in de novo synthesis of AChE (105). Thus, because AChE activity recovers completely in all brain regions, it is unlikely that the cholinergic systems contribute significantly to spontaneously recurrent seizures and subsequent neuropathology, or the increases in anxiety-like behavior observed after nerve agent exposure. Rather, it may be that inhibitory synaptic transmission, resulting from deficits to cholinergic receptor modulation of GABAergic inhibition, or increases in glutamatergic excitability, may be responsible for BLA hyperexcitability and the long-lasting increases in anxiety-like behavior.

ACUTE AND DELAYED NEUROPATHOLOGY AFTER NERVE AGENT INDUCED STATUS EPILEPTICUS

Following nerve agent induced SE, humans and animals display severe neuropathology. Severely affected individuals from the Japan attack showed continued EEG, ECG, and nerve conduction abnormalities 18 months after the attack, but these abnormalities disappeared within 5 years (296). Six to 10 years after the attack, however, victims of the Japan attack had significant decreases in regional gray matter volume in the right insular, right temporal cortex, left hippocampus, anterior cingulate cortex, and amygdala. Regional white matter volume was reduced in the left temporal stem and white matter integrity was disrupted in widespread bilateral brain regions including the parietal

lobe, temporal stem, and brainstem (243; 295). Crucially, the severity of damage correlated with the loss of AChE levels at the time of the incident (295), though it went unreported whether victims developed seizures after exposure.

Within 24 hours of soman induced SE, animals display significant neuronal loss and ongoing neurodegeneration in many brain regions, including the amygdala (90; 231). Neuropathology was observed as early as 7 hours after exposure in the amygdala (107) and MRI imaging revealed pathology within 12 hours after exposure (35). The initial neuronal loss is likely due to the convulsive activity as no neuropathology or neurodegeneration occurred in animals that did not develop seizures (49; 230). However, delayed neuropathology has been observed in the absence of convulsions in the amygdala, hippocampus, and thalamus of monkeys (117; 222), suggesting that nerve agents might have long-term harmful effects on brain structures and function (53; 127). In our hands, however, neuropathology only occurred in animals that had seizures; no additional loss of neurons was observed after 24 hours. The relative stability in neuronal loss after 24 hours may be attributed to the initiation of neuroregenerative processes (59; 60), including the proliferation of neural progenitors (58). However, it is not until 30 and 90 days after soman exposure before there is a significant increase in the total number of neurons in the BLA (60).

An important finding discussed in Chapter 3 was that 24 hours after soman exposure, there was not a significant loss of GABAergic interneurons in the BLA (90; 231); the loss of GABAergic interneurons after soman exposure was delayed (231). Chronically degenerating neurons after SE has been observed in other models of SE (285) and may be GABAergic interneurons, as one study observed that after pilocarpine-

induced SE, the majority of chronically degenerating neurons exhibited GAD-immunoreactivity (285). While the mechanisms responsible for the delayed death of interneurons are not completely known, one hypothesis may be that the delayed loss of GABAergic interneurons is due to an upregulation of D-serine (160), a D-amino acid that has been found to regulate NMDA signaling by selectively binding to the glycine site of NMDA receptors on GABAergic interneurons in the amygdala and other brain regions. D-serine acts as an endogenous co-agonist for NMDA receptor activation (160; 191; 291), triggering NMDA receptor over-activation and excitotoxic damage under epileptic conditions (160).

The delayed loss of GABAergic interneurons highlights an important finding 14 and 30 days after exposure: a decrease in the ratio of interneurons to the total neuronal count (231). The ability to regulate BLA excitability requires a balance between excitation and inhibition. Prior to a nerve agent exposure, approximately 15-20% of the BLA is comprised of GABAergic interneurons (172; 245; 268). However, the approximately 46% decrease in GABAergic interneurons 7 days after exposure to soman disrupts this balance, which shifts the balance towards a net increase in excitability and may contribute to BLA hyperactivity and subsequent increases in anxiety-like behavior. Thus, if similar morphological alterations occurred in humans, then the significant loss of neurons, including the loss of GABAergic interneurons in the BLA, may contribute to the volumetric loss in the amygdala more than a decade after the Japan attack (243), but also to BLA hyperexcitability, which would reinforce and sustain anxiety- and PTSD-like symptoms (209; 296).

INCREASED ANXIETY-LIKE BEHAVIOR AND PATHOPHYSIOLOGICAL ALTERATIONS AFTER EXPOSURE TO A NERVE AGENT

Many victims of the Japan terrorist attacks had symptoms of PTSD ranging from nightmares and flashbacks to fear of riding trains (295). Animals exposed to soman also display anxiety- and fear-like behaviors after soman exposure, although these behaviors manifest as avoidance of being in an open space or freezing responses. Eight days following soman exposure, animals do not develop a fear response (i.e., freezing) during an auditory fear-conditioning paradigm (187), but display increased startle behavior (150). However, 30 but not 90 days after soman exposure, animals froze to a greater extent in auditory fear conditioning paradigms (61). A number of variables may account for the differences in freezing responses, including the species tested, time of conditioning, and pattern of neurotoxicity (187). We modeled, at the cellular level, the recovery of fear learning processes, as animals did show recovery of fear learning by 30 days. At 24 hours, 7 days, and 14 days after exposure, LTP of synaptic plasticity in the BLA was significantly impaired, but recovered by 30 days post exposure (231). The recovery of synaptic plasticity over time may be related to synaptic re-organization (182; 265), though this was not tested in our experiments.

In addition to fear related behaviors, animals also show increases in anxiety-like behavior. We demonstrated that within 14 days of exposure, animals display increases in the time spent around the periphery of an open field as well as increased startle response, both indicators of increased anxiety. Anxiety-like behavior was sustained up to 90 days after exposure (61; 165). The results of our studies and additional animal studies (124; 295; 296) are corroborated with the clinical manifestations of anxiety disorders observed after a nerve agent exposure, but the mechanisms underlying the development of anxiety

disorders after a nerve agent exposure were unknown. Hyperexcitability of the BLA is a characteristic feature of anxiety-like behaviors in animals (44; 67; 231; 246) and anxiety disorders in humans (143; 240; 282). Therefore, it is likely that the anxiety-like behaviors observed after exposure to a nerve agent may be due to pathophysiological alterations to the BLA, causing amygdalar hyperexcitability.

We observed, indirectly, reduced inhibitory synaptic transmission within 24 hours of soman exposure; loss of GABAergic inhibition was reflected as an increase in the duration of the field potentials evoked in the BLA, and the increased paired pulse ratio (231). To test whether inhibitory synaptic transmission was reduced directly, we recorded spontaneous and miniature IPSCs. We found that there was a significant decrease in inhibitory synaptic transmission within 24 hours of soman exposure. The loss of inhibition in the BLA could be attributed to impaired release of GABA early after soman exposure or the regional loss of GABAergic interneurons. Importantly, the loss of inhibition reflected presynaptic rather than postsynaptic mechanisms, as no change in mIPSC amplitude was observed after soman exposure. Thus, the loss of inhibition in the BLA likely shifts the balance of inhibitory control to hyperexcitability.

The loss of GABAergic interneurons may have contributed significantly to deficits in inhibitory synaptic transmission; however mechanisms that modulate GABAergic inhibition may have also been damaged after SE. The cholinergic system densely innervates the BLA and activation of α_7 -nAChRs enhance inhibitory synaptic transmission (183; 193; 225). After soman exposure, α_7 -nAChR mediated enhancement of inhibitory but not excitatory synaptic transmission was reduced. This reduction may be due to differences in the density of α_7 -nAChRs expressed on principal neurons versus

interneurons, receptor stoichiometry, or the loss of cholinergic innervation (225).

Damage to the basal forebrain has also been found to cause significant increases in anxiety-like behavior and failures in recovering from stressful situations (169); reduced cholinergic innervation, as occurs in Alzheimer's disease, also results in the inactivation of α_7 -nAChRs and subsequently enhances anxiety and fear behaviors (80; 87). Most likely, however, due to the disproportionately large loss of GABAergic interneurons, the cholinergic control of GABAergic interneurons in the BLA is reduced, thereby impairing α_7 -nAChR mediated enhancement of inhibitory synaptic transmission.

CONCLUSIONS AND FUTURE DIRECTIONS

The present studies describe the progression of biochemical, pathological, and pathophysiological alteration that occur from seizure generation to the development of anxiety-like behavior after a nerve agent exposure. The duration of the study, 30 days in rats, corresponds to approximately 3 years of human life (250). We show that SE onset occurs when AChE is significantly inhibited by soman, and suggest that AChE inhibition in the BLA is necessary for the generation of seizures after nerve agent exposure. Inhibition of AChE causes an accumulation of ACh at cholinergic synapses and hyperactivation of cholinergic receptors, initiating seizures. Cholinergic receptor hyperstimulation gives way to glutamatergic receptor hyperactivation, which sustains and reinforces seizures, leading to profound neuropathology (Figure 19A). Although slow, AChE recovers over 14 days from soman exposure, but can have both acute and long-term consequences on cholinergic modulation of neuronal excitability (231). Primary cell death occurs within the first 24 hours of soman exposure, but there is a delayed loss of GABAergic interneurons; neurons do continue to show signs of death/degeneration up to

30 days after exposure, however, with time the chronically degenerating neurons, which appear to be GABAergic interneurons, die. The loss of GABAergic interneurons in the BLA subsequently leads to reduced inhibition, but mechanisms modulating GABAergic inhibition are also impaired (Figure 19B). The loss of inhibition leads to greater excitability within the BLA, increased excitatory synaptic transmission, and the long-lasting increases in anxiety-like behavior.

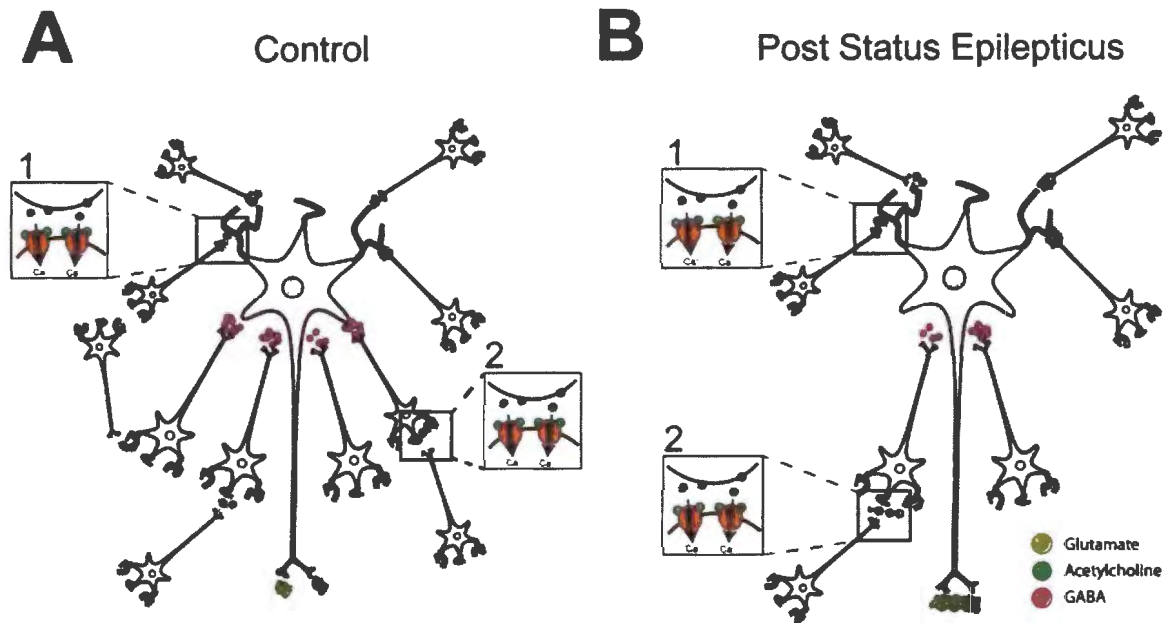


Figure 19 Summary of mechanisms involved with the onset of nerve agent induced seizures and pathophysiological alterations after status epilepticus. **(A)** Excitation within the BLA is tightly regulated by GABAergic inhibition (blue neurons, red circles). ACh (green circles) released from cholinergic fibers in the basal forebrain synapse, in part, on α_7 -nAChRs. While activation of α_7 -nAChRs enhances both excitation (1) and inhibition (2), α_7 -nAChR mediated enhancement of GABAergic inhibition predominates (see Appendix 1). Nerve agent exposure rapidly and irreversibly inhibits AChE, leading to an accumulation of ACh at the synapse and hyperstimulation of cholinergic receptors. SE onset occurs only after AChE is sufficiently inhibited in the BLA, leading to hyperstimulation of mAChR and nAChR, and subsequent neuronal depolarization; α_7 -nAChRs rapidly desensitize and reduce α_7 -nAChR mediated enhancement of inhibitory synaptic transmission. SE is sustained and reinforced when excessive glutamate (gold circles) is released, subsequently causing hyperstimulation of glutamatergic receptors (e.g., AMPA, NMDA, kainate receptors). **(B)** Within 24 hours of SE onset, approximately 35% of neurons die in the BLA and within 7 days of SE 46% of GABAergic interneurons die. α_7 -nAChR mediated enhancement of excitatory transmission remains unchanged (1), but α_7 -nAChR mediated inhibitory synaptic transmission is reduced, likely because of the loss of GABAergic interneurons and not because of alterations to receptor activation (2). Reduced GABAergic inhibition, and deficits to mechanisms that modulate GABAergic inhibition, subsequently dysregulate the tight control GABAergic inhibition has over excitation in the BLA; reduced GABAergic inhibition, leads to significant increases in excitatory synaptic transmission and subsequently BLA hyperexcitability, which may manifest as anxiety disorders.

While the loss of GABAergic inhibition may be one of the causes of BLA hyperexcitability after nerve agent exposure, this work does not confirm that similar alterations occur in other brain regions. For example, we have previously provided evidence that there is not a significant loss of GABAergic interneurons in the CA1 hippocampal regions 7 days after SE (90). In addition, unpublished data suggest that 24 hours after soman induced SE, LTP is enhanced, but 7 days after exposure, we were unable to induce or maintain LTP in the CA1 hippocampal region; LTP recovers to baseline levels within 14 days of exposure to soman. While the direct effects of soman exposure on GABAergic inhibition in the CA1 hippocampal region remain unknown, it may be that rather than a significant loss of GABAergic interneurons, nerve agent induced SE may lead to desensitization and internalization of GABA_A receptors; thus, the effects in the CA1 hippocampal region may be predominately postsynaptic rather than presynaptic as observed in the BLA. Evidence in support of this hypothesis includes reductions in GABA_A receptor mediated synaptic transmission and the internalization of GABA_A receptors during seizure activity after pilocarpine-induced SE in the CA1 (100; 101; 201). While deficits to inhibitory synaptic transmission may be due to the death of interneurons in the BLA, in the CA1 hippocampal region, deficits in inhibitory synaptic transmission may be the result of desensitization and internalization of GABA_A receptors. Future studies should examine how deficits in inhibitory synaptic transmission differ in other brain regions that are damaged by nerve agents.

Though deficits in inhibitory synaptic transmission are a major theme in this dissertation, long-lasting increases in excitatory synaptic transmission were also observed after SE. These increases were likely due to the loss of inhibition in the BLA, but may

also reflect increases in the surface expression of glutamatergic receptors. Increases in excitatory synaptic transmission were observed while recording field potentials from the CA1 region (unpublished data) and may be due to the accumulation of NMDA receptors at the synapse after SE (200). Because long-lasting increases in excitatory synaptic transmission are feasible in both the amygdala and hippocampus, it is plausible that increases in excitatory synaptic transmission may be prominent in other brain regions as well. Moreover, the increased excitability may make victims of a nerve agent attack more susceptible to anxiety and other neurological disorders (e.g., epilepsy). Therefore, it is imperative that steps are to be taken to reduce the hyperexcitability. These steps should bypass the inhibitory system as the mechanisms regulating inhibitory synaptic transmission may be damaged in region specific manners. By regulating the excitability of the brain, pharmacotherapy may be beneficial in reducing anxiety-like behavior and prevent the development of neurological impairments.

In summary, this dissertation described the long lasting pathological and pathophysiological alterations in the GABAergic system after soman induced SE. The loss of inhibition, and subsequent increases in excitatory synaptic transmission, are reflected behaviorally as increases in anxiety-like behavior in rodents and anxiety disorders in humans. The damage to the inhibitory system also reflects why treatments targeting the GABAergic system are less effective in mitigating anxiety-like behavior. It may be too late to deliver medical countermeasures against nerve agent intoxication to civilians in Syria, but it is not too late to treat the survivors for the long-term neuropsychiatric impairments that are likely to occur. By demonstrating that a nerve agent exposure severely disrupts the inhibitory system, we conclude that it is essential

that treatments are developed to target and subsequently decrease the hyperexcitability observed after a nerve agent exposure in an effort to mitigate the lasting neuropsychiatric impairments.

Appendix 1: α_7 -Containing Nicotinic Acetylcholine Receptors on Interneurons of the Basolateral Amygdala and Their Role in the Regulation of the Network Excitability

Volodymyr I. Pidoplichko¹, Eric M. Prager^{1,3}, Vasiliki Aroniadou-Anderjaska^{1,2,3},
Maria F.M. Braga^{1,2,3*}

¹Department of Anatomy, Physiology, and Genetics

²Department of Psychiatry

³Program in Neuroscience

Uniformed Services University of the Health Sciences

4301 Jones Bridge Road

Bethesda, MD 20814, USA

Abbreviated title: Functional α_7 -nAChRs on amygdalar interneurons

*Corresponding Author:

Maria F.M. Braga, D.D.S., Ph.D.

Department of Anatomy, Physiology, and Genetics

Uniformed Services University of the Health Sciences

4301 Jones Bridge Road

Bethesda, MD 20814

Phone: (301) 295-3524

Fax: (301) 295-3566

Email: maria.braga@usuhs.edu

ABSTRACT

The basolateral amygdala (BLA) plays a key role in fear-related learning and memory, in the modulation of cognitive functions, and in the overall regulation of emotional behavior. Pathophysiological alterations involving hyperexcitability in this brain region underlie anxiety and other emotional disorders, as well as some forms of epilepsy. GABAergic interneurons exert a tight inhibitory control over the BLA network; understanding the mechanisms that regulate their activity is necessary for understanding physiological and disordered BLA functions. The BLA receives dense cholinergic input from the basal forebrain, affecting both normal functions and dysfunctions of the amygdala, but the mechanisms involved in the cholinergic regulation of inhibitory activity in the BLA are unclear. Using whole-cell recordings in rat amygdala slices, here we demonstrate that the α_7 -containing nicotinic acetylcholine receptors (α_7 -nAChRs) are present on somatic or somatodendritic regions of BLA interneurons. These receptors are active in the basal state enhancing GABAergic inhibition, and their further – exogenous – activation produces a transient but dramatic increase of spontaneous inhibitory postsynaptic currents (sIPSCs) in principal BLA neurons. In the absence of AMPA/kainate receptor antagonists, activation of α_7 -nAChRs in the BLA network, increases both GABAergic and glutamatergic spontaneous currents in BLA principal cells, but the inhibitory currents are enhanced significantly more than the excitatory currents, reducing overall excitability. The anxiolytic effects of nicotine, as well as the role of the α_7 -nAChRs in seizure activity involving the amygdala and in mental illnesses, such as schizophrenia and Alzheimer's disease, may be better understood in light of the present findings.

Key words: α_7 -nAChR, GABA_A receptor, inhibition, basolateral amygdala

INTRODUCTION

The amygdala is a group of nuclei in the temporal lobe that receives information from all sensory modalities, locally processes this information for its emotional significance, and plays a key role in the orchestration of the behavioral response (226; 245). The amygdala is particularly responsive to fear-evoking stimuli, and it appears to be the site where fear-related memories are consolidated and stored (97; 152; 153; 192; 215). Amygdalar dysfunction that involves hyperexcitability and hyperactivity is a key feature of anxiety disorders, including posttraumatic stress disorder (67; 82; 240; 258). Furthermore, the amygdala is very prone to seizure generation, and, along with the hippocampus, it is the epileptic focus in certain types of epilepsy (20; 99; 227). Therefore, knowledge of the mechanisms that regulate the excitability of the amygdala can have significant implications in understanding the pathophysiology of and treatment for anxiety and seizure disorders.

Neuronal excitability in the basolateral nucleus of the amygdala (BLA) is particularly relevant to both anxiety (66; 67; 81; 82; 152) and seizure generation (20; 130; 257). GABAergic inhibition plays a primary role in the regulation of the excitability of neuronal networks (e.g., (149)). Although GABAergic interneurons in the BLA make up only a small proportion (about 20%) of the total neuronal population (172; 245; 268), they tightly regulate principal cell excitability (149; 268; 293). A number of neuromodulatory systems participate in the regulation of GABAergic synaptic transmission in the BLA (22; 39; 40; 140; 208; 238). The cholinergic system is prominently present in the BLA (31; 193; 229), but its involvement in the regulation of GABAergic synaptic transmission is not well understood.

The cholinergic projections to the BLA arise primarily from the nucleus basalis magnocellularis (48; 79; 197; 294), a collection of neurons in the substantia innominata of the basal forebrain. Afferents from these neurons synapse on both pyramidal cells and interneurons (47; 193; 206), targeting nicotinic and/or muscarinic acetylcholine receptors, which are abundantly present in the BLA (119; 170; 193; 249; 270; 279; 298).

Neuronal nicotinic acetylcholine receptors (nAChRs) are pentameric and are composed, in different subunit combinations, of α_2 - α_{10} and β_2 - β_4 subunits (7; 63; 64; 180). The homomeric α_7 and heteromeric $\alpha_4\beta_2$ are the two major subtypes of nAChRs found in the mammalian brain (4; 103). α_7 -nAChRs play an important role in the regulation of neuronal excitability in different brain regions, either by presynaptically modulating neurotransmitter release (30; 70; 161; 235), or by their position on somatodendritic sites of interneurons and pyramidal cells, where they directly regulate neuronal activity (6; 9-11; 18; 132; 138; 141). In the BLA, α_7 -nAChRs are present on somatodendritic regions of glutamatergic neurons (141), and they are also involved in presynaptically facilitating glutamate release (29; 128). It is unclear if α_7 -nAChRs are also present on somatodendritic sites of BLA interneurons. There is only one study in the literature addressing this question, where it is reported that in the BLA of neonatal (P7-10) rats, an increase in the frequency of spontaneous inhibitory postsynaptic currents (sIPSCs) by application of acetylcholine or nicotine was not reduced by the specific α_7 -nAChR antagonists alpha-bungarotoxin (α -BgTx) or methyllycaconitine, suggesting that α_7 -nAChRs do not play an important role in the regulation of GABAergic activity in the BLA (298). The focus of the present study was to delineate the role of α_7 -nAChRs in

the regulation of GABAergic activity in the BLA, and determine the net effect of α_7 -nAChR activation on the excitability of the BLA network.

MATERIALS AND METHODS

Animals

Experiments were performed using 25-40 day old, male, Sprague-Dawley rats (Taconic Farms, Derwood, MD). Animals were housed in an environmentally controlled room (20-23°C, 44% humidity, 12-h light/12-h dark cycle [350-400 lux], lights on at 6:00 am), with food (Harlan Teklad Global Diet 2018, 18% protein rodent diet; Harlan Laboratories; Indianapolis, IN) and water available *ad libitum*. Cages were cleaned weekly and had no physical enrichment within the cage (232). All animal experiments were conducted following the Guide for the Care and Use of Laboratory Animals (Institute of Laboratory Animal Resources, National Research Council), and were approved by the Institutional Animal Care and Use Committee.

Electrophysiological Experiments.

Animals were anesthetized with isoflurane before decapitation. Coronal brain slices (400 μm -thick) containing the amygdala (-2.64 to -3.36 from bregma) were cut using a vibratome (Leica VT 1200 S; Leica Microsystems, Buffalo Grove, IL), in ice-cold cutting solution consisting of (in mM): 115 sucrose, 70 NMDG, 1 KCl, 2 CaCl₂, 4 MgCl₂, 1.25 NaH₂PO₄, 30 NaHCO₃, 25 D-glucose. The slices were transferred to a holding chamber, at room temperature, in a bath solution containing (in mM): 125 NaCl, 2.5 KCl, 1.25 NaH₂PO₄, 21 NaHCO₃, 2 CaCl₂, 1 MgCl₂, and 11 D-glucose. Recording solution was the same as the holding bath solution. For field potential recordings the bath/recording solution was same as above, except for the concentration of MgCl₂ (1.5

mM) and KCl (3 mM). All solutions were saturated with 95% O₂ / 5% CO₂ to achieve a pH near 7.4. For whole-cell recordings, the slice chamber (0.7 mL capacity) had continuously flowing ACSF (~8 mL/min) at temperature 32~33°C. The osmolarity of this external solution was adjusted to 325 mOsm with D-glucose. Field potential recordings were obtained in an interface-type chamber, maintained at 32~33°C, with a flow rate of the ACSF at 1.5 ml/min.

For whole-cell recordings, neurons were visualized under infrared light using Nomarski optics of an upright microscope (Zeiss Axioskop 2, Thronwood, NY) through a 40x water immersion objective, equipped with a CCD-100 camera (Dage-MTI, Michigan City, IN(90)). The patch electrodes had resistances of 3.5–4.5 MΩ when filled with the internal solution (in mM): 60 CsCH₃SO₃, 60 KCH₃SO₃, 10 KCl, 10 EGTA, 10 HEPES, 5 Mg-ATP, 0.3 Na₃GTP (pH 7.2), 290 mOsm. When sIPSCs and sEPSCs were recorded simultaneously, the internal chloride concentration was 1 mM, and osmolarity was adjusted with potassium gluconate. We use KCl bridge electrode holders (ALA Scientific Instruments Inc., Farmingdale, NY), which provide stable offset potentials, and make the concentration of Cl⁻ in the pipette solution irrelevant (the Ag⁺/AgCl wires are in constant contact with 2M KCl). Tight-seal (over 1 GΩ) whole-cell recordings were obtained from the cell body of pyramidal-shaped neurons in the BLA region and from the cell body of interneurons, which were identified on the basis of their electrophysiological properties (218; 245). Access resistance (5–24 MΩ) was regularly monitored during recordings, and cells were rejected if the resistance changed by more than 15% during the experiment. Agonists of α₇-nAChRs were applied either to the bath or by pressure injection. Pressure application was performed with the help of a push–pull experimental arrangement (224),

as utilized previously (89; 290). A motorizer (Newport, Fountain Valley, CA) was coupled with the approach/withdrawal (push–pull) actuator of a micromanipulator (Burleigh PCS-5000 series; EXFO Photonic Solution Inc., Mississauga, Ontario, Canada). Motorizer movement and duration of application pulses were controlled with a Master-8 digital stimulator (AMPI; Jerusalem, Israel). The pipette was placed approximately 50 μm away from the soma of the recorded neuron, and pressure was applied for 70 to 100 ms, via a Picospritzer (General Valve Division, Parker Hannifin Corp., Fairfield, NJ), set between 14 and 30 psi. Ionic currents and action potentials were amplified and filtered (1 kHz) using the Axopatch 200B amplifier (Axon Instruments, Foster City, CA) with a four-pole, low-pass Bessel filter, were digitally sampled (up to 2 kHz) using the pClamp 10.2 software (Molecular Devices, Sunnyvale, CA), and further analyzed using the Mini Analysis program (Synaptosoft Inc., Fort Lee, NJ) and Origin (OriginLab Corporation, Northampton, MA). In some experiments, the charge transferred by postsynaptic currents was calculated, using the Mini60 software by Synaptosoft (Synaptosoft Inc., Fort Lee, NJ).

Field potentials were evoked by stimulation of the external capsule, at 0.05 Hz. Recording glass pipettes were filled with ACSF, and had a resistance of approximately 5 M Ω . Stimulation was applied with a bipolar concentric stimulating electrode made of tungsten (World Precision Instruments, Sarasota, FL). Signals were digitized using the pClamp 10.2 software (Molecular Devices, Union City, CA), analyzed using Clampfit 10.2, and final presentation was prepared using Origin (OriginLab Corporation, Northampton, MA) or Graphpad Prism (GraphPad Software, La Jolla, CA).

Drugs used were as follows: bicuculline methiodide, a GABA_A receptor antagonist, atropine sulphate, a muscarinic AChR antagonist, dihydro- β -erythroidine (DH β E), an $\alpha_4\beta_2$ nicotinic receptor antagonist, choline chloride and tricholine citrate, α_7 agonists, α -bungarotoxin (α -BgTx), an α_7 antagonist, CNQX, an AMPA/kainate receptor antagonist (all purchased from Sigma-Aldrich, St. Louis; MO). We also used D-AP5, an NMDA receptor antagonist, SCH50911, a GABA_B receptor antagonist, α -conotoxin Au1B, an $\alpha_3\beta_4$ nicotinic receptor antagonist, LY 341495, a metabotropic glutamate group II/III receptor antagonist (all purchased from Tocris, Ellisville, MO).

Statistical Analysis.

Electrophysiological studies were analyzed using the Paired-Student's t-tests. Results were considered statistically significant when $P < 0.05$. Data are presented as Mean \pm standard error (SE) of the mean. Sample size " n " refers to the number of neurons for the whole-cell experiments, and the number of slices for the field potential recordings.

RESULTS

Functional α_7 -nAChRs are present on BLA interneurons

Whole-cell recordings were obtained from presumed interneurons in the BLA, which were identified on the basis of their small size compared to pyramidal/principal cells, their firing pattern in response to depolarizing current pulses in the current clamp mode, and the absence of a current activated by hyperpolarizing voltage-steps, in the voltage-clamp mode. Depolarizing current injections generated a high-frequency series of fast, non-accommodating action potentials (Figure 20B, *right panel*), which is typical of a significant subpopulation of BLA interneurons (21; 245; 272). Voltage-clamp recordings

demonstrated linear change in leakage current and the absence of I_h (Figure 20B, *right panel*), which is a cationic current activated by hyperpolarizing voltage steps, that is commonly present in principal neurons of the BLA (21; 218; 292).

To determine if α_7 -nAChRs are present on BLA interneurons, we pressure-applied tricholine citrate (5 mM, n = 7), or choline chloride (10 mM, n = 13), while recording from interneurons in the presence of α -conotoxin Au1B (1 μ M), DH β E (10 μ M), atropine sulfate (0.5 μ M), D-AP5 (50 μ M), CNQX (20 μ M), SCH50911 (10 μ M), LY 3414953 (3 μ M), and bicuculline (20 μ M). The concentrations of the α_7 -nAChR agonists that we used have been shown in the hippocampus (12) or neocortical layer I interneurons (54) to selectively activate α_7 -nAChRs; furthermore, the presence of the $\alpha_4\beta_2$ and the $\alpha_3\beta_4$ nicotinic receptor antagonists in the slice medium can increase confidence that tricholine citrate and choline chloride selectively activated α_7 -nAChRs. Out of 20 cells, 12 responded to the “puff-application” of the α_7 -nAChR agonist with a fast-inactivating inward current of an amplitude 83.1 ± 8.4 pA (Figure 20A, left trace). The remaining 8 cells, responded with a slow current of an amplitude 236 ± 52.1 pA (Figure 20A, right trace). The fast or slow kinetics of the evoked currents had no relation to whether tricholine citrate or choline chloride was applied. In the current-clamp mode, puff-application of the α_7 -nAChR agonist elicited a brief train of action potentials (Figure 1B, left panel, *upper trace*). The fast-inactivating currents were blocked equally effectively by either 250 nM (n = 4, Figure 20C, upper trace) or 1 μ M (n = 5, Figure 19C, lower trace) α -BgTx, within 2 to 4 min of bath application of the toxin; the mean reduction was $94.5 \pm 2.0\%$ (n = 9). The slow currents were only partially reduced by 250 nM, 500 nM, or 1 μ M of α -BgTx. The blockade ($36.5 \pm 4.8\%$, n = 6) was slow (required

at least 8 min of perfusion), and appeared to be more effective at the high concentration of the toxin (1 μM , Figure 20D).

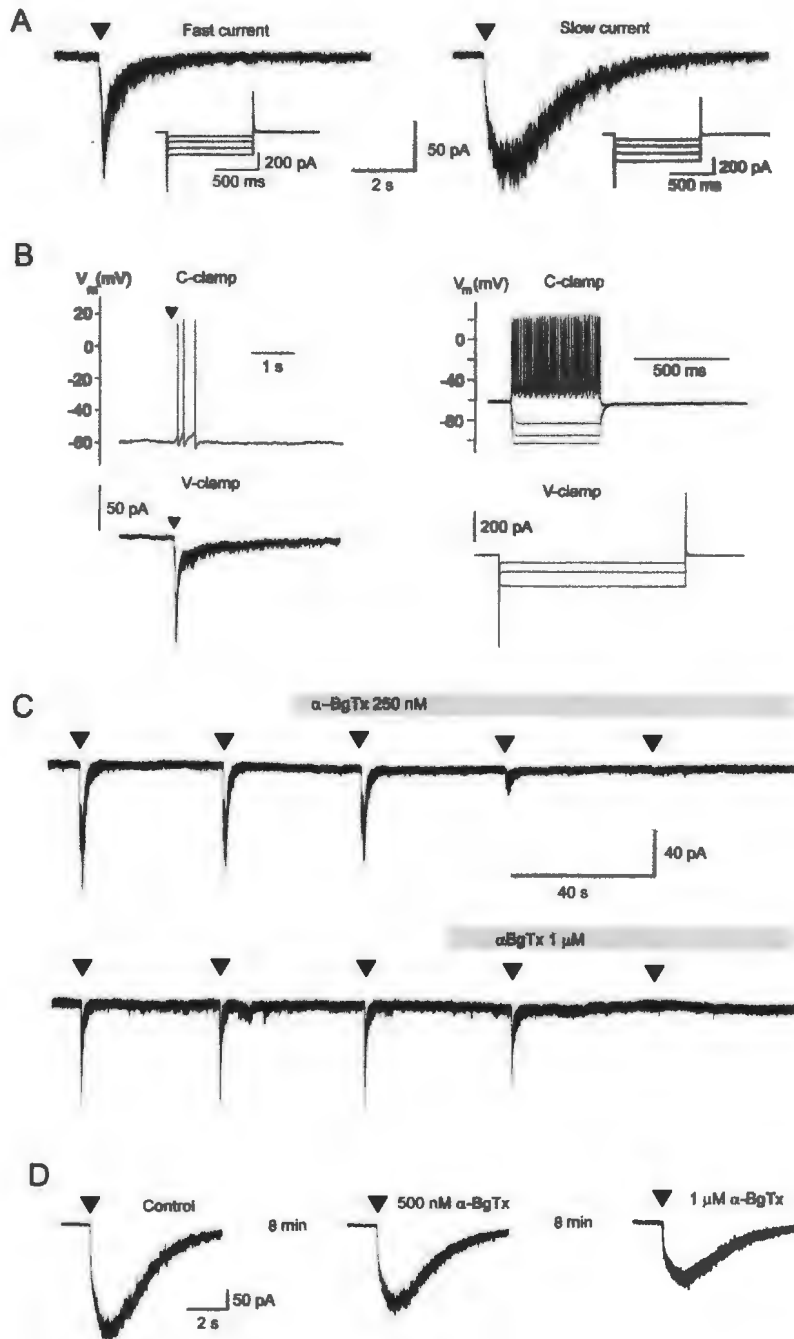


Figure 20 α_7 -nAChRs are present on BLA interneurons. Recordings were obtained from electrophysiologically identified interneurons in the BLA, in the presence of α -conotoxin Au1B (1 μ M), DH β E (10 μ M), atropine sulfate (0.5 μ M), D-AP5 (50 μ M), CNQX (20 μ M), SCH50911 (10 μ M), LY 3414953 (3 μ M), and bicuculline (20 μ M). *A*: Examples of fast and slow currents evoked by pressure-application of 10 mM choline chloride (arrowhead; 100 ms; 30 psi; $V_h = -70$ mV; $[Cl^-]_{int.} = 10$ mM). The insets show the absence of the current activated by hyperpolarization (I_h). *B*: In the current-clamp mode, pressure application of 5 mM tricholine citrate (arrowhead) induced brief spiking (*upper left panel*; the membrane potential was held at -60 mV by passing low-amplitude depolarizing current). The *lower left panel* shows the inward current evoked in the same cell by tricholine citrate (5 mM; arrowhead) in the voltage-clamp mode (holding potential (V_h), -70 mV). The *right panel* shows the fast, non-accommodating spiking of the same neuron, in response to depolarizing current injections, and the absence of a “sag” in response to hyperpolarizing current injections (*upper panel*), as well as the linear changes in leakage current (absence of I_h) during 1 s-long, 10 mV hyperpolarizing steps, starting from the holding potential of -70 mV (*lower panel*). *C*: The fast current activated by sequential (40 s interval) pressure-application of 10 mM choline chloride (arrowheads; same settings as in “A”) was blocked by bath application of either 250 nM α -BgTx (*upper trace*), or 1 μ M α -BgTx (*lower trace*). Upper and lower traces are from two different neurons. Grey bars over the recordings mark the duration of bath-application of α -BgTx. *D*: Example of the low sensitivity of choline-evoked, slow currents to α -BgTx. Arrowheads show the time point of pressure application of 10 mM choline chloride. α -BgTx was bath applied, initially at the concentration of 500 nM, followed by 1 μ M (duration of application, 8 min at each concentration; flow rate, 8 ml/min).

Glutamatergic excitation of interneurons following α_7 -nAChR activation.

The experiments described above indicate that α_7 -nAChRs are present on somatic or somatodendritic regions of BLA interneurons, and their activation depolarizes these cells. Since α_7 -nAChRs are also present on principal BLA neurons (141), as well as on glutamatergic terminals (29; 128), we investigated whether α_7 -nAChR activation in the BLA network, in addition to depolarizing interneurons directly, also depolarizes interneurons by increasing glutamatergic activity. Therefore, we conducted similar experiments as those shown in Figure 20, except that CNQX was not included in the slice

medium. Under these conditions, pressure-application of 5 mM tricholine citrate induced long-lasting, high-frequency firing in the current-clamp mode, and a transient inward current accompanied by spontaneous excitatory postsynaptic currents (sEPSCs), in the voltage-clamp mode (n = 7, Figure 21A). Similarly, when choline chloride (2.5 mM) was applied to the bath, it also induced repetitive, high-frequency firing of BLA interneurons (n = 4, Figure 21B). Thus, α_7 -nAChR activation in the BLA increases the activity of interneurons not only via direct depolarization, but also indirectly due to an enhancement of glutamatergic activity.

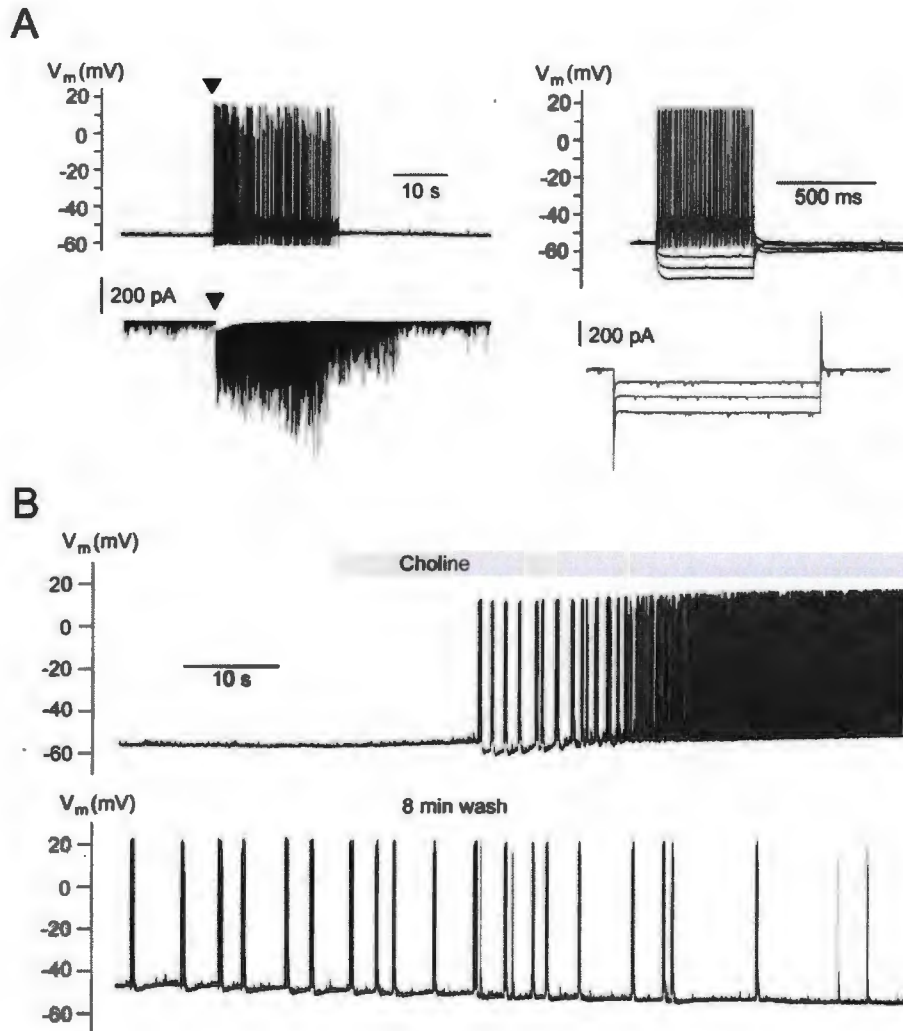


Figure 21 Indirect excitation of interneurons by activation of α_7 -nAChRs. Recordings are from electrophysiologically identified interneurons, in the presence of α -conotoxin Au1B (1 μ M), DH β E (10 μ M), atropine sulfate (0.5 μ M), D-AP5 (50 μ M), SCH50911 (10 μ M), LY 3414953 (3 μ M), and bicuculline (20 μ M). *A*: Pressure application of tricholine citrate (5 mM; arrowhead) induced high frequency firing in the current-clamp mode (*upper left panel*) and a transient inward current along with high-frequency sEPSCs in the voltage-clamp mode (*lower left panel*; V_h , -70 mV). The electrophysiological characteristics of this neuron are shown on the right panel. Responses to depolarizing or hyperpolarizing current injections (*upper right panel*) and hyperpolarizing voltage steps (*lower right panel*) are consistent with the properties of interneurons. *B*: In current-clamp mode, bath application of choline chloride (2.5 mM) induced high-frequency spiking.

Activation of α_7 -nAChRs enhances spontaneous GABA_A receptor-mediated inhibitory postsynaptic currents (sIPSCs)

The neurons we recorded from in the experiments described above were presumed to be GABAergic interneurons. Therefore, the data presented would predict that activation of α_7 -nAChRs will enhance GABAergic inhibition in the BLA. To determine if α_7 -nAChR activation increases GABA_A receptor-mediated sIPSCs, we bath applied choline chloride while recording from principal neurons ($n = 12$), in the presence of α -conotoxin AulB ($1 \mu\text{M}$), DH β E ($10 \mu\text{M}$), atropine sulfate ($0.5 \mu\text{M}$), D-AP5 ($50 \mu\text{M}$), CNQX ($20 \mu\text{M}$), SCH50911 ($10 \mu\text{M}$), and LY 3414953 ($3 \mu\text{M}$). Neurons were identified as principal cells based on their size and pyramidal-like shape, as well as on their firing patterns in response to depolarizing current pulses, and the presence of I_h (21; 218; 245). Choline chloride (5 mM) was bath-applied at a flow rate of 8 ml/min . The effect was immediate and consisted of the appearance of a barrage of sIPSCs (Figure 22). The frequency of sIPSCs was increased by choline from $22 \pm 1 \text{ Hz}$ to $50 \pm 3 \text{ Hz}$ ($n = 12$; $P < 0.001$); the measurements of the sIPSC frequency in the presence of choline were made for a 20 s time window within a time period of 30 s after the initiation of the effect. The effect subsided within 40 s to 2 min , despite the continual presence of choline, suggesting desensitization of the receptors. Reapplication of choline after only partial wash out of the initially-applied choline, had virtually no effect, probably due to the lasting desensitization of the receptors while the exogenous choline was still present. However, after washing out choline for at least 8 min , reapplication of choline could evoke a similar effect, suggesting that desensitization was not lasting after removal of the 5 mM exogenous agonist. Higher concentrations of choline (we tried 10 mM and 20 mM)

produced a similar increase in sIPSC amplitude and frequency, but longer wash-out times were required in order to be able to reproduce the effect upon reapplication of choline.

In some experiments, we washed out choline for 8 min, and then applied α -BgTx (1 μ M) for another 4 min. Subsequent application of 5 mM choline chloride (in the presence of α -BgTx) increased the frequency of sIPSCs from 18 ± 3 Hz to 37 ± 4 Hz ($n = 9$; $P < 0.01$, Figure 22D). Thus, even in the presence of α -BgTx, choline increased sIPSCs significantly, probably because of the activation of interneurons that respond to choline by generating a slow current with low sensitivity to α -BgTx (Figure 20D). However, the increase in the frequency of sIPSCs in the presence of α -BgTx was significantly smaller than the increase in the absence of the α_7 -nAChR antagonist ($P < 0.001$, Figure 22D), probably reflecting the blockade of the α -BgTx-sensitive α_7 -nAChRs on interneurons that generate fast-inactivating currents in response to choline (Figure 20C).

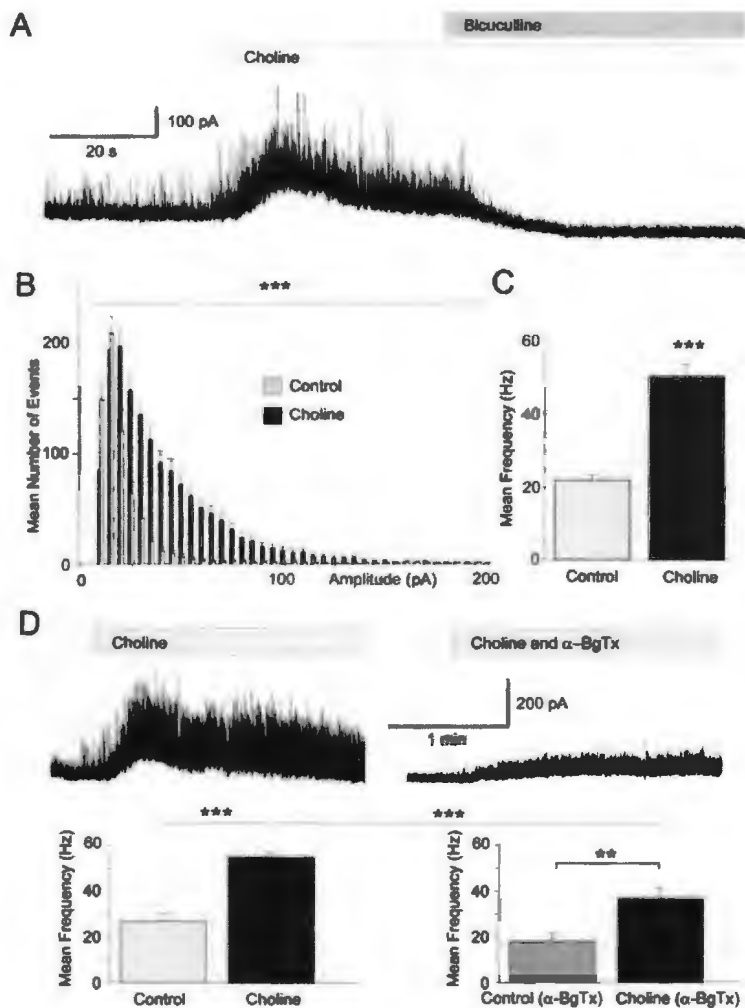


Figure 22 Activation of α_7 -nAChRs enhances spontaneous GABA_A receptor-mediated IPSCs. Recordings are from BLA principal cells, in the presence of α -conotoxin Au1B (1 μ M), DH β E (10 μ M), atropine sulfate (0.5 μ M), D-AP5 (50 μ M), CNQX (20 μ M), SCH50911 (10 μ M), and LY 3414953 (3 μ M), at V_h +30 mV and internal chloride 10 mM. *A*: Bath application of choline chloride (5 mM) induced a transient outward cationic current and increased the frequency and amplitude of sIPSCs. The sIPSCs were blocked by 20 μ M bicuculline, indicating that they were mediated by GABA_A receptors. *B*: Amplitude-frequency histogram of the effect of choline on sIPSCs ($n = 12$, *** $P < 0.001$). *C*: Group data (mean \pm SE) of the change in the frequency of sIPSCs by bath application of choline chloride ($n = 12$, *** $P < 0.001$). *D*: Pretreatment of the slices with α -BgTx reduced significantly the effects of choline. Traces show an example of the response of a principal neuron to bath application of choline chloride (5 mM), and the response of the same neuron when choline chloride was applied in the presence of α -BgTx (1 μ M). The group data are shown in the bar graphs below (*** $P < 0.001$, ** $P < 0.01$, $n = 9$).

The net effect of α_7 -nAChR activation in the BLA

Since activation of α_7 -nAChRs in the BLA can increase both glutamatergic and GABAergic activity, an important question that arises is whether the overall, net effect of α_7 -nAChR activation is enhancement or suppression of excitatory activity in the BLA. To answer this question we recorded both sIPSCs and sEPSCs, simultaneously, from principal neurons in the presence of α -conotoxin Au1B (1 μ M), DH β E (10 μ M), atropine sulfate (0.5 μ M), D-AP5 (50 μ M), SCH50911 (10 μ M), and LY 3414953 (3 μ M), at a holding potential of -58 mV and internal chloride concentration of 1 mM. Bath application of choline chloride (5 mM) increased both sIPSCs and sEPSCs (Figure 23). Out of 9 cells, in 3 cells there was only a small increase in sEPSCs while sIPSCs were dramatically increased (as in the example shown in Figure 23A), in 5 cells both sEPSCs and sIPSCs were increased but the increase in sIPSCs was clearly more prominent (as in the example shown in Figure 23B), while 1 cell showed dramatic increase in both sIPSCs and sEPSCs. To quantify these effects we calculated the total charge transferred. The charge, in pico Coulombs, was calculated as the area delimited by the inhibitory or excitatory current and the baseline. Current areas were analyzed for a time period of 5s. On the average, the charge transferred by sIPSCs was increased from 1.3 ± 0.3 pC in control medium to 97 ± 24 pC in the presence of choline ($n = 9$; $P < 0.01$; Figure 23C, left graph), while the charge transferred by sEPSCs was increased from 1.5 ± 0.3 pC to 20 ± 4 pC ($n = 9$; $P < 0.01$; Figure 23C, right graph), during the initial phase of bath application of choline chloride (during a 5 sec period after the initiation of the effect). The charge transferred by sIPSCs was significantly larger than the charge transferred by sEPSCs ($n = 9$, $P < 0.01$), suggesting that the net effect of α_7 -nAChR activation is

inhibitory. As in the case where only sIPSCs were recorded (Figure 22), the effects of choline subsided in less than 2 min, despite the continual presence of the agonist. Lower concentrations of bath-applied choline chloride (1 mM, n = 2, and 0.5 mM, n = 3) had qualitatively similar effects (Figure 22D).

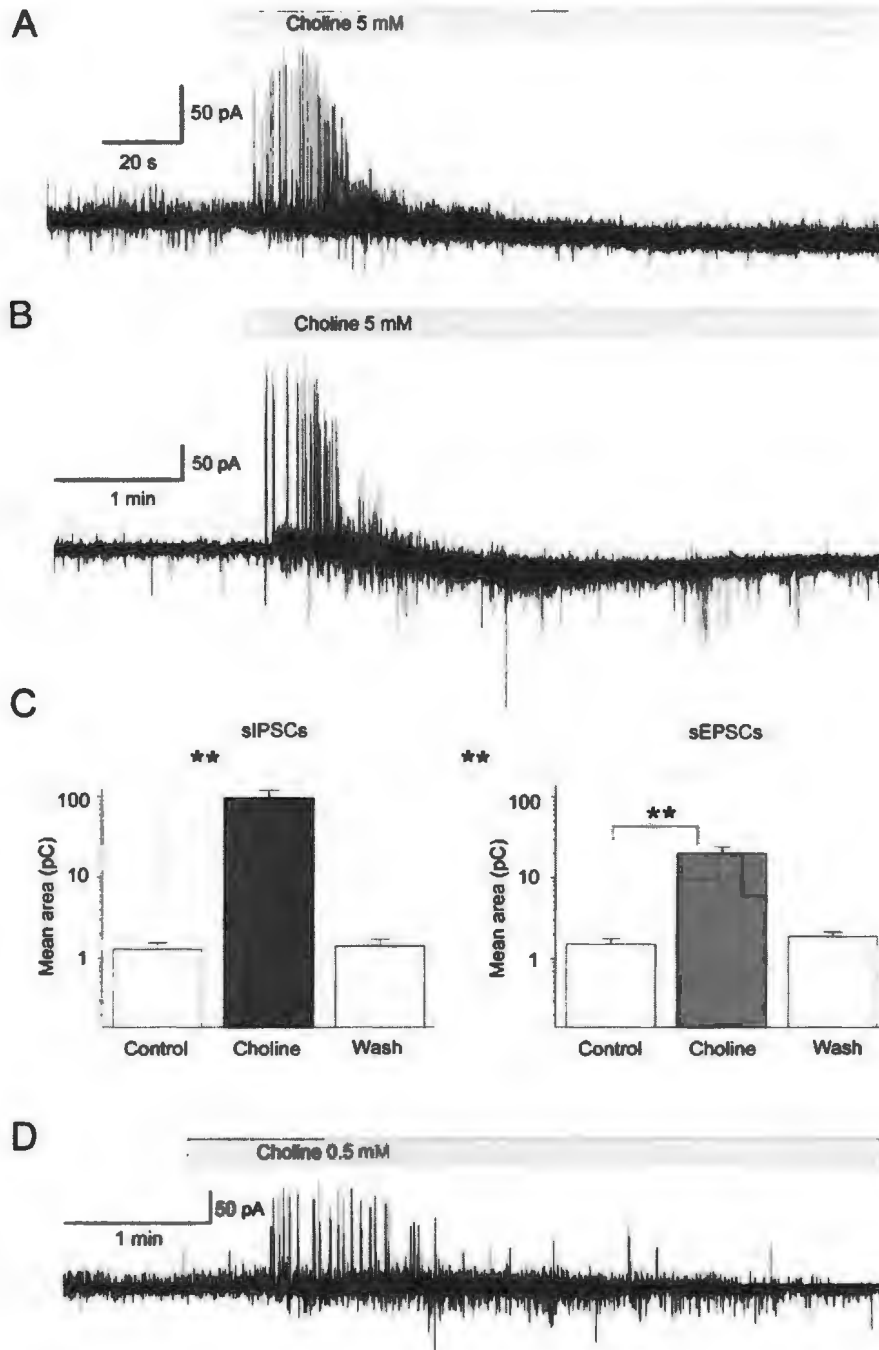


Figure 23 Effects of α_7 -nAChR activation on simultaneously recorded sIPSCs and sEPSCs. Recordings were obtained from principal neurons in the presence of α -conotoxin AulB (1 μ M), DH β E (10 μ M), atropine sulfate (0.5 μ M), D-AP5 (50 μ M), SCH50911 (10 μ M), and LY 3414953 (3 μ M), at a holding potential of -58 mV and internal chloride concentration of 1 mM. *A*: Bath application of choline chloride (5 mM) induced a transient increase in the frequency and amplitude of both sIPSCs (outward currents) and sEPSCs (inward currents), but the increase in sIPSCs was more pronounced. *B*: Another example of the effects

of choline chloride (5 mM) on sIPSCs and sEPSCs. The increase in sEPSCs is more apparent in this cell compared to the cell in *A*. *C*: Group data (mean \pm SE) showing the effects of 5 mM choline chloride on sIPSCs (*left*) and sEPSCs (*right*). Application of choline significantly increased the mean charge transferred by sIPSCs and sEPSCs ($n = 9$, $**P < 0.01$), measured during the 5 sec period after the initiation of the effect. During this 5 sec period, the charge transferred by sIPSCs was significantly larger than the charge transferred by sEPSCs ($n = 9$, $**P < 0.01$). *D*: Lower concentrations of choline produced a similar effect; an example is shown where 500 μ M choline chloride was bath applied.

Since α_7 -nAChR activation enhances spontaneous GABAergic activity to a greater extent than glutamatergic activity, this effect should be reflected in the population responses. An enhanced “tonic” inhibition (sIPSCs) in the BLA network can be expected to reduce overall excitability. Field potentials in the BLA are reduced in amplitude by the GABA_A agonist muscimol and are enhanced by bicuculline (unpublished observations), which implies significant presence of synchronized spiking activity (somatic and/or dendritic) in the generation of the field responses. Since choline enhances GABAergic inhibition, the amplitude of evoked population responses should be reduced in the presence of choline. To test this prediction we bath-applied choline chloride while recording field potentials in the BLA, evoked by stimulation of the external capsule. In these experiments, slices were placed in an interface chamber, which has a much slower flow rate than in the whole-cell recording experiments; the gradual exposure of the slice to low – and slowly rising – concentrations of choline chloride could desensitize the receptors, rendering the effect undetectable. Therefore, we used a high concentration of choline chloride (20 mM) in order to detect the effect. Choline chloride reversibly decreased the amplitude of the field response from 0.49 ± 0.02 to 0.34 ± 0.02 mV ($n = 8$; $P < 0.001$; Figure 24). In percentages, choline reduced the evoked field potential to 71.87

$\pm 4.11\%$ of the control amplitude ($P < 0.001$; Figure 24C). These results are consistent with the view that activation of α_7 -nAChRs reduces the excitability of the BLA network.

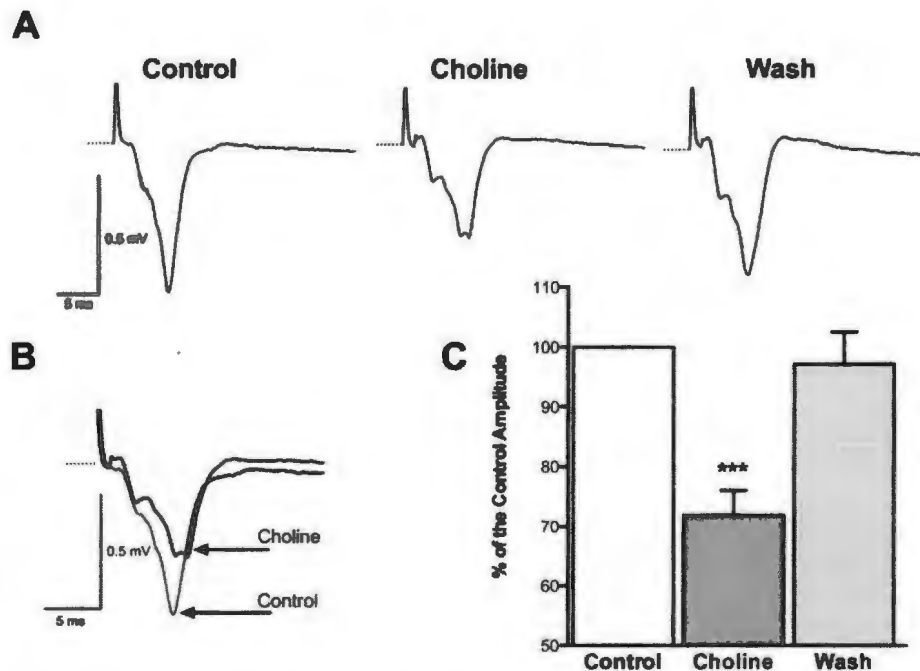


Figure 24 Activation of α_7 -nAChRs reduces evoked field potentials in the BLA. *A*: An example of field potentials evoked in the BLA by stimulation of the external capsule, before, during, and after wash out of choline chloride (20 mM). Each trace is an average of 10 sweeps. *B*: Same field potentials as in *A*, in control medium and in the presence of choline, superimposed for a clearer view of the effect of choline. *C*: Group data from 8 slices showing the amplitude of the field responses as percentages of the control responses before, during, and after bath application of choline ($n = 8$; $***P < 0.001$).

α_7 -nAChRs are active in the basal state contributing to background inhibition

Considering that α_7 -nAChRs have low affinity for their endogenous agonists, acetylcholine and choline, and desensitize rapidly (4), it is important to ask if these receptors can be activated by ambient concentrations of acetylcholine or choline, thereby contributing to the background levels of inhibitory and/or excitatory activity. To answer this question, first we examined the effects of bath-applied α -BgTx (1 μ M) on sIPSCs

recorded from principal BLA neurons. The frequency of sIPSCs was reduced by bath application of α -BgTx, from 43 ± 9 Hz in control medium to 22 ± 8 Hz in α -BgTx ($n = 4$; $P < 0.01$; Figure 25A, B). Next, we tested the effects of α -BgTx on simultaneously recorded sIPSCs and sEPSCs, from principal neurons. α -BgTx ($1\mu\text{M}$) significantly decreased the frequency of sIPSCs from 24 ± 3 Hz to 12 ± 3 Hz ($n=4$; $P = 0.0316$), while the frequency of sEPSCs was reduced from 22 ± 4 Hz in control medium to 15 ± 3 Hz in the presence of α -BgTx ($n = 4$; $P = 0.141$). These results suggest that basal activation of α_7 -nAChRs on interneurons (whether it is the postsynaptic α_7 -nAChRs demonstrated in the present study or/and presynaptic α_7 -nAChRs on GABAergic terminals) contributes significantly to spontaneous inhibitory activity.

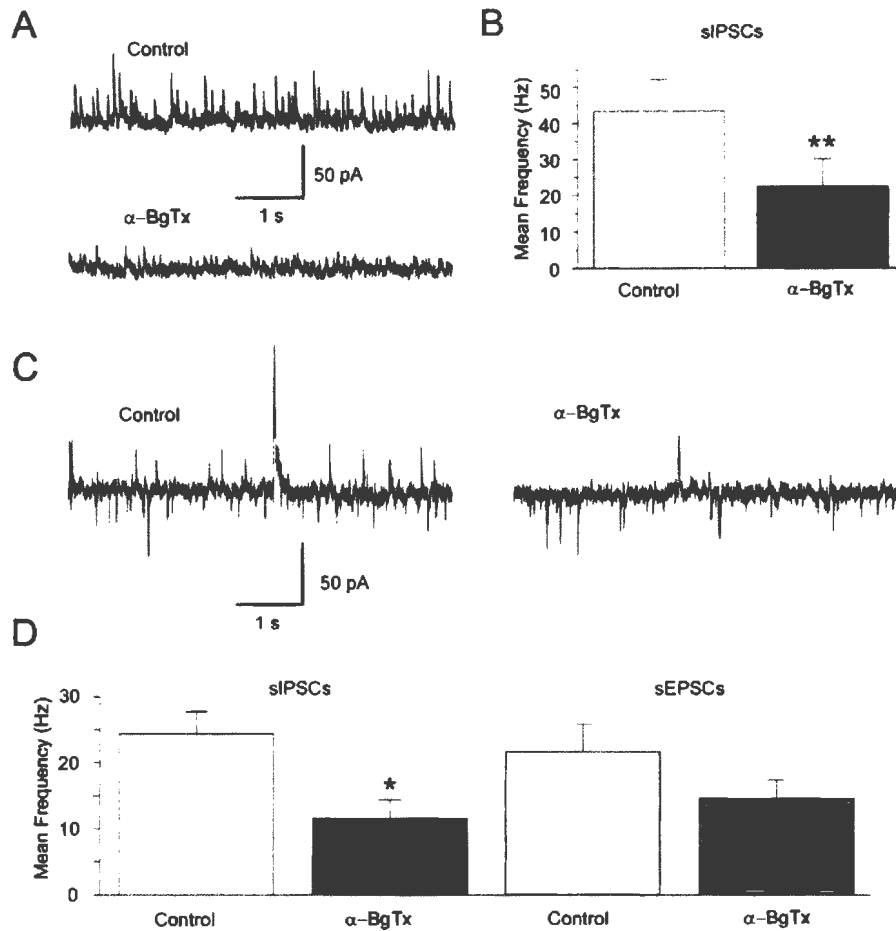


Figure 25 Blockade of α_7 -nAChRs in the basal state decreases the frequency of sIPSCs. *A*: An example from a principal cell displaying high inhibitory synaptic activity in control medium, and the effect of α -BgTx (1 μ M) on sIPSCs ($V_h = +30$ mV); the reduction of the sIPSCs by α -BgTx was irreversible. The slice medium contains α -conotoxin Au1B (1 μ M), DH β E (10 μ M), atropine sulfate (0.5 μ M), CNQX (20 μ M), D-AP5 (50 μ M), SCH50911 (10 μ M), and LY 3414953 (3 μ M). *B*: Group data showing the effect of α -BgTx on the frequency of sIPSCs ($n = 4$, $**P < 0.01$). *C*: An example from another principal cell where sIPSCs and sEPSCs were recorded simultaneously ($V_h = -58$ mV, internal chloride concentration is 1 mM). The reduction of the sIPSCs by α -BgTx (1 μ M) was more pronounced than the reduction of sEPSCs. The slice medium contains α -conotoxin Au1B (1 μ M), DH β E (10 μ M), atropine sulfate (0.5 μ M), D-AP5 (50 μ M), SCH50911 (10 μ M), and LY 3414953 (3 μ M). *D*: Group data showing the effect of α -BgTx on the frequency of sIPSCs ($n = 4$, $*P < 0.05$) and sEPSCs ($n = 4$, $P > 0.05$).

DISCUSSION

This study demonstrated the presence of functional α_7 -nAChRs on somatic or somatodendritic regions of electrophysiologically-identified interneurons in the BLA. Activation of α_7 -nAChRs by choline directly depolarized interneurons and elicited action potentials. In addition, α_7 -nAChR activation increased the frequency of sEPSCs recorded from interneurons, probably due to α_7 -nAChR-mediated depolarization of principal – glutamatergic – neurons and/or presynaptic facilitation of glutamate release. The increase in interneuronal activity by α_7 -nAChR activation produced a dramatic increase in the frequency and amplitude of GABA_A receptor-mediated sIPSCs recorded from BLA principal cells. Simultaneous recordings of sIPSCs and sEPSCs from principal neurons revealed that activation of α_7 -nAChRs by choline increases both types of currents, but the increase of the inhibitory currents is larger than the increase of the excitatory currents. This observation, along with the reduction of the population field response in the presence of choline, suggests that the net effect of α_7 -nAChR activation in the BLA network is suppression of excitability. This function of α_7 -nAChRs appears to be in effect even in the basal state, as blockade of these receptors decreased the frequency of sIPSCs.

The α_7 subunit of the nicotinic receptors is expressed in the BLA (298), and functional α_7 -nAChRs are present on somatodendritic regions of principal BLA neurons (141). However, it was unknown if α_7 -nAChRs are also present on somatodendritic regions of BLA interneurons. This is the first study investigating the responses of BLA interneurons to the activation of α_7 -nAChRs by a specific agonist. We found that 60% of the recorded interneurons responded with a fast-inactivating current, which was blocked

by α -BgTx; these characteristics are typical of the currents mediated by homomeric α_7 -nAChRs (4; 139). However, the remaining interneurons displayed a slow current, which was only partly sensitive to α -BgTx. Since this current was activated by choline in the presence of antagonists of all cholinergic receptors except for the α_7 -nAChRs, it was probably mediated by α_7 -nAChRs. The slow kinetics and the partial resistance to α -BgTx may suggest that the α_7 -nAChRs mediating this current are not homomeric. A different composition and stoichiometry of these α_7 -containing receptors may be responsible for the different kinetics and pharmacology of the currents they mediate. For example, the $\alpha_7\beta_2$ subunit combination has different pharmacological properties and produces currents with slower kinetics compared to the homomeric α_7 -nAChRs (139). The presence of heteromeric α_7 -containing nicotinic receptors ($\alpha_7\beta_2$ subunit combination) has been demonstrated in rat basal forebrain cholinergic neurons (159); it is possible, therefore, that such heteromeric α_7 -nAChRs exist also in other brain regions, including the BLA.

In regard to the role that α_7 -nAChRs play in the regulation of GABAergic activity in the rat BLA, there is only one previous study, showing that α_7 -nAChR antagonists did not reduce the acetylcholine-induced increase in the frequency of sIPSCs recorded from BLA principal cells; therefore, it was suggested that α_7 -nAChRs may not participate in the regulation of inhibitory activity in the BLA (298). One factor that may have contributed to the disparity between our results and those of Zhu et al. (2005) could be the age of the animals used, as the latter study was performed in neonatal rats (P7-10), and, at least in hippocampal interneurons, α_7 -nAChR-mediated currents increase with age (12). A more likely possibility, however, which the authors (298) suggested, is that

the increase in sIPSCs by acetylcholine (the agonist used in the Zhu et al. study) was not reduced by subsequent application of specific α_7 -nAChR antagonists because it was sustained only by non- α_7 nicotinic receptor subtypes that are slow to desensitize (the α_7 -nAChRs were already desensitized). This explanation for the divergent conclusions regarding the importance of α_7 -nAChRs in the regulation of GABAergic activity in the BLA, is consistent with the present results, where the effect of the specific α_7 -nAChR agonist, choline, on the sIPSCs did not last for more than 1 to 2 min, which probably reflects the fast desensitization of the α_7 -nAChRs.

What are the functional implications of the involvement of the α_7 -nAChRs in the regulation of GABAergic activity in the BLA? Like the α_7 -nAChRs on hippocampal interneurons (13), the α_7 -nAChRs in the BLA appear to be active in the basal state, preferentially increasing inhibitory activity. Therefore, even without significant activation of the cholinergic inputs to the amygdala above the basal level, these receptors may participate in the regulation of normal amygdala functions, primarily by limiting excitation. It should be considered, however, that since α_7 -nAChRs are present on both inhibitory and excitatory BLA neurons, their *in vivo* activation in the functioning BLA may promote either excitatory or inhibitory activity depending on a number of factors, such as: a) the concentration of acetylcholine at the vicinity of α_7 -nAChRs, and the temporal pattern of its increase, which may differentially affect the desensitization of α_7 -nAChRs on principal cells versus interneurons, b) the role of presynaptic α_7 -nAChRs on glutamatergic terminals (29; 128), and c) possible effects of other concomitantly acting neurotransmitters and neuromodulators that could potentially alter the neurons' response

to α_7 -nAChR stimulation. Our results show only that inhibition is favored over excitation when α_7 -nAChRs are uniformly activated throughout the BLA network.

Relatively uniform activation of α_7 -nAChRs in the BLA can be expected during cigarette smoking, and our results suggest that these receptors may, in part, mediate the anxiolytic effects of nicotine. On an acute basis, nicotine is known to have anxiolytic (32; 52; 56; 133; 273) and antidepressant effects (116; 281). The amygdala, and the BLA in particular, plays a central role in anxiety and depression (66; 67; 73; 81; 113; 152; 185). Our results suggest that the α_7 -nAChR-mediated increase in GABAergic activity in the BLA may be one of the mechanisms by which nicotine suppresses BLA excitability, thereby reducing anxiety and alleviating depression. This view receives support by the finding that systemic administration of an α_7 -nAChR agonist, in mice, has anxiolytic effects (88). Because of the pronounced but only transient increase of inhibitory activity upon activation of α_7 -nAChRs, followed by desensitization of the receptor, the anxiolytic effect of nicotine may be stronger when α_7 -nAChRs are stimulated in an intermittent fashion, as it probably occurs during cigarette smoking. Due to their low affinity for nicotine (86), the α_7 -nAChRs may be transiently activated only during the peak levels of nicotine, while they recover from desensitization during the troughs.

Considering that the amygdala is a seizure-prone structure with an important role in certain forms of epilepsy (20), the question arises as to whether α_7 -nAChRs, by regulating both GABAergic and glutamatergic activity in the BLA, play a significant role in seizure generation and/or suppression. An involvement of the α_7 -nAChR in epilepsy is suggested by the association of juvenile myoclonic epilepsy with a mutation in the gene coding for the α_7 subunit (78). In addition, systemic administration of an α_7 -nAChR

agonist, in mice, showed anticonvulsant potential in the audiogenic seizure paradigm (88), which is known to involve the amygdala (85; 120). This finding, along with the present data showing a preferential increase of inhibitory activity in the BLA by α_7 -nAChR activation, suggest that in the amygdala these receptors may contribute to suppression of seizures.

The α_7 -nAChRs are known to be important in learning and memory (37; 118; 155; 242; 280), including memory involving the amygdala (1). In the BLA of Alzheimer's patients, there is accumulation of β -amyloid protein in GABAergic and glutamatergic neurons (80), which interacts and forms a protein complex with the α_7 -nAChRs (75; 219); the resulting inactivation of α_7 -nAChRs is considered to be important in the pathogenesis of Alzheimer's disease (219). Alzheimer's patients display impaired fear conditioning (112; 123) – a form of fear-related memory – as well as increased fear and anxiety (80; 87); these symptoms may be related to the inactivation of α_7 -nAChRs by β -amyloid protein, producing hyperexcitability in the BLA.

The involvement of α_7 -nAChRs in the regulation of GABAergic inhibition in the BLA may also have implications in the pathophysiology of schizophrenia. The expression and function of α_7 -nAChRs is reduced in schizophrenia (2; 106; 168; 211). The dysfunction of the amygdala in schizophrenic patients (5; 33; 151) and, in particular, the abnormally high activation of the amygdala during processing of stimuli that should not evoke fear (111) may imply dysregulation of inhibitory activity in the BLA, which could be due, in part, to abnormalities in α_7 -nAChR function.

In conclusion, we demonstrated that α_7 -nAChRs are expressed on somatic and/or dendritic regions of GABAergic interneurons in the BLA, and that activation of these

receptors increases GABA_A receptor-mediated sIPSCs, even in the basal state. In addition, we showed that although activation of α_7 -nAChRs increases both sIPSCs and sEPSCs, the net effect is a preferential enhancement of inhibition. The presence of functional α_7 -nAChRs on GABAergic interneurons in the BLA may suggest a site for therapeutic treatments of diseases associated with amygdalar hyperactivity.

ACKNOWLEDGMENTS

Grants: This work was supported by the CounterACT Program, National Institutes of Health, Office of the Director and the National Institute of Neurologic Disorders and Stroke [Grant Number 5U01NS058162-07], and the Defense Threat Reduction Agency-Joint Science and Technology Office, Medical S&T Division [Grant Numbers CBM.NEURO.01.10.US.18 and CBM.NEURO.01.10.US.15].

Disclosures: No conflicts of interest, financial or otherwise, are declared by the authors.

Author Contributions: M.F.M.B., V. A-A., V.I.P., E.M.P., conception and design of research; V.I.P. and E.M.P., performed experiments; V.I.P. and E.M.P., analyzed data and prepared figures; V. A-A., V.I.P., M.F.M.B., E.M.P. interpreted results of experiments; E.M.P. prepared draft of the manuscript; V.A-A., revised manuscript; E.M.P., V.I.P., M.F.M.B., provided comments on the manuscript; M.F.M.B., V. A-A., V.I.P., E.M.P. approved final version of manuscript; M.F.M.B., V. A-A., acquired funding for the research.

REFERENCES

1. Addy NA, Nakijama A, Levin ED. 2003. Nicotinic mechanisms of memory: effects of acute local DHbetaE and MLA infusions in the basolateral amygdala. *Brain Res Cogn Brain Res* 16:51-7
2. Adler LE, Olincy A, Waldo M, Harris JG, Griffith J, et al. 1998. Schizophrenia, sensory gating, and nicotinic receptors. *Schizophr Bull* 24:189-202
3. Akaike A, Takada-Takatori Y, Kume T, Izumi Y. 2010. Mechanisms of neuroprotective effects of nicotine and acetylcholinesterase inhibitors: role of alpha4 and alpha7 receptors in neuroprotection. *J Mol Neurosci* 40:211-6
4. Albuquerque EX, Pereira EF, Alkondon M, Rogers SW. 2009. Mammalian nicotinic acetylcholine receptors: from structure to function. *Physiol Rev* 89:73-120
5. Aleman A, Kahn RS. 2005. Strange feelings: do amygdala abnormalities dysregulate the emotional brain in schizophrenia? *Prog Neurobiol* 77:283-98
6. Alkondon M, Albuquerque EX. 2001. Nicotinic acetylcholine receptor alpha7 and alpha4beta2 subtypes differentially control GABAergic input to CA1 neurons in rat hippocampus. *J Neurophysiol* 86:3043-55
7. Alkondon M, Albuquerque EX. 2004. The nicotinic acetylcholine receptor subtypes and their function in the hippocampus and cerebral cortex. *Prog Brain Res* 145:109-20
8. Alkondon M, Albuquerque EX. 2005. Nicotinic receptor subtypes in rat hippocampal slices are differentially sensitive to desensitization and early in vivo functional up-regulation by nicotine and to block by bupropion. *J Pharmacol Exp Ther* 313:740-50
9. Alkondon M, Braga MF, Pereira EF, Maelicke A, Albuquerque EX. 2000. alpha7 nicotinic acetylcholine receptors and modulation of gabaergic synaptic transmission in the hippocampus. *Eur J Pharmacol* 393:59-67
10. Alkondon M, Pereira EF, Albuquerque EX. 1996. Mapping the location of functional nicotinic and gamma-aminobutyric acidA receptors on hippocampal neurons. *J Pharmacol Exp Ther* 279:1491-506
11. Alkondon M, Pereira EF, Albuquerque EX. 1998. alpha-bungarotoxin- and methyllycaconitine-sensitive nicotinic receptors mediate fast synaptic transmission in interneurons of rat hippocampal slices. *Brain Res* 810:257-63
12. Alkondon M, Pereira EF, Albuquerque EX. 2007. Age-dependent changes in the functional expression of two nicotinic receptor subtypes in CA1 stratum radiatum interneurons in the rat hippocampus. *Biochem Pharmacol* 74:1134-44

13. Alkondon M, Pereira EF, Eisenberg HM, Albuquerque EX. 1999. Choline and selective antagonists identify two subtypes of nicotinic acetylcholine receptors that modulate GABA release from CA1 interneurons in rat hippocampal slices. *J Neurosci* 19:2693-705
14. Ankarcrona M, Dypbukt JM, Bonfoco E, Zhivotovsky B, Orrenius S, et al. 1995. Glutamate-induced neuronal death: a succession of necrosis or apoptosis depending on mitochondrial function. *Neuron* 15:961-73
15. Apland JP, Aroniadou-Anderjaska V, Braga MF. 2009. Soman induces ictogenesis in the amygdala and interictal activity in the hippocampus that are blocked by a GluR5 kainate receptor antagonist in vitro. *Neuroscience* 159:380-9
16. Apland JP, Aroniadou-Anderjaska V, Figueiredo TH, Green CE, Swezey R, et al. 2013. Efficacy of the GluK1/AMPA receptor antagonist LY293558 against seizures and neuropathology in a soman-exposure model without pretreatment and its pharmacokinetics after intramuscular administration. *J Pharmacol Exp Ther* 344:133-40
17. Apland JP, Figueiredo TH, Qashu F, Aroniadou-Anderjaska V, Souza AP, Braga MF. 2010. Higher susceptibility of the ventral versus the dorsal hippocampus and the posteroventral versus anterodorsal amygdala to soman-induced neuropathology. *Neurotoxicology* 31:485-92
18. Arnaiz-Cot JJ, Gonzalez JC, Sobrado M, Baldelli P, Carbone E, et al. 2008. Allosteric modulation of alpha 7 nicotinic receptors selectively depolarizes hippocampal interneurons, enhancing spontaneous GABAergic transmission. *Eur J Neurosci* 27:1097-110
19. Aroniadou-Anderjaska V, Figueiredo TH, Apland JP, Qashu F, Braga MF. 2009. Primary brain targets of nerve agents: the role of the amygdala in comparison to the hippocampus. *Neurotoxicology* 30:772-6
20. Aroniadou-Anderjaska V, Fritsch B, Qashu F, Braga MF. 2008. Pathology and pathophysiology of the amygdala in epileptogenesis and epilepsy. *Epilepsy Res* 78:102-16
21. Aroniadou-Anderjaska V, Pidoplichko VI, Figueiredo TH, Almeida-Suhett CP, Prager EM, Braga MF. 2012. Presynaptic facilitation of glutamate release in the basolateral amygdala: a mechanism for the anxiogenic and seizurogenic function of GluK1 receptors. *Neuroscience* 221:157-69
22. Aroniadou-Anderjaska V, Qashu F, Braga MF. 2007. Mechanisms regulating GABAergic inhibitory transmission in the basolateral amygdala: implications for epilepsy and anxiety disorders. *Amino Acids* 32:305-15
23. Baille V, Clarke PG, Brochier G, Dorandeu F, Verna JM, et al. 2005. Soman-induced convulsions: the neuropathology revisited. *Toxicology* 215:1-24

24. Bajgar J. 1997. Differential inhibition of the brain acetylcholinesterase molecular forms following sarin, soman and VX intoxication in laboratory rats. *Acta Medica (Hradec Kralove)* 40:89-94
25. Bajgar J. 2004. Organophosphates/nerve agent poisoning: mechanism of action, diagnosis, prophylaxis, and treatment. *Adv Clin Chem* 38:151-216
26. Bajgar J. 2005. Complex view on poisoning with nerve agents and organophosphates. *Acta Medica (Hradec Kralove)* 48:3-21
27. Bajgar J, Fusek J, Kassa J, Jun D, Kuca K, Hajek P. 2008. An attempt to assess functionally minimal acetylcholinesterase activity necessary for survival of rats intoxicated with nerve agents. *Chem Biol Interact* 175:281-5
28. Balali-Mood M, Saber H. 2012. Recent advances in the treatment of organophosphorous poisonings. *Iran J Med Sci* 37:74-91
29. Barazangi N, Role LW. 2001. Nicotine-induced enhancement of glutamatergic and GABAergic synaptic transmission in the mouse amygdala. *J Neurophysiol* 86:463-74
30. Barik J, Wonnacott S. 2006. Indirect modulation by alpha7 nicotinic acetylcholine receptors of noradrenaline release in rat hippocampal slices: interaction with glutamate and GABA systems and effect of nicotine withdrawal. *Mol Pharmacol* 69:618-28
31. Ben-Ari Y, Zigmond RE, Shute CC, Lewis PR. 1977. Regional distribution of choline acetyltransferase and acetylcholinesterase within the amygdaloid complex and stria terminalis system. *Brain Res* 120:435-44
32. Bencan Z, Levin ED. 2008. The role of alpha7 and alpha4beta2 nicotinic receptors in the nicotine-induced anxiolytic effect in zebrafish. *Physiol Behav* 95:408-12
33. Benes FM. 2010. Amygdalocortical circuitry in schizophrenia: from circuits to molecules. *Neuropsychopharmacology* 35:239-57
34. Bergstrom HC, McDonald CG, Dey S, Tang H, Selwyn RG, Johnson LR. 2013. The structure of Pavlovian fear conditioning in the amygdala. *Brain Struct Funct* 218:1569-89
35. Bhagat YA, Obenaus A, Hamilton MG, Kendall EJ. 2001. Magnetic resonance imaging predicts neuropathology from soman-mediated seizures in the rodent. *Neuroreport* 12:1481-7
36. Bodjarian N, Carpentier P, Blanchet G, Baubichon D, Lallement G. 1993. Cholinergic activation of phosphoinositide metabolism during soman-induced seizures. *Neuroreport* 4:1191-3

37. Boess FG, De Vry J, Erb C, Flessner T, Hendrix M, et al. 2007. The novel alpha7 nicotinic acetylcholine receptor agonist N-[(3R)-1-azabicyclo[2.2.2]oct-3-yl]-7-[2-(methoxy)phenyl]-1-benzofuran-2-carboxamide improves working and recognition memory in rodents. *J Pharmacol Exp Ther* 321:716-25
38. Bradford MM. 1976. A rapid and sensitive method for the quantitation of microgram quantities of protein utilizing the principle of protein-dye binding. *Anal Biochem* 72:248-54
39. Braga MF, Aroniadou-Anderjaska V, Manion ST, Hough CJ, Li H. 2004. Stress impairs alpha(1A) adrenoceptor-mediated noradrenergic facilitation of GABAergic transmission in the basolateral amygdala. *Neuropsychopharmacology* 29:45-58
40. Braga MF, Aroniadou-Anderjaska V, Xie J, Li H. 2003. Bidirectional modulation of GABA release by presynaptic glutamate receptor 5 kainate receptors in the basolateral amygdala. *J Neurosci* 23:442-52
41. Braun P, Greenberg D, Dasberg H, Lerer B. 1990. Core symptoms of posttraumatic stress disorder unimproved by alprazolam treatment. *J Clin Psychiatry* 51:236-8
42. Brown DA. 2010. Muscarinic acetylcholine receptors (mAChRs) in the nervous system: some functions and mechanisms. *J Mol Neurosci* 41:340-6
43. Browning ET. 1971. Free choline formation by cerebral cortical slices from rat brain. *Biochem Biophys Res Commun* 45:1586-90
44. Bueno CH, Zangrossi H, Jr., Viana MB. 2005. The inactivation of the basolateral nucleus of the rat amygdala has an anxiolytic effect in the elevated T-maze and light/dark transition tests. *Braz J Med Biol Res* 38:1697-701
45. Callicott JH, Bertolino A, Mattay VS, Langheim FJ, Duyn J, et al. 2000. Physiological dysfunction of the dorsolateral prefrontal cortex in schizophrenia revisited. *Cereb Cortex* 10:1078-92
46. Cardona D, Lopez-Granero C, Canadas F, Llorens J, Flores P, et al. 2013. Dose-dependent regional brain acetylcholinesterase and acylpeptide hydrolase inhibition without cell death after chlorpyrifos administration. *J Toxicol Sci* 38:193-203
47. Carlsen J, Heimer L. 1986. A correlated light and electron microscopic immunocytochemical study of cholinergic terminals and neurons in the rat amygdaloid body with special emphasis on the basolateral amygdaloid nucleus. *J Comp Neurol* 244:121-36

48. Carlsen J, Zaborszky L, Heimer L. 1985. Cholinergic projections from the basal forebrain to the basolateral amygdaloid complex: a combined retrograde fluorescent and immunohistochemical study. *J Comp Neurol* 234:155-67
49. Carpentier P, Foquin A, Rondouin G, Lerner-Natoli M, de Groot DM, Lallement G. 2000. Effects of atropine sulphate on seizure activity and brain damage produced by soman in guinea-pigs: ECoG correlates of neuropathology. *Neurotoxicology* 21:521-40
50. Carpentier P, Testylier G, Dorandeu F, Segebarth C, Montigon O, et al. 2008. Hyperosmolar treatment of soman-induced brain lesions in mice: evaluation of the effects through diffusion-weighted magnetic resonance imaging and through histology. *Toxicology* 253:97-103
51. Cates ME, Bishop MH, Davis LL, Lowe JS, Woolley TW. 2004. Clonazepam for treatment of sleep disturbances associated with combat-related posttraumatic stress disorder. *Ann Pharmacother* 38:1395-9
52. Cheeta S, Irvine EE, Tucci S, Sandhu J, File SE. 2001. In adolescence, female rats are more sensitive to the anxiolytic effect of nicotine than are male rats. *Neuropsychopharmacology* 25:601-7
53. Chen Y. 2012. Organophosphate-induced brain damage: mechanisms, neuropsychiatric and neurological consequences, and potential therapeutic strategies. *Neurotoxicology* 33:391-400
54. Christophe E, Roebuck A, Staiger JF, Lavery DJ, Charpak S, Audinat E. 2002. Two types of nicotinic receptors mediate an excitation of neocortical layer I interneurons. *J Neurophysiol* 88:1318-27
55. Clement JG, Rosario S, Bessette E, Erhardt N. 1991. Soman and sarin inhibition of molecular forms of acetylcholinesterase in mice. Time course of recovery and reactivation by the oxime HI-6. *Biochem Pharmacol* 42:329-35
56. Cohen A, Young RW, Velazquez MA, Groysman M, Noorbehesht K, et al. 2009. Anxiolytic effects of nicotine in a rodent test of approach-avoidance conflict. *Psychopharmacology* 204:541-9
57. Collombet JM. 2011. Nerve agent intoxication: recent neuropathophysiological findings and subsequent impact on medical management prospects. *Toxicol Appl Pharmacol* 255:229-41
58. Collombet JM, Beracochea D, Liscia P, Pierard C, Lallement G, Filliat P. 2011. Long-term effects of cytokine treatment on cognitive behavioral recovery and neuronal regeneration in soman-poisoned mice. *Behav Brain Res* 221:261-70

59. Collombet JM, Carpentier P, Baille V, Four E, Bernabe D, et al. 2006. Neuronal regeneration partially compensates the delayed neuronal cell death observed in the hippocampal CA1 field of soman-poisoned mice. *Neurotoxicology* 27:201-9
60. Collombet JM, Pierard C, Beracochea D, Coubard S, Burckhart MF, et al. 2008. Long-term consequences of soman poisoning in mice Part 1. Neuropathology and neuronal regeneration in the amygdala. *Behav Brain Res* 191:88-94
61. Coubard S, Beracochea D, Collombet JM, Philippin JN, Krazem A, et al. 2008. Long-term consequences of soman poisoning in mice: part 2. Emotional behavior. *Behav Brain Res* 191:95-103
62. Cruickshank JW, Brudzynski SM, McLachlan RS. 1994. Involvement of M1 muscarinic receptors in the initiation of cholinergically induced epileptic seizures in the rat brain. *Brain Res* 643:125-9
63. Dani JA. 2001. Overview of nicotinic receptors and their roles in the central nervous system. *Biol Psychiatry* 49:166-74
64. Dani JA, Bertrand D. 2007. Nicotinic acetylcholine receptors and nicotinic cholinergic mechanisms of the central nervous system. *Annu Rev Pharmacol Toxicol* 47:699-729
65. Davidson JR, Brady K, Mellman TA, Stein MB, Pollack MH. 2007. The efficacy and tolerability of tiagabine in adult patients with post-traumatic stress disorder. *J Clin Psychopharmacol* 27:85-8
66. Davis M. 1998. Are different parts of the extended amygdala involved in fear versus anxiety? *Biol Psychiatry* 44:1239-47
67. Davis M, Rainnie D, Cassell M. 1994. Neurotransmission in the rat amygdala related to fear and anxiety. *Trends Neurosci* 17:208-14
68. de Araujo Furtado M, Lumley LA, Robison C, Tong LC, Lichtenstein S, Yourick DL. 2010. Spontaneous recurrent seizures after status epilepticus induced by soman in Sprague-Dawley rats. *Epilepsia* 51:1503-10
69. Demoy M, Minko T, Kopeckova P, Kopecek J. 2000. Time- and concentration-dependent apoptosis and necrosis induced by free and HPMA copolymer-bound doxorubicin in human ovarian carcinoma cells. *J Control Release* 69:185-96
70. Dickinson JA, Kew JN, Wonnacott S. 2008. Presynaptic alpha 7- and beta 2-containing nicotinic acetylcholine receptors modulate excitatory amino acid release from rat prefrontal cortex nerve terminals via distinct cellular mechanisms. *Mol Pharmacol* 74:348-59

71. Didenko VV, Wang X, Yang L, Hornsby PJ. 1996. Expression of p21(WAF1/CIP1/SDI1) and p53 in apoptotic cells in the adrenal cortex and induction by ischemia/reperfusion injury. *J Clin Invest* 97:1723-31
72. Dolgin E. 2013. Syrian gas attack reinforces need for better anti-sarin drugs. *Nat Med* 19:1194-5
73. Drevets WC. 1999. Prefrontal cortical-amygdalar metabolism in major depression. *Ann N Y Acad Sci* 877:614-37
74. Drewes LR, Singh AK. 1988. Choline transport and metabolism in soman- or sarin-intoxicated brain. *J Neurochem* 50:868-75
75. Dziewczapolski G, Glogowski CM, Masliah E, Heinemann SF. 2009. Deletion of the alpha 7 nicotinic acetylcholine receptor gene improves cognitive deficits and synaptic pathology in a mouse model of Alzheimer's disease. *J Neurosci* 29:8805-15
76. Eglen RM. 2006. Muscarinic receptor subtypes in neuronal and non-neuronal cholinergic function. *Auton Autacoid Pharmacol* 26:219-33
77. Ellman GL, Courtney KD, Andres V, Jr., Feather-Stone RM. 1961. A new and rapid colorimetric determination of acetylcholinesterase activity. *Biochem Pharmacol* 7:88-95
78. Elmslie FV, Rees M, Williamson MP, Kerr M, Kjeldsen MJ, et al. 1997. Genetic mapping of a major susceptibility locus for juvenile myoclonic epilepsy on chromosome 15q. *Hum Mol Genet* 6:1329-34
79. Emson PC, Paxinos G, Le Gal La Salle G, Ben-Ari Y, Silver A. 1979. Choline acetyltransferase and acetylcholinesterase containing projections from the basal forebrain to the amygdaloid complex of the rat. *Brain Res* 165:271-82
80. Espana J, Gimenez-Llort L, Valero J, Minano A, Rabano A, et al. 2010. Intraneuronal beta-amyloid accumulation in the amygdala enhances fear and anxiety in Alzheimer's disease transgenic mice. *Biol Psychiatry* 67:513-21
81. Etkin A, Klemenhagen KC, Dudman JT, Rogan MT, Hen R, et al. 2004. Individual differences in trait anxiety predict the response of the basolateral amygdala to unconsciously processed fearful faces. *Neuron* 44:1043-55
82. Etkin A, Wager TD. 2007. Functional neuroimaging of anxiety: a meta-analysis of emotional processing in PTSD, social anxiety disorder, and specific phobia. *Am J Psychiatry* 164:1476-88
83. Faraday MM, Elliott BM, Grunberg NE. 2001. Adult vs. adolescent rats differ in biobehavioral responses to chronic nicotine administration. *Pharmacol Biochem Behav* 70:475-89

84. Faraday MM, Grunberg NE. 2000. The importance of acclimation in acoustic startle amplitude and pre-pulse inhibition testing of male and female rats. *Pharmacol Biochem Behav* 66:375-81
85. Feng HJ, Faingold CL. 2002. Repeated generalized audiogenic seizures induce plastic changes on acoustically evoked neuronal firing in the amygdala. *Brain Res* 932:61-9
86. Fenster CP, Rains MF, Noerager B, Quick MW, Lester RA. 1997. Influence of subunit composition on desensitization of neuronal acetylcholine receptors at low concentrations of nicotine. *J Neurosci* 17:5747-59
87. Ferretti L, McCurry SM, Logsdon R, Gibbons L, Teri L. 2001. Anxiety and Alzheimer's disease. *J Geriatr Psychiatry Neurol* 14:52-8
88. Feuerbach D, Lingenhoehl K, Olpe HR, Vassout A, Gentsch C, et al. 2009. The selective nicotinic acetylcholine receptor alpha7 agonist JN403 is active in animal models of cognition, sensory gating, epilepsy and pain. *Neuropharmacology* 56:254-63
89. Figueiredo TH, Aroniadou-Anderjaska V, Qashu F, Apland JP, Pidoplichko V, et al. 2011. Neuroprotective efficacy of caramiphen against soman and mechanisms of its action. *Br J Pharmacol* 164:1495-505
90. Figueiredo TH, Qashu F, Apland JP, Aroniadou-Anderjaska V, Souza AP, Braga MF. 2011. The GluK1 (GluR5) Kainate/{alpha}-amino-3-hydroxy-5-methyl-4-isoxazolepropionic acid receptor antagonist LY293558 reduces soman-induced seizures and neuropathology. *J Pharmacol Exp Ther* 336:303-12
91. Filliat P, Coubard S, Pierard C, Liscia P, Beracochea D, et al. 2007. Long-term behavioral consequences of soman poisoning in mice. *Neurotoxicology* 28:508-19
92. Fishman EB, Siek GC, MacCallum RD, Bird ED, Volicer L, Marquis JK. 1986. Distribution of the molecular forms of acetylcholinesterase in human brain: alterations in dementia of the Alzheimer type. *Ann Neurol* 19:246-52
93. Fix AS, Horn JW, Wightman KA, Johnson CA, Long GG, et al. 1993. Neuronal vacuolization and necrosis induced by the noncompetitive N-methyl-D-aspartate (NMDA) antagonist MK(+)-801 (dizocilpine maleate): a light and electron microscopic evaluation of the rat retrosplenial cortex. *Exp Neurol* 123:204-15
94. Flynn CJ, Wecker L. 1986. Elevated choline levels in brain. A non-cholinergic component of organophosphate toxicity. *Biochem Pharmacol* 35:3115-21
95. Fucile S. 2004. Ca²⁺ permeability of nicotinic acetylcholine receptors. *Cell Calcium* 35:1-8

96. Fujikawa DG. 2005. Prolonged seizures and cellular injury: understanding the connection. *Epilepsy Behav* 7 Suppl 3:S3-11
97. Gale GD, Anagnostaras SG, Godsil BP, Mitchell S, Nozawa T, et al. 2004. Role of the basolateral amygdala in the storage of fear memories across the adult lifetime of rats. *J Neurosci* 24:3810-5
98. Giniatullin R, Nistri A, Yakel JL. 2005. Desensitization of nicotinic ACh receptors: shaping cholinergic signaling. *Trends Neurosci* 28:371-8
99. Gloor P. 1992. Role of the amygdala in temporal lobe epilepsy. In *The amygdala: neurobiological aspects of emotion, memory, and mental dysfunction*, ed. JP Aggleton:505-38. New York: Wiley-Liss. Number of 505-38 pp.
100. Goodkin HP, Joshi S, Mchedlishvili Z, Brar J, Kapur J. 2008. Subunit-specific trafficking of GABA(A) receptors during status epilepticus. *J Neurosci* 28:2527-38
101. Goodkin HP, Yeh JL, Kapur J. 2005. Status epilepticus increases the intracellular accumulation of GABAA receptors. *J Neurosci* 25:5511-20
102. Goossens L, Sunaert S, Peeters R, Griez EJ, Schruers KR. 2007. Amygdala hyperfunction in phobic fear normalizes after exposure. *Biol Psychiatry* 62:1119-25
103. Gotti C, Clementi F, Fornari A, Gaimarri A, Guiducci S, et al. 2009. Structural and functional diversity of native brain neuronal nicotinic receptors. *Biochem Pharmacol* 78:703-11
104. Grifman M, Arbel A, Ginzberg D, Glick D, Elgavish S, et al. 1997. In vitro phosphorylation of acetylcholinesterase at non-consensus protein kinase A sites enhances the rate of acetylcholine hydrolysis. *Brain Res Mol Brain Res* 51:179-87
105. Grubic Z, Sketelj J, Klinar B, Brzin M. 1981. Recovery of acetylcholinesterase in the diaphragm, brain, and plasma of the rat after irreversible inhibition by soman: a study of cytochemical localization and molecular forms of the enzyme in the motor end plate. *J Neurochem* 37:909-16
106. Guan ZZ, Zhang X, Blennow K, Nordberg A. 1999. Decreased protein level of nicotinic receptor alpha7 subunit in the frontal cortex from schizophrenic brain. *Neuroreport* 10:1779-82
107. Gullapalli RP, Aracava Y, Zhuo J, Helal Neto E, Wang J, et al. 2010. Magnetic resonance imaging reveals that galantamine prevents structural brain damage induced by an acute exposure of guinea pigs to soman. *Neurotoxicology* 31:67-76
108. Gundersen HJ, Jensen EB, Kieu K, Nielsen J. 1999. The efficiency of systematic sampling in stereology--reconsidered. *J Microsc* 193:199-211

109. Gunderson CH, Lehmann CR, Sidell FR, Jabbari B. 1992. Nerve agents: a review. *Neurology* 42:946-50
110. Hajek P, Slizova D, Krs O, Bajgar J. 2004. Comparison of changes in AChE activity in the brain of the laboratory rat after soman and tabun intoxication. *Biomed Pap Med Fac Univ Palacky Olomouc Czech Repub* 148:209-11
111. Hall J, Whalley HC, McKirdy JW, Romaniuk L, McGonigle D, et al. 2008. Overactivation of fear systems to neutral faces in schizophrenia. *Biol Psychiatry* 64:70-3
112. Hamann S, Monarch ES, Goldstein FC. 2002. Impaired fear conditioning in Alzheimer's disease. *Neuropsychologia* 40:1187-95
113. Hamilton JP, Siemer M, Gotlib IH. 2008. Amygdala volume in major depressive disorder: a meta-analysis of magnetic resonance imaging studies. *Mol Psychiatry* 13:993-1000
114. Hamilton MG, Posavad C. 1991. Alteration of calcium influx in rat cortical synaptosomes by soman. *Neuroreport* 2:273-6
115. Harrison PK, Sheridan RD, Green AC, Scott IR, Tattersall JE. 2004. A guinea pig hippocampal slice model of organophosphate-induced seizure activity. *J Pharmacol Exp Ther* 310:678-86
116. Hawkins JW. 1997. Antidepressant effects of nicotine. *J Clin Psychiatry* 58:324-5
117. Hayward IJ, Wall HG, Jaax NK, Wade JV, Marlow DD, Nold JB. 1990. Decreased brain pathology in organophosphate-exposed rhesus monkeys following benzodiazepine therapy. *J Neurol Sci* 98:99-106
118. Hellier JL, Arevalo NL, Smith L, Xiong KN, Restrepo D. 2012. alpha7-Nicotinic acetylcholine receptor: role in early odor learning preference in mice. *PloS One* 7:e35251
119. Hill JA, Jr., Zoli M, Bourgeois JP, Changeux JP. 1993. Immunocytochemical localization of a neuronal nicotinic receptor: the beta 2-subunit. *J Neurosci* 13:1551-68
120. Hirsch E, Danober L, Simler S, Pereira de Vasconcelos A, Maton B, et al. 1997. The amygdala is critical for seizure propagation from brainstem to forebrain. *Neuroscience* 77:975-84
121. Hirsch JC, Agassandian C, Merchan-Perez A, Ben-Ari Y, DeFelipe J, et al. 1999. Deficit of quantal release of GABA in experimental models of temporal lobe epilepsy. *Nat Neurosci* 2:499-500

122. Hitchcock JM, Davis M. 1987. Fear-potentiated startle using an auditory conditioned stimulus: effect of lesions of the amygdala. *Physiol Behav* 39:403-8
123. Hoefer M, Allison SC, Schauer GF, Neuhaus JM, Hall J, et al. 2008. Fear conditioning in frontotemporal lobar degeneration and Alzheimer's disease. *Brain* 131:1646-57
124. Hoffman A, Eisenkraft A, Finkelstein A, Schein O, Rotman E, Dushnitsky T. 2007. A decade after the Tokyo sarin attack: a review of neurological follow-up of the victims. *Mil Med* 172:607-10
125. Holmes GL. 2002. Seizure-induced neuronal injury: animal data. *Neurology* 59:S3-6
126. Howerton TC, Murphy MR, Miller SA, Hartgraves SL. 1991. Differential sensitivity of CNS regions to acetylcholinesterase inhibition following chronic low-dose soman treatment in the rat. *Psychopharmacology* 105:400-6
127. Jett DA. 2007. Neurological aspects of chemical terrorism. *Ann Neurol* 61:9-13
128. Jiang L, Role LW. 2008. Facilitation of cortico-amygdala synapses by nicotine: activity-dependent modulation of glutamatergic transmission. *J Neurophysiol* 99:1988-99
129. Jimmerson VR, Shih TM, Mailman RB. 1989. Variability in soman toxicity in the rat: correlation with biochemical and behavioral measures. *Toxicology* 57:241-54
130. Joy RM, Albertson TE, Stark LG. 1984. An analysis of the actions of progabide, a specific GABA receptor agonist, on kindling and kindled seizures. *Exp Neurol* 83:144-54
131. Kadar T, Cohen G, Sahar R, Alkalai D, Shapira S. 1992. Long-term study of brain lesions following soman, in comparison to DFP and metrazol poisoning. *Hum Exp Toxicol* 11:517-23
132. Kalappa BI, Gusev AG, Uteshev VV. 2010. Activation of functional alpha7-containing nAChRs in hippocampal CA1 pyramidal neurons by physiological levels of choline in the presence of PNU-120596. *PloS One* 5:e13964
133. Kassel JD, Unrod M. 2000. Smoking, anxiety, and attention: support for the role of nicotine in attentionally mediated anxiety. *J Abnorm Psychol* 109:161-6
134. Kawana N, Ishimatsu S, Kanda K. 2001. Psycho-physiological effects of the terrorist sarin attack on the Tokyo subway system. *Mil Med* 166:23-6
135. Kazi AI, Oommen A. 2012. The effect of acute severe monocrotophos poisoning on inhibition, expression and activity of acetylcholinesterase in different rat brain regions. *Neurotoxicology* 33:1284-90

136. Kemppainen S, Pitkanen A. 2000. Distribution of parvalbumin, calretinin, and calbindin-D(28k) immunoreactivity in the rat amygdaloid complex and colocalization with gamma-aminobutyric acid. *J Comp Neurol* 426:441-67
137. Kerkut GA. 1984. Acetylcholinesterase (AChE) (EC 3.1.1.7.). *Gen Pharmacol* 15:375-8
138. Khiroug L, Giniatullin R, Klein RC, Fayuk D, Yakel JL. 2003. Functional mapping and Ca²⁺ regulation of nicotinic acetylcholine receptor channels in rat hippocampal CA1 neurons. *J Neurosci* 23:9024-31
139. Khiroug SS, Harkness PC, Lamb PW, Sudweeks SN, Khiroug L, et al. 2002. Rat nicotinic ACh receptor alpha7 and beta2 subunits co-assemble to form functional heteromeric nicotinic receptor channels. *J Physiol* 540:425-34
140. Kishimoto K, Koyama S, Akaike N. 2000. Presynaptic modulation of synaptic gamma-aminobutyric acid transmission by tandospirone in rat basolateral amygdala. *Eur J Pharmacol* 407:257-65
141. Klein RC, Yakel JL. 2006. Functional somato-dendritic alpha7-containing nicotinic acetylcholine receptors in the rat basolateral amygdala complex. *J Physiol* 576:865-72
142. Kobayashi H, Suzuki T, Sakamoto M, Hashimoto W, Kashiwada K, et al. 2007. Brain regional acetylcholinesterase activity and muscarinic acetylcholine receptors in rats after repeated administration of cholinesterase inhibitors and its withdrawal. *Toxicol Appl Pharmacol* 219:151-61
143. Koenigs M, Grafman J. 2009. Posttraumatic stress disorder: the role of medial prefrontal cortex and amygdala. *Neuroscientist* 15:540-8
144. Kozhemyakin M, Rajasekaran K, Kapur J. 2010. Central cholinesterase inhibition enhances glutamatergic synaptic transmission. *J Neurophysiol* 103:1748-57
145. Lallement G, Carpentier P, Collet A, Baubichon D, Pernot-Marino I, Blanchet G. 1992. Extracellular acetylcholine changes in rat limbic structures during soman-induced seizures. *Neurotoxicology* 13:557-67
146. Lallement G, Carpentier P, Collet A, Pernot-Marino I, Baubichon D, Blanchet G. 1991. Effects of soman-induced seizures on different extracellular amino acid levels and on glutamate uptake in rat hippocampus. *Brain Res* 563:234-40
147. Lallement G, Carpentier P, Collet A, Pernot-Marino I, Baubichon D, et al. 1991. [Involvement of glutamatergic system of amygdala in generalized seizures induced by soman: comparison with the hippocampus]. *C R Acad Sci III* 313:421-6

148. Lang EJ, Pare D. 1997. Similar inhibitory processes dominate the responses of cat lateral amygdaloid projection neurons to their various afferents. *J Neurophysiol* 77:341-52
149. Lang EJ, Pare D. 1998. Synaptic responsiveness of interneurons of the cat lateral amygdaloid nucleus. *Neuroscience* 83:877-89
150. Langston JL, Wright LK, Connis N, Lumley LA. 2012. Characterizing the behavioral effects of nerve agent-induced seizure activity in rats: increased startle reactivity and perseverative behavior. *Pharmacol Biochem Behav* 100:382-91
151. Lawrie SM, Whalley HC, Job DE, Johnstone EC. 2003. Structural and functional abnormalities of the amygdala in schizophrenia. *Ann N Y Acad Sci* 985:445-60
152. LeDoux J. 2003. The emotional brain, fear, and the amygdala. *Cell Mol Neurobiol* 23:727-38
153. LeDoux JE. 1995. Emotion: clues from the brain. *Annu Rev Psychol* 46:209-35
154. LeDoux JE. 2000. Emotion circuits in the brain. *Annu Rev Neurosci* 23:155-84
155. Levin ED. 2012. alpha7-Nicotinic receptors and cognition. *Curr Drug Target* 13:602-6
156. Li L, Du Y, Li N, Wu X, Wu Y. 2009. Top-down modulation of prepulse inhibition of the startle reflex in humans and rats. *Neurosci Biobehav Rev* 33:1157-67
157. Li L, Fulton JD, Yeomans JS. 1999. Effects of bilateral electrical stimulation of the ventral pallidum on acoustic startle. *Brain Res* 836:164-72
158. Lintern MC, Wetherell JR, Smith ME. 1998. Differential recovery of acetylcholinesterase in guinea pig muscle and brain regions after soman treatment. *Hum Exp Toxicol* 17:157-62
159. Liu Q, Huang Y, Xue F, Simard A, DeChon J, et al. 2009. A novel nicotinic acetylcholine receptor subtype in basal forebrain cholinergic neurons with high sensitivity to amyloid peptides. *J Neurosci* 29:918-29
160. Liu YH, Wang L, Wei LC, Huang YG, Chen LW. 2009. Up-regulation of D-serine might induce GABAergic neuronal degeneration in the cerebral cortex and hippocampus in the mouse pilocarpine model of epilepsy. *Neurochem Res* 34:1209-18
161. Livingstone PD, Srinivasan J, Kew JN, Dawson LA, Gotti C, et al. 2009. alpha7 and non-alpha7 nicotinic acetylcholine receptors modulate dopamine release in vitro and in vivo in the rat prefrontal cortex. *Eur J Neurosci* 29:539-50

162. Mahanty NK, Sah P. 1998. Calcium-permeable AMPA receptors mediate long-term potentiation in interneurons in the amygdala. *Nature* 394:683-7
163. Mahanty NK, Sah P. 1999. Excitatory synaptic inputs to pyramidal neurons of the lateral amygdala. *Eur J Neurosci* 11:1217-22
164. Malenka RC, Nicoll RA. 1999. Long-term potentiation--a decade of progress? *Science* 285:1870-4
165. Mamczarz J, Pereira EF, Aracava Y, Adler M, Albuquerque EX. 2010. An acute exposure to a sub-lethal dose of soman triggers anxiety-related behavior in guinea pigs: interactions with acute restraint. *Neurotoxicology* 31:77-84
166. Maren S. 1996. Synaptic transmission and plasticity in the amygdala. An emerging physiology of fear conditioning circuits. *Mol Neurobiol* 13:1-22
167. Marrs TC, Rice P, Vale JA. 2006. The role of oximes in the treatment of nerve agent poisoning in civilian casualties. *Toxicol Rev* 25:297-323
168. Martin LF, Kem WR, Freedman R. 2004. Alpha-7 nicotinic receptor agonists: potential new candidates for the treatment of schizophrenia. *Psychopharmacology* 174:54-64
169. Martinowich K, Schloesser RJ, Lu Y, Jimenez DV, Paredes D, et al. 2012. Roles of p75(NTR), long-term depression, and cholinergic transmission in anxiety and acute stress coping. *Biol Psychiatry* 71:75-83
170. Mash DC, Potter LT. 1986. Autoradiographic localization of M1 and M2 muscarinic receptors in the rat brain. *Neuroscience* 19:551-64
171. Mattson MP. 2000. Apoptosis in neurodegenerative disorders. *Nat Rev Mol Cell Biol* 1:120-9
172. McDonald AJ, Mascagni F. 2002. Immunohistochemical characterization of somatostatin containing interneurons in the rat basolateral amygdala. *Brain Res* 943:237-44
173. McDonald AJ, Mascagni F. 2010. Neuronal localization of m1 muscarinic receptor immunoreactivity in the rat basolateral amygdala. *Brain Struct Funct* 215:37-48
174. McDonough JH, Jr., Dochterman LW, Smith CD, Shih TM. 1995. Protection against nerve agent-induced neuropathology, but not cardiac pathology, is associated with the anticonvulsant action of drug treatment. *Neurotoxicology* 16:123-32

175. McDonough JH, Jr., McLeod CG, Jr., Nipwoda MT. 1987. Direct microinjection of soman or VX into the amygdala produces repetitive limbic convulsions and neuropathology. *Brain Res* 435:123-37
176. McDonough JH, Jr., Shih TM. 1993. Pharmacological modulation of soman-induced seizures. *Neurosci Biobehav Rev* 17:203-15
177. McDonough JH, Jr., Shih TM. 1997. Neuropharmacological mechanisms of nerve agent-induced seizure and neuropathology. *Neurosci Biobehav Rev* 21:559-79
178. McDonough JH, Jr., Zoefel LD, McMonagle J, Copeland TL, Smith CD, Shih TM. 2000. Anticonvulsant treatment of nerve agent seizures: anticholinergics versus diazepam in soman-intoxicated guinea pigs. *Epilepsy Res* 38:1-14
179. McDonough JH, McMonagle JD, Shih TM. 2010. Time-dependent reduction in the anticonvulsant effectiveness of diazepam against soman-induced seizures in guinea pigs. *Drug Chem Toxicol* 33:279-83
180. McGehee DS, Role LW. 1995. Physiological diversity of nicotinic acetylcholine receptors expressed by vertebrate neurons. *Annu Rev Physiol* 57:521-46
181. Meerson A, Cacheaux L, Goosens KA, Sapolsky RM, Soreq H, Kaufer D. 2010. Changes in brain MicroRNAs contribute to cholinergic stress reactions. *J Mol Neurosci* 40:47-55
182. Mello LE, Cavaleiro EA, Tan AM, Kupfer WR, Pretorius JK, et al. 1993. Circuit mechanisms of seizures in the pilocarpine model of chronic epilepsy: cell loss and mossy fiber sprouting. *Epilepsia* 34:985-95
183. Mesulam MM, Hersh LB, Mash DC, Geula C. 1992. Differential cholinergic innervation within functional subdivisions of the human cerebral cortex: a choline acetyltransferase study. *J Comp Neurol* 318:316-28
184. Michalek H, Meneguz A, Bisso GM. 1981. Molecular forms of rat brain acetylcholinesterase in DFP intoxication and subsequent recovery. *Neurobehav Toxicol Teratol* 3:303-12
185. Mitra R, Ferguson D, Sapolsky RM. 2009. SK2 potassium channel overexpression in basolateral amygdala reduces anxiety, stress-induced corticosterone secretion and dendritic arborization. *Mol Psychiatry* 14:847-55, 27
186. Modak AT, Stavinoha WB, Weintraub ST. 1975. Dichlorvos and the cholinergic system: effects on cholinesterase and acetylcholine and choline contents of rat tissues. *Arch Int Pharmacodyn Ther* 217:293-301
187. Moffett MC, Schultz MK, Schwartz JE, Stone MF, Lumley LA. 2011. Impaired auditory and contextual fear conditioning in soman-exposed rats. *Pharmacol Biochem Behav* 98:120-9

188. Mohapel P, Dufresne C, Kelly ME, McIntyre DC. 1996. Differential sensitivity of various temporal lobe structures in the rat to kindling and status epilepticus induction. *Epilepsy Res* 23:179-87
189. Morita H, Yanagisawa N, Nakajima T, Shimizu M, Hirabayashi H, et al. 1995. Sarin poisoning in Matsumoto, Japan. *Lancet* 346:290-3
190. Moshiri M, Darchini-Maragheh E, Balali-Mood M. 2012. Advances in toxicology and medical treatment of chemical warfare nerve agents. *Daru* 20:81
191. Mothet JP, Parent AT, Wolosker H, Brady RO, Jr., Linden DJ, et al. 2000. D-serine is an endogenous ligand for the glycine site of the N-methyl-D-aspartate receptor. *Proc Natl Acad Sci U S A* 97:4926-31
192. Muller J, Corodimas KP, Fridel Z, LeDoux JE. 1997. Functional inactivation of the lateral and basal nuclei of the amygdala by muscimol infusion prevents fear conditioning to an explicit conditioned stimulus and to contextual stimuli. *Behav Neurosci* 111:683-91
193. Muller JF, Mascagni F, McDonald AJ. 2011. Cholinergic innervation of pyramidal cells and parvalbumin-immunoreactive interneurons in the rat basolateral amygdala. *J Comp Neurol* 519:790-805
194. Murata K, Araki S, Yokoyama K, Okumura T, Ishimatsu S, et al. 1997. Asymptomatic sequelae to acute sarin poisoning in the central and autonomic nervous system 6 months after the Tokyo subway attack. *J Neurol* 244:601-6
195. Myhrer T. 2007. Neuronal structures involved in the induction and propagation of seizures caused by nerve agents: implications for medical treatment. *Toxicology* 239:1-14
196. Myhrer T. 2010. Identification of neuronal target areas for nerve agents and specification of receptors for pharmacological treatment. *Neurotoxicology* 31:629-38
197. Nagai T, Kimura H, Maeda T, McGeer PL, Peng F, McGeer EG. 1982. Cholinergic projections from the basal forebrain of rat to the amygdala. *J Neurosci* 2:513-20
198. Nagao M, Takatori T, Matsuda Y, Nakajima M, Iwase H, Iwadata K. 1997. Definitive evidence for the acute sarin poisoning diagnosis in the Tokyo subway. *Toxicol Appl Pharmacol* 144:198-203
199. Nakajima T, Ohta S, Fukushima Y, Yanagisawa N. 1999. Sequele of sarin toxicity at one and three years after exposure in Matsumoto, Japan. *J Epidemiol* 9:337-43

200. Naylor DE, Liu H, Niquet J, Wasterlain CG. 2013. Rapid surface accumulation of NMDA receptors increases glutamatergic excitation during status epilepticus. *Neurobio Dis* 54:225-38
201. Naylor DE, Liu H, Wasterlain CG. 2005. Trafficking of GABA(A) receptors, loss of inhibition, and a mechanism for pharmacoresistance in status epilepticus. *J Neurosci* 25:7724-33
202. Newmark J. 2004. The birth of nerve agent warfare: lessons from Syed Abbas Foroutan. *Neurology* 62:1590-6
203. Newmark J. 2007. Nerve agents. *Neurologist* 13:20-32
204. Niquet J, Baldwin RA, Allen SG, Fujikawa DG, Wasterlain CG. 2003. Hypoxic neuronal necrosis: protein synthesis-independent activation of a cell death program. *Proc Natl Acad Sci U S A* 100:2825-30
205. Nishiwaki Y, Maekawa K, Ogawa Y, Asukai N, Minami M, et al. 2001. Effects of sarin on the nervous system in rescue team staff members and police officers 3 years after the Tokyo subway sarin attack. *Environ Health Perspect* 109:1169-73
206. Nitecka L, Frotscher M. 1989. Organization and synaptic interconnections of GABAergic and cholinergic elements in the rat amygdaloid nuclei: single- and double-immunolabeling studies. *J Comp Neurol* 279:470-88
207. Nozaki H, Aikawa N, Shinozawa Y, Hori S, Fujishima S, et al. 1995. Sarin poisoning in Tokyo subway. *Lancet* 345:980-1
208. Ohshiro H, Kubota S, Murakoshi T. 2011. Dopaminergic modulation of oscillatory network inhibition in the rat basolateral amygdala depends on initial activity state. *Neuropharmacology* 61:857-66
209. Ohtani T, Iwanami A, Kasai K, Yamasue H, Kato T, et al. 2004. Post-traumatic stress disorder symptoms in victims of Tokyo subway attack: a 5-year follow-up study. *Psychiatry Clin Neurosci* 58:624-9
210. Okumura T, Takasu N, Ishimatsu S, Miyanoki S, Mitsunashi A, et al. 1996. Report on 640 victims of the Tokyo subway sarin attack. *Ann Emerg Med* 28:129-35
211. Olincy A, Stevens KE. 2007. Treating schizophrenia symptoms with an alpha7 nicotinic agonist, from mice to men. *Biochem Pharmacol* 74:1192-201
212. Ottersen OP. 1982. Connections of the amygdala of the rat. IV: Corticoamygdaloid and intraamygdaloid connections as studied with axonal transport of horseradish peroxidase. *J Comp Neurol* 205:30-48

213. Padilla S, Lassiter TL, Hunter D. 1999. Biochemical measurement of cholinesterase activity. *Methods Mol Med* 22:237-45
214. Pan BX, Dong Y, Ito W, Yanagawa Y, Shigemoto R, Morozov A. 2009. Selective gating of glutamatergic inputs to excitatory neurons of amygdala by presynaptic GABA_B receptor. *Neuron* 61:917-29
215. Pape HC, Pare D. 2010. Plastic synaptic networks of the amygdala for the acquisition, expression, and extinction of conditioned fear. *Physiol Rev* 90:419-63
216. Pare D, Gaudreau H. 1996. Projection cells and interneurons of the lateral and basolateral amygdala: distinct firing patterns and differential relation to theta and delta rhythms in conscious cats. *J Neurosci* 16:3334-50
217. Pare D, Smith Y, Pare JF. 1995. Intra-amygdaloid projections of the basolateral and basomedial nuclei in the cat: Phaseolus vulgaris-leucoagglutinin anterograde tracing at the light and electron microscopic level. *Neuroscience* 69:567-83
218. Park K, Lee S, Kang SJ, Choi S, Shin KS. 2007. Hyperpolarization-activated currents control the excitability of principal neurons in the basolateral amygdala. *Biochem Biophys Res Commun* 361:718-24
219. Parri HR, Hernandez CM, Dineley KT. 2011. Research update: Alpha7 nicotinic acetylcholine receptor mechanisms in Alzheimer's disease. *Biochem Pharmacol* 82:931-42
220. Paxinos G, Watson C. 2005. *The Rat Brain in Stereotaxic Coordinates*. New York NY: Elsevier
221. Petras JM. 1981. Soman neurotoxicity. *Fundam Appl Toxicol* 1:242
222. Petras JM. 1994. Neurology and neuropathology of Soman-induced brain injury: an overview. *J Exp Anal Behav* 61:319-29
223. Phelps EA, LeDoux JE. 2005. Contributions of the amygdala to emotion processing: from animal models to human behavior. *Neuron* 48:175-87
224. Pidoplichko VI, Dani JA. 2005. Applying small quantities of multiple compounds to defined locations of in vitro brain slices. *J Neurosci Methods* 142:55-66
225. Pidoplichko VI, Prager EM, Aroniadou-Anderjaska V, Braga MF. 2013. alpha7-containing nicotinic acetylcholine receptors on interneurons of the basolateral amygdala and their role in the regulation of the network excitability. *J Neurophysiol* 110:2358-69
226. Pitkanen A, Stefanacci L, Farb CR, Go GG, LeDoux JE, Amaral DG. 1995. Intrinsic connections of the rat amygdaloid complex: projections originating in the lateral nucleus. *J Comp Neurol* 356:288-310

227. Pitkanen A, Tuunanen J, Kalviainen R, Partanen K, Salmenpera T. 1998. Amygdala damage in experimental and human temporal lobe epilepsy. *Epilepsy Res* 32:233-53
228. Popescu AT, Pare D. 2011. Synaptic interactions underlying synchronized inhibition in the basal amygdala: evidence for existence of two types of projection cells. *J Neurophysiol* 105:687-96
229. Power AE. 2004. Muscarinic cholinergic contribution to memory consolidation: with attention to involvement of the basolateral amygdala. *Curr Med Chem* 11:987-96
230. Prager EM, Aroniadou-Anderjaska V, Almeida-Suhett CP, Figueiredo TH, Apland JP, Braga MF. 2013. Acetylcholinesterase inhibition in the basolateral amygdala plays a key role in the induction of status epilepticus after soman exposure. *Neurotoxicology* 38:84-90
231. Prager EM, Aroniadou-Anderjaska V, Almeida-Suhett CP, Figueiredo TH, Apland JP, et al. 2013. The recovery of acetylcholinesterase activity and the progression of neuropathological and pathophysiological alterations in the rat basolateral amygdala after soman-induced status epilepticus: relation to anxiety-like behavior. *Neuropharmacology*
232. Prager EM, Bergstrom HC, Grunberg NE, Johnson LR. 2011. The importance of reporting housing and husbandry in rat research. *Front Behav Neurosci* 5:38
233. Prut L, Belzung C. 2003. The open field as a paradigm to measure the effects of drugs on anxiety-like behaviors: a review. *Eur J Pharmacol* 463:3-33
234. Qashu F, Figueiredo TH, Aroniadou-Anderjaska V, Apland JP, Braga MF. 2010. Diazepam administration after prolonged status epilepticus reduces neurodegeneration in the amygdala but not in the hippocampus during epileptogenesis. *Amino Acids* 38:189-97
235. Quarta D, Naylor CG, Barik J, Fernandes C, Wonnacott S, Stolerman IP. 2009. Drug discrimination and neurochemical studies in alpha7 null mutant mice: tests for the role of nicotinic alpha7 receptors in dopamine release. *Psychopharmacology* 203:399-410
236. Racine R, Rose PA, Burnham WM. 1977. Afterdischarge thresholds and kindling rates in dorsal and ventral hippocampus and dentate gyrus. *Can J Neurol Sci* 4:273-8
237. Racine RJ. 1972. Modification of seizure activity by electrical stimulation. II. Motor seizure. *Electroencephalogr Clin Neurophysiol* 32:281-94
238. Rainnie DG. 1999. Serotonergic modulation of neurotransmission in the rat basolateral amygdala. *J Neurophysiol* 82:69-85

239. Rauch SL, Shin LM, Phelps EA. 2006. Neurocircuitry models of posttraumatic stress disorder and extinction: human neuroimaging research--past, present, and future. *Biol Psychiatry* 60:376-82
240. Rauch SL, Whalen PJ, Shin LM, McInerney SC, Macklin ML, et al. 2000. Exaggerated amygdala response to masked facial stimuli in posttraumatic stress disorder: a functional MRI study. *Biol Psychiatry* 47:769-76
241. Ravindran LN, Stein MB. 2009. Pharmacotherapy of PTSD: premises, principles, and priorities. *Brain Res* 1293:24-39
242. Robinson L, Platt B, Riedel G. 2011. Involvement of the cholinergic system in conditioning and perceptual memory. *Behav Brain Res* 221:443-65
243. Rogers MA, Yamasue H, Abe O, Yamada H, Ohtani T, et al. 2009. Smaller amygdala volume and reduced anterior cingulate gray matter density associated with history of post-traumatic stress disorder. *Psychiatry Res* 174:210-6
244. Rossetti F, de Araujo Furtado M, Pak T, Bailey K, Shields M, et al. 2012. Combined diazepam and HDAC inhibitor treatment protects against seizures and neuronal damage caused by soman exposure. *Neurotoxicology* 33:500-11
245. Sah P, Faber ES, Lopez De Armentia M, Power J. 2003. The amygdaloid complex: anatomy and physiology. *Physiol Rev* 83:803-34
246. Sanders SK, Morzorati SL, Shekhar A. 1995. Priming of experimental anxiety by repeated subthreshold GABA blockade in the rat amygdala. *Brain Res* 699:250-9
247. Schmitz C, Hof PR. 2000. Recommendations for straightforward and rigorous methods of counting neurons based on a computer simulation approach. *J Chem Neuroanat* 20:93-114
248. Schmued LC, Albertson C, Slikker W, Jr. 1997. Fluoro-Jade: a novel fluorochrome for the sensitive and reliable histochemical localization of neuronal degeneration. *Brain Res* 751:37-46
249. Segal M, Dudai Y, Amsterdam A. 1978. Distribution of an alpha-bungarotoxin-binding cholinergic nicotinic receptor in rat brain. *Brain Res* 148:105-19
250. Sengupta P. 2011. A scientific review of age determination for a laboratory rat: How old is it in comparison with human age? *Biomedicine International* 2:81-9
251. Sheffler DJ, Williams R, Bridges TM, Xiang Z, Kane AS, et al. 2009. A novel selective muscarinic acetylcholine receptor subtype 1 antagonist reduces seizures without impairing hippocampus-dependent learning. *Mol Pharmacol* 76:356-68
252. Shekhar A, Truitt W, Rainnie D, Sajdyk T. 2005. Role of stress, corticotrophin releasing factor (CRF) and amygdala plasticity in chronic anxiety. *Stress* 8:209-19

253. Sheline YI, Barch DM, Donnelly JM, Ollinger JM, Snyder AZ, Mintun MA. 2001. Increased amygdala response to masked emotional faces in depressed subjects resolves with antidepressant treatment: an fMRI study. *Biol Psychiatry* 50:651-8
254. Shih TM. 1982. Time course effects of soman on acetylcholine and choline levels in six discrete areas of the rat brain. *Psychopharmacology* 78:170-5
255. Shih TM, Duniho SM, McDonough JH. 2003. Control of nerve agent-induced seizures is critical for neuroprotection and survival. *Toxicol Appl Pharmacol* 188:69-80
256. Shih TM, Kan RK, McDonough JH. 2005. In vivo cholinesterase inhibitory specificity of organophosphorus nerve agents. *Chem Biol Interact* 157-158:293-303
257. Shin C, Rigsbee LC, McNamara JO. 1986. Anti-seizure and anti-epileptogenic effect of gamma-vinyl gamma-aminobutyric acid in amygdaloid kindling. *Brain Res* 398:370-4
258. Shin LM, Orr SP, Carson MA, Rauch SL, Macklin ML, et al. 2004. Regional cerebral blood flow in the amygdala and medial prefrontal cortex during traumatic imagery in male and female Vietnam veterans with PTSD. *Arch Gen Psychiatry* 61:168-76
259. Sidell FR. 1997. Nerve Agents. In *Textbook of Military Medicine: Medical Aspects of Chemical and Biological Warfare*, ed. FR Sidell, TE Takafuji, DR Franz:129-79. Falls Church, VA: Office of the Surgeon General, U.S. Army. Number of 129-79 pp.
260. Siek GC, Katz LS, Fishman EB, Korosi TS, Marquis JK. 1990. Molecular forms of acetylcholinesterase in subcortical areas of normal and Alzheimer disease brain. *Biol Psychiatry* 27:573-80
261. Siesjo BK, Siesjo P. 1996. Mechanisms of secondary brain injury. *Eur J Anaesthesiol* 13:247-68
262. Simmons AN, Matthews SC, Strigo IA, Baker DG, Donovan HK, et al. 2011. Altered amygdala activation during face processing in Iraqi and Afghanistani war veterans. *Biol Mood Anxiety Disord* 1:6
263. Sirin GS, Zhou Y, Lior-Hoffmann L, Wang S, Zhang Y. 2012. Aging mechanism of soman inhibited acetylcholinesterase. *J Phys Chem B* 116:12199-207
264. Skovira JW, McDonough JH, Shih TM. 2010. Protection against sarin-induced seizures in rats by direct brain microinjection of scopolamine, midazolam or MK-801. *J Mol Neurosci* 40:56-62

265. Sloviter RS. 1999. Status epilepticus-induced neuronal injury and network reorganization. *Epilepsia* 40 Suppl 1:S34-9; discussion S40-1
266. Smith Y, Pare JF, Pare D. 1998. Cat intraamygdaloid inhibitory network: ultrastructural organization of parvalbumin-immunoreactive elements. *J Comp Neurol* 391:164-79
267. Soreq H, Seidman S. 2001. Acetylcholinesterase--new roles for an old actor. *Nat Rev Neurosci* 2:294-302
268. Spanpanato J, Polepalli J, Sah P. 2011. Interneurons in the basolateral amygdala. *Neuropharmacology* 60:765-73
269. Stein MB, Stein DJ. 2008. Social anxiety disorder. *Lancet* 371:1115-25
270. Swanson LW, Simmons DM, Whiting PJ, Lindstrom J. 1987. Immunohistochemical localization of neuronal nicotinic receptors in the rodent central nervous system. *J Neurosci* 7:3334-42
271. Szinicz L. 2005. History of chemical and biological warfare agents. *Toxicology* 214:167-81
272. Szinyei C, Heinbockel T, Montagne J, Pape HC. 2000. Putative cortical and thalamic inputs elicit convergent excitation in a population of GABAergic interneurons of the lateral amygdala. *J Neurosci* 20:8909-15
273. Szyndler J, Sienkiewicz-Jarosz H, Maciejak P, Siemiatkowski M, Rokicki D, et al. 2001. The anxiolytic-like effect of nicotine undergoes rapid tolerance in a model of contextual fear conditioning in rats. *Pharmacol Biochem Behav* 69:511-8
274. Tetz LM, Rezk PE, Ratcliffe RH, Gordon RK, Steele KE, Nambiar MP. 2006. Development of a rat pilocarpine model of seizure/status epilepticus that mimics chemical warfare nerve agent exposure. *Toxicol Ind Health* 22:255-66
275. Teyler TJ, DiScenna P. 1987. Long-term potentiation. *Annu Rev Neurosci* 10:131-61
276. Thiermann H, Worek F, Kehe K. 2013. Limitations and challenges in treatment of acute chemical warfare agent poisoning. *Chem Biol Interact*
277. Truitt WA, Johnson PL, Dietrich AD, Fitz SD, Shekhar A. 2009. Anxiety-like behavior is modulated by a discrete subpopulation of interneurons in the basolateral amygdala. *Neuroscience* 160:284-94
278. Tu AT. 1996. Basic information on nerve gas and the use of sarin by Aum Shinrikyo. *J Mass Spectrom Soc Jpn* 44:293-320

279. van der Zee EA, Luiten PG. 1999. Muscarinic acetylcholine receptors in the hippocampus, neocortex and amygdala: a review of immunocytochemical localization in relation to learning and memory. *Prog Neurobiol* 58:409-71
280. Van Kampen M, Selbach K, Schneider R, Schiegel E, Boess F, Schreiber R. 2004. AR-R 17779 improves social recognition in rats by activation of nicotinic alpha7 receptors. *Psychopharmacology* 172:375-83
281. Vazquez-Palacios G, Bonilla-Jaime H, Velazquez-Moctezuma J. 2004. Antidepressant-like effects of the acute and chronic administration of nicotine in the rat forced swimming test and its interaction with fluoxetine [correction of flouxetine]. *Pharmacol Biochem Behav* 78:165-9
282. Villarreal G, King CY. 2001. Brain imaging in posttraumatic stress disorder. *Semin Clin Neuropsychiatry* 6:131-45
283. Wang H, Sun X. 2005. Desensitized nicotinic receptors in brain. *Brain Res Brain Res Rev* 48:420-37
284. Wang JM, Wang BB, Xie Y, Sun SS, Gu ZY, et al. 2014. Functional study on the mutations in the silkworm (*Bombyx mori*) acetylcholinesterase type 1 gene (*ace1*) and its recombinant proteins. *Mol Biol Rep* 41:429-37
285. Wang L, Liu YH, Huang YG, Chen LW. 2008. Time-course of neuronal death in the mouse pilocarpine model of chronic epilepsy using Fluoro-Jade C staining. *Brain Res* 1241:157-67
286. Wang Y, Boeck AT, Duysen EG, Van Keuren M, Saunders TL, Lockridge O. 2004. Resistance to organophosphorus agent toxicity in transgenic mice expressing the G117H mutant of human butyrylcholinesterase. *Toxicol Appl Pharmacol* 196:356-66
287. White LE, Price JL. 1993. The functional anatomy of limbic status epilepticus in the rat. I. Patterns of ¹⁴C-2-deoxyglucose uptake and Fos immunocytochemistry. *J Neurosci* 13:4787-809
288. White LE, Price JL. 1993. The functional anatomy of limbic status epilepticus in the rat. II. The effects of focal deactivation. *J Neurosci* 13:4810-30
289. Wiener SW, Hoffman RS. 2004. Nerve agents: a comprehensive review. *J Intensive Care Med* 19:22-37
290. Williams LR, Aroniadou-Anderjaska V, Qashu F, Finne H, Pidoplichko V, et al. 2011. RDX binds to the GABA(A) receptor-convulsant site and blocks GABA(A) receptor-mediated currents in the amygdala: a mechanism for RDX-induced seizures. *Environ Health Perspect* 119:357-63

291. Wolosker H. 2007. NMDA receptor regulation by D-serine: new findings and perspectives. *Mol Neurobiol* 36:152-64
292. Womble MD, Moises HC. 1993. Hyperpolarization-activated currents in neurons of the rat basolateral amygdala. *J Neurophysiol* 70:2056-65
293. Woodruff AR, Sah P. 2007. Inhibition and synchronization of basal amygdala principal neuron spiking by parvalbumin-positive interneurons. *J Neurophysiol* 98:2956-61
294. Woolf NJ. 1991. Cholinergic systems in mammalian brain and spinal cord. *Prog Neurobiol* 37:475-524
295. Yamasue H, Abe O, Kasai K, Suga M, Iwanami A, et al. 2007. Human brain structural change related to acute single exposure to sarin. *Ann Neurol* 61:37-46
296. Yanagisawa N, Morita H, Nakajima T. 2006. Sarin experiences in Japan: acute toxicity and long-term effects. *J Neurol Sci* 249:76-85
297. Yang RJ, Mozhui K, Karlsson RM, Cameron HA, Williams RW, Holmes A. 2008. Variation in mouse basolateral amygdala volume is associated with differences in stress reactivity and fear learning. *Neuropsychopharmacology* 33:2595-604
298. Zhu PJ, Stewart RR, McIntosh JM, Weight FF. 2005. Activation of nicotinic acetylcholine receptors increases the frequency of spontaneous GABAergic IPSCs in rat basolateral amygdala neurons. *J Neurophysiol* 94:3081-91
299. Zinebi F, Russell RT, McKernan M, Shinnick-Gallagher P. 2001. Comparison of paired-pulse facilitation of AMPA and NMDA synaptic currents in the lateral amygdala. *Synapse* 42:115-27